

Secondary Organic Aerosol (SOA) Formation from Monoterpene Ozonolysis in the Presence of
Inorganic Aerosols:
Acid effects on SOA yields

Amanda Laura Northcross

A dissertation submitted to the faculty of the University of North Carolina at Chapel Hill in partial fulfillment of the requirements for the degree of doctor of philosophy in the Department of Environmental Sciences and Engineering, School of Public Health

Chapel Hill
2007

Approved by:
Dr. Myoseon Jang
Dr. Edward Edney
Dr. Donald Fox
Dr. Harvey Jefferies
Dr. David Leith
Dr. Howard Weinberg

© 2007
Amanda Laura Northcross
ALL RIGHTS RESERVED

ABSTRACT

Secondary Organic Aerosol (SOA) Formation from Monoterpene Ozonolysis in the Presence of Inorganic Aerosols: Acid effects on SOA yields

Traditionally SOA formation has been predicted using a thermodynamic partitioning theory which does not take into consideration the presence of inorganic aerosols although SOA mass has been shown to be affected by the presence inorganic acidic aerosols. Acid particles are able to catalyze the formation of higher molecular weight structures within SOA and alter the thermodynamic partitioning equilibrium. The equilibrium is reestablished when additional mass partitions the aerosols increasing the particulate mass formed.

The effects of preexisting acidic particles on the SOA formation of a series of biogenic precursor gases has been investigated experimentally using an indoor smog chamber and modeled using mathematical models describing the gas, and particle phase chemistry. The model predicts the total SOA mass and the fraction of heterogeneous acid-catalyzed aerosol mass formed. The effect of varying acidity and relative humidity on the heterogeneous acid-catalyzed aerosol mass produced is also captured. Thermal gravimetric analysis was used to quantify the fraction of heterogeneous acid catalyzed aerosol mass in SOA, and to evaluate model predictions. The developed model more accurately describes the SOA formation process as it occurs in the ambient atmosphere by including the influence of inorganic aerosols.

DEDICATION

Mom and Dad I love you. Thanks you for everything.

ACKNOWLEDGMENTS

I first would like to acknowledge for whom without nothing occurs. I thank my parents and family for all their support. I also would like to thank my doctoral committee and especially my advisor for all of their time and effort which as helped me to develop into a doctoral scholar.

Friends and lab mates are invaluable and have helped me to stay balanced and focused, thank you.

TABLE OF CONTENTS

ABSTRACT	iii
LIST OF TABLES	x
LIST OF FIGURES.....	xi
LIST OF ABBREVIATIONS.....	xv
Chapter 1 Introduction.....	1
1.1 Background.....	1
1.1.1 Environmental and Health Effects of PM2.5.....	1
1.1.2 Sources of PM2.5.....	2
1.2 Motivation.....	8
1.3 Objective.....	9
1.4 Project description.....	9
1.5 References.....	12
Chapter 2	16
Heterogeneous SOA Yield from Ozonolysis of Monoterpenes in the Presence of Inorganic Acid	
ABSTRACT.....	17
2.1. Introduction.....	18
2.2. Experimental Section	19
2.3. Results and Discussion.....	23
2.3.1 Aerosol yields.....	23
2.3.2 Acidity and Inorganic Aerosols	25
2.3.3 Acidity Effect on SOA Yields	25
2.4. Conclusion	34

2.5. Acknowledgments.....	34
2.6 References.....	35
Chapter 3	38
Quantifying the nonvolatile fraction of biogenic secondary organic aerosols formed in the presence of inorganic aerosols through thermal analysis.	
ABSTRACT.....	39
3.1. Introduction.....	40
3.2. Experimental Methods	42
3.2.1 Chamber Operation.....	42
3.2.2 Aerosol Sampling	43
3.2.3 Thermal Gravimetric Analysis.....	43
3.2.4 FTIR Analysis of TGA Samples.....	44
3.3. Theory	44
3.3.1. Classification of Chemical Species in Aerosols	44
3.3.2 TGA Data Analysis.....	46
3.3.3 Thermogram of Inorganic Seed Aerosol	48
3.3.4 Thermograms of Organics in the Presence of Inorganics.....	48
3.3.5 FTIR Spectral Analysis of TGA Samples.....	52
3.3.6 Decoupling Organic and Inorganic Aerosol Mass.....	55
3.4. Results.....	60
3.4.1 Experimental Yield.....	60
3.4.2 Effect of Particle Acidity on SOA Formation.....	61
3.4.3 Types of Terpenes.....	61
3.5. Conclusion	62
3.6 Acknowledgments.....	63
Chapter 4	67
Modeling Formation of SOA from Thermodynamic Partitioning and Heterogeneous Acid Catalyzed Reactions in the Presence of Inorganic Aerosols	

4.1 Introduction.....	68
4.2 Experimental Methods.....	70
4.3 Model Development.....	71
4.3.1 Gas Phase Mechanism.....	71
4.3.2 OM _H Model.....	76
4.3.3 OM _P Model.....	77
4.4 Results and Discussion.....	79
4.4.1 Product Distribution.....	80
4.4.2 Total SOA Production.....	81
4.4.3 Oligomer Estimation.....	84
4.4.4 Acidic Inorganic Seed Concentration and SOA Mass.....	85
4.4.5 Uncertainty Analysis.....	86
4.5 Conclusion.....	88
CHAPTER 5.....	92
Summary of Key Findings, Implications and Recommendation for Future Studies	
5.1 Key Findings and Implications.....	92
5.2 Recommendations for Future Studies.....	93
5.2.1 Aerosol Chemistry Related Future Studies.....	94
5.2.2 Environmental Future Studies.....	96
5.3 References.....	97
Appendix.....	98
A.1 Experimental Instrumentation Description and Calibration.....	99
A.2 Experiment Protocol.....	102
A.2 Experiment Protocol.....	102
A.2.1 Smog Chamber Experiments.....	102
A.2.2 Aerosol Analysis.....	104

A.3 Instrument Calibration and Measurement Comparison.....	108
A.3.1 Gas Chromatograph Calibration	108
A.3.2 Mass Concentration Comparison SMPS/CNC vs. Filters.....	108
A.3.3 Ozone Monitor Calibration.....	109
A.3.4 TGA Calibration	110
A.4 Chamber Wall Loss.....	111
A.5 Nebulizer Seed Aerosol Size Distribution.....	112

LIST OF TABLES

Table 2.1 22
 Experimental Conditions and average SOA yields for neutral ($\bar{Y}_{neutral}$) and acidic seed (\bar{Y}_{acid}) experiments at 20% and 40% RH.
 a: Initial ozone concentrations.
 b: α -pinene data used to determine relationship between seed mass and aerosol yield. Figure 2.2.
 c. Average Y of acidic seed experiments for a given relative humidity.
 d. Average Y of neutral seed experiments for a given relative humidity.
 e. One experiment was conducted
 n.a.: not applicable

Table 3.1 42
 Experimental Conditions for TGA analysis of SOA T constant at 23°C. All values are average for experimental conditions.

Table 4.1 70
 Experimental conditions for chamber generated SOA formed from the ozonolysis of α -pinene, d-limonene, and terpinolene in the presence inorganic aerosols

Table 4.2 75
 Stoichiometric coefficients and representative product group structures from the MCM product distribution for the ozonolysis of α -pinene, d-limonene, and terpinolene.

Table 4.3 87
 Stoichiometric coefficients (α_i) for the product group from with the highest partitioning constant and highest reaction rate constant for α -pinene, terpinolene, and limonene.

Table A.1 109
 SMPS/CNC estimated mass concentration for SOA from α -pinene ozonolysis in comparison to filter sample derived aerosol concentration.

Table A.2 111
 Particle wall loss coefficients.

LIST OF FIGURES

Figure 1.1.....	1
Source contribution to primary PM2.5 in Charlotte, NC.	
Figure 1.2a	4
Average daily PM2.5 aerosol composition in Queens, NY Drewnick et al, 2004a.	
Figure 1.2b	4
Average daily PM2.5 aerosol composition in Houston TX Russell et al, 2004.	
Figure 1.3.....	6
Hypothesized reaction mechanisms for acid catalyzed heterogeneous reactions	
Figure 1.4.....	9
Molecular structures for terpenes used in modeling study	
Figure 2.1.....	21
A. α - pinene, β -pinene Δ^2 -carene and major ozonolysis products a: total molar yield (<i>Yu et al. 1999</i>), b: aerosol phase molar yield (<i>Grosjean et al. 1993</i>), c: gas phase molar yield (<i>Hakola et al. 1994</i>) B. Terpinolene and Limonene and major ozonolysis products B. a: total molar yield (<i>Yu et al. 1999</i>), b: aerosol phase molar yield (<i>Grosjean et al. 1993</i>), c: gas phase molar yield (<i>Hakola et al. 1994</i>), d: structural reference (<i>Glasius et al. 2000</i>)	
Figure 2.2.....	24
SOA aerosol yield (Y) from ozonolysis of α -pinene in the presence of inorganic acidic seed aerosol vs. inorganic seed aerosol mass (M_{seed_acid}). $Y = \Delta M / \Delta HC$ measuring the change in aerosol mass ΔM ($\mu\text{g}/\text{m}^3$) and dividing by the amount of hydrocarbons reacted ΔHC ($\mu\text{g}/\text{m}^3$). %RH = 16-19 and temperature = 297 K.	
Figure 2.3.....	26
Normalized SOA yield difference (ΔY^*) between acid and neutral at %RH = 20 and 40.	
$\Delta Y^* = \frac{Y_{acid} - \bar{Y}_{neutral}}{M_{seed_acid}}$, where Y_{acid} is the SOA yield with acidic seed and $\bar{Y}_{neutral}$ is the average SOA yield with neutral seed at %RH = 40. Errors were calculated using standard deviation from experimental SOA data.	

Figure 2.4.....	28
(log ΔY^* - log a_w) vs. X (excess acidity) for ozonolysis of various terpenes in the presence of an acid catalyst. Inorganic seed composition was 2:3 mole ratio of H_2SO_4 to NH_4HSO_4 . Regression line equations: β -pinene = $0.50X - 5.13$, α -pinene = $1.37X - 6.31$ ($R^2 = 0.84$), Δ^2 -carene = $0.99X - 5.30$ ($R^2=0.66$), terpinolene = $0.70X - 4.65$ ($R^2= 0.79$). a_w (water activity) was calculated using AIM (43-45).	
Figure 3.1.....	47
Thermograms of simulated $(NH_4)_2SO_4$ seed, NH_4HSO_4 - H_2SO_4 aqueous solution, neutral seeded α -pinene SOA, self-nucleated α -pinene SOA. The temperatures for inflection points are shown for each system. Inflection points at 240°C and 340° C are for $(NH_4)_2SO_4$ seed. Inflection points at 60°C, 240°C, and 328°C are for aqueous acidic seed solution ($H_2SO_4:NH_4HSO_4 = 2:3$).	
Figure 3.2.....	49
Thermograms of pinonic acid (2.2mg), and pinonic acid (0.5 mg) with nonanol (3.0 μ L), water, and acid seed solution (207mg NH_4HSO_4 , 2mL H_2SO_4 , 2ml H_2O).	
Figure 3.3.....	50
Isothermal analysis thermograms of nonanol (1.7 mg), acid seed solution (composition: 207 mg NH_4HSO_4 , 2 mL H_2SO_4 , 2 ml H_2O), and nonanol (1.71mg) with acid seed solution (7.4 mg) Isothermal temperature program was 80 minutes at 70°C and then ramped from 70°C to 600°C at 10°C/min.	
Figure 3.4.....	51
DTA thermograms of acidic seed solution and nonanol (65% _{wt}), and acid seed solution and pinonic acid (15% _{wt}), and acidic seed solution.	
Figure 3.5.....	53-54
FTIR spectra of pinonic acid and mixtures of pinonic acid with acidic seed solutions before and after TGA analysis. A. pure pinonic acid B. Mildly acidic mixture: 2.3 mg pinonic acid and 9.4 mg mildly acidic seed solution (16 g NH_4HSO_4 , 8 mL H_2O and 5 mL of H_2SO_4) C. Strongly acidic mixture: 4.8 mg of pinonic acid and 8.5 mg of strongly acidic seed solution (1.0 g NH_4HSO_4 , 1 mL H_2O and 1.5 mL of H_2SO_4)	
Figure 3.6.....	57
DTA thermograms A: aqueous $(NH_4)_2SO_4$ solution and aqueous solution containing both $(NH_4)_2SO_4$ (16% _{wt}) and pinonic acid (13% _{wt}). B: T shifted ($\Delta T=80^\circ C$) aqueous $(NH_4)_2SO_4$ solution and aqueous solution containing both $(NH_4)_2SO_4$ (16% _{wt}) and pinonic acid (13% _{wt}).	

Figure 3.7.....	59
DTA thermograms. A: aqueous neutral seed solution and neutral seeded α -pinene SOA; B: T shifted ($\Delta T=100^\circ\text{C}$) neutral seed solution and neutral seeded α -pinene SOA; C: OM only decoupled from neutral seeded α -pinene SOA using equation 2 and self nucleated α -pinene SOA (no seed used). The arrow shows the slope change used to determine the monomer T_f .	
Figure 3.8.....	60
Composition of aerosol. A: neutral seeded α -pinene SOA, $M_{\text{seed}}/\Delta\text{HC} = 0.5$; B: acidic seeded α -pinene SOA, $M_{\text{seed}}/\Delta\text{HC} = 0.25$; C: acidic seeded α -pinene SOA, $M_{\text{seed}}/\Delta\text{HC} = 0.1$; D: acidic seeded terpinolene SOA, $M_{\text{seed}}/\Delta\text{HC} = 0.15$.	
Figure 4.1.....	73
Gas phase terpene ozonolysis model estimation and smog chamber data. MCM model and protocol simulation for the decay of α -pinene, limonene and terpinolene with ozone and smog chamber experimental data for terpene and ozone decays. Terpene concentrated measured using GC/FID, ozone concentration measured using ozone monitor. Started adding ozone at time=0.	
Figure 4.2.....	79
Stoichiometric coefficients from terpene ozonolysis, grouped based on thermodynamic partitioning: very high partitioning (VHP), high partitioning (HP), medium partitioning (MP), low partitioning (LP) and very low partitioning (VLP), and heterogeneous reactivity: highly reactive (HR), medium reactivity (MR), low reactivity (LR), and non-reactive (NR). A. α -pinene ozonolysis, B terpinolene ozonolysis, C limonene ozonolysis.	
Figure 4.3.....	83
Total SOA mass from terpene ozonolysis in the presence of inorganic aerosols at low and high %RH. Acid seed: 2:3 $\text{H}_2\text{SO}_4/\text{NH}_4\text{HSO}_4$ Mid-acid seed 3:7 $\text{H}_2\text{SO}_4/\text{NH}_4\text{HSO}_4$, neutral seed $(\text{NH}_4)_2\text{SO}_4$. Black bar represent SOA from the smog chamber experiments, shaded bars are model results.	
Figure 4.4.....	84
Comparison of oligomer fraction of the organic SOA. Oligomer fraction measured using TGA, OM_H estimated using equation 4.3. Black bars are experimentally measured TGA oligomer fractions, shaded bars are model results from oligomer fractions estimated using the shown acidity and relative humidity.	
Figure A.1.....	99
Smog chamber schematic	
Figure A.2.....	103
Terpene injection manifold	

Figure A.3	108
Example of calibration curve. α -pinene in a Teflon bag with serial dilutions using clean air for concentrations from 2.25 ppm - 0.32 ppm.	
Figure A.4	112
Particle wall loss for α -pinene ozonolysis and neutral seed. Loss calculation starts at end of seed injection.	
Figure A.5	112
Acid seed particle number distribution, 25%RH Mode: 103 nm	
Figure A.6	113
Mid acid seed particle number distribution 25%RH Mode 89 nm	
Figure A.7	113
Neutral seed particle distribution 42%RH Mode 98 nm	

LIST OF ABBREVIATIONS

%RH	Relative percent humidity
$(\text{NH}_4)_2\text{SO}_4$	Ammonium sulfate
$[\text{B}_i]$	Slope
$[\text{H}^+]_{\text{mass}\%}$	Mass percent of proton concentration
$^{\circ}\text{C}$	Degree Celsius
A	Derived constant that describes the sensitivity of SOA formation
a_{B}	Activity of a base
a_{BH^+}	Activity of a protonated base
a_{H^+}	Activity of a proton
α_i	Stoichiometric coefficient
a_{w}	Activity of water
$C^*_{\text{sat},i}$	Gas phase saturation concentration of compound i
$\text{C}=\text{O}$	Carbonyl functional group
$C_{\text{aer},a}$	Aerosols phase concentration of all partitioned oxidized products
$C_{\text{aer},i}$	Aerosol phase concentration of compound i

C_{aerosol}	Aerosol phase concentration
CAM	Community Airshed Model
C_{gas}	Gas phase concentration
C_{H^+}	Proton concentration
CI	Crige Intermediate
C_{init}	Concentration of reactive intermediate
Cm	Centimeter
CNC	Condensation nuclei counter
ΔHC	Change in hydrocarbon concentration
ΔM	Change in aerosol mass concentration
ΔS_{vap}	Change in enthalpy of vaporization
ΔY^*	Change acid catalyzed heterogenous aerosol yield for an acid system above neutral conditions
e.g.	Example
f_h	Fraction of aerosol to reactive organic gas
FID-GC	Flame ionization detector – gas chromatograph
f_{om}	Fraction of organic matter
FTIR	Fourier transform infrared radiation

γ_{om}	Activity coefficient of organic matter
H ₂ SO ₄	Sulfuric acid
HP	Highly partitioning
HR	Highly reactive
HULIS	Humic like substances
<i>I</i>	Structural indicator for ability of compound to react heterogeneously
k'_{app}	Applied rate constant for heterogenous reactions
K_{BH^+}	Equilibrium constant for base protonation
kcal	Kilocalories
K_{hyd}	Hydration equilibrium constant
$K_{om,i}$	Thermodynamic partitioning constant
kPa	Kilopascals
LP	Low partitioning
M	Molar
m ³	Cubic meter
MALDI	Matrix assisted laser desorption ionization
MCM	Master chemical mechanism

μg	Micrograms
mg	Milligrams
min	Minutes
mL	Millileters
mm	Millimeters
M_{olig}	Mass of oligomer
$M_{\text{org-sul}}$	Mass of organic sulfate
MP	Medium partitioning
MR	Medium reactivity
MS	Mass spectrometry
M_{seed}	Mass of inorganic seed
$M_{\text{seed_acid}}$	Mass of acidic inorganic seed
M_{SOC}	Mass of semi-volatile carbon
M_{TOT}	Total aerosol mass
MW_{om}	Average molecular weight of organic mass
N_2	Nitrogen
NH_3	Ammonia

NH ₄ ⁺	Ammonium
NH ₄ HSO ₄	Ammonium hydrogen sulfate
nm	Nanometers
NO	Nitrogen oxide
NR	Nonreactive
O ₃	Ozone
OH	Hydroxyl radical
OM	Organic matter
OM _H	Organic matter from heterogeneous acid catalyzed reactions
OM _{H-A}	Organic matter associated only with heterogeneous acid catalyzed reaction in acidic systems
OM _P	Organic matter solely formed by thermodynamic partitioning
p _{L,i}	Saturated liquid vapor pressure
PM ₁₀	10 μm aerodynamic diameter particulate matter
PM _{2.5}	2.5 μm aerodynamic diameter particulate matter
R	Ideal gas law constant
ROG	Reactive organic gas

SAPRC	Statewide air pollution research center
SMPS	Scanning mobility particle sizer
SO ₃	Sulfur trioxide
SO ₄ ²⁻	Sulfate ion
SOA	Secondary organic aerosol
SOC	Semivolatile organic carbon
SOGRAM	Secondary organic aerosol model
T	Temperature
<i>t</i>	Time
T _b	Boiling point temperature
TGA	Thermal gravimetric analysis
UNC	University of North Carolina
USEPA	United States Environmental Protection Agency
UV	Ultra violet
VHP	Very highly partitioning
VLP	Very low partitioning
VOCs	Volatile organic carbon

wt%	Weight percent
X	Excess acidity
Y	Yield
Y_{acid}	SOA yield formed in presence of acidic inorganic aerosols
$Y_{neutral}$	SOS yield formed in presence of neutral inorganic aerosols

Chapter 1 Introduction

1.1 Background

1.1.1 Environmental and Health Effects of PM_{2.5}

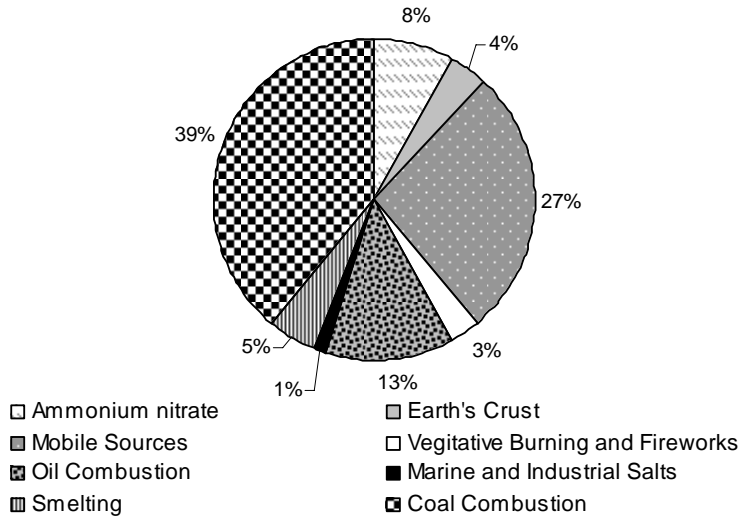


Figure 1.1 Source contribution to primary PM_{2.5} in Charlotte, NC.

Air pollution is composed of both gas phase and particle phase components which can pose health risks for humans. The risks linked to particles in particular, have been linked to concentration, composition, and particle size through epidemiological studies (Pope et al. 2004; Laden et al. 2000). Due to the deleterious

health effects of air pollution the United States Environmental Protection Agency (USEPA) regulates ambient concentrations of six criteria pollutants including particulate matter (PM).

Particulate matter in the ambient atmosphere is divided into two size modes, particulate matter with diameters less than 2.5 μ m (PM_{2.5}) and particulate matter with diameters less than 10 μ m (PM₁₀). PM_{2.5}, the fine mode of particulate matter, has been found to have very serious health effects which are directly related to size. Fine particulate matter is able to transverse the bends in the upper airway and able to deposit deep into the lungs, while the coarse mode (PM₁₀) typically impacts at the back of the nasal passage and is cleared through the mucocilliary elevator. The ability of PM_{2.5} to deposit into the deep lungs increases its ability to cause damage. PM_{2.5} has been shown to increase the incidences of bronchitis, asthma, decreased lung function and other respiratory illnesses

as well as increased risk to both morbidity and mortality (Laden et al. 2000; Neuberger et al. 2004; Pope et al. 2004).

Beyond health risks, particulate matter also affects environmental conditions such as visibility, cloud condensation nuclei, and radiative forcing. PM is able to alter the light and solar radiation which reaches the Earth's surface (Kogan et al. 1997; Schulz et al. 2007). The ability of PM to absorb and reflect solar radiation alters the radiative forcing of the earth which may have consequences for global climate change. The fine portion of PM may also act as cloud condensation nuclei, enhancing cloud formation (Fitzgerald and Spyers-Duran 1973). Cloud formation can also indirectly affect radiative forcing as clouds reflect solar radiation (Ghan and Easter 2007; Kaufman 2007). Both the health and environmental effects of particulate matter are rationales for the USEPA regulations of ambient PM_{2.5}.

1.1.2 Sources of PM_{2.5}

Regulating concentrations of PM_{2.5} is harder than simply controlling emissions. Particulates are emitted directly into the atmosphere and formed in the atmosphere through secondary processes. Primary sources of particulate matter include emissions of organic and elemental carbon particulate from coal fired power plants, and automobile exhausts. Figure 1.1 contains the results from a source apportionment study of primary PM_{2.5} in Charlotte, NC (Office of Air Quality Planning and Standards Emissions, Monitoring, and Analysis Division USEPA). Coal combustion and mobile sources are the two largest sources followed by oil combustion which is indicative of industrial processing.

Many of the sources responsible for emitting primary particulate matter also emit volatile organic carbon gases (VOCs), which have the ability to react in the atmosphere with photochemically produced oxidants such as hydroxyl radicals (OH·) and nitrogen oxide (NO) as well as ozone (O₃). The products of these gas phase reactions have lower vapor pressures than the original precursor VOCs providing them the ability to be present in both the gas and particle phase through thermodynamic partitioning. When oxidized products partition to the particle phase or self-nucleate

the aerosol mass is called secondary organic aerosols (SOA). Sources of VOCs are not limited to anthropogenic processes such as those named above but also include biogenic sources. Biogenic VOCs are emitted from vegetation and are comprised of several classes including isoprene (C_5H_{10}), monoterpenes ($C_{10}H_{16}$), sesquiterpenes ($C_{15}H_{24}$) and oxygenated terpenes (e.g., $C_{10}H_{18}O$, $C_{10}H_{12}O$). The average total mixing ratio of ambient terpenes has been measured to be as high as 0.5 ppm (Sakulyanontvittaya, 2007). Of the biogenic VOCs the monoterpenes are largest contributors to atmospheric concentrations of SOA. Lathiere et al. (2006) estimated the total monoterpene emissions to be approximately 117 Tg of carbon per year which is ~16% of the total biogenic emissions. The monoterpenes include Δ^3 -carene, *d*-limonene, myrcene, α -pinene, β -pinene, sabinene, camphene, β -phellandrene, α -thujene, terpinolene, α -terpinene, γ -terpinene, ρ -cymene, and ocimene. The structure of the terpene varies by plant species, as does the emission rates. The atmospheric concentrations and the subsequent aerosol yields also vary by terpene.

Ambient aerosols are composed of both anthropogenic and biogenically derived SOA, primary particulates as well as inorganic compounds and elemental components. Figures 1.2a and 1.2b provide a chemical characterization of ambient aerosols collected from Queens, NY (Drewnick et al. 2004) and Houston, TX (Russell et al. 2004) respectively. The aerosol characterizations highlight the significant concentrations of both organic carbon and inorganic species in both cities. Although aerosol compositions vary from city to city the relative concentrations of organic carbon to inorganic compounds is expected to be similar. The organic fraction of ambient aerosols is composed of both biogenic and anthropogenic fractions. Measuring the biogenic fraction of ambient aerosols is vital because natural sources create the background concentrations of ambient particulate matter and can influence anthropogenic PM regulations. Carbon dating techniques have been used to deduce the fraction of biogenic SOA from the total organic mass of ambient aerosols. Anthropogenic carbon has an older carbon date than biogenic carbon. In Zurich, during the summer when biogenic emissions are at a maximum, Szidat et al. (2006) determined the biogenic fraction of aerosols with an maximum

aerodynamic diameter of 10 μ m (PM10) to be as much as 60% while fossil fuels contributed 30% of the organic carbon fraction throughout the year. Lewis et al. (2004) reported that 60-71% of the PM2.5 organic fraction of ambient aerosols collected near Nashville, TN during a summer investigation was of biogenic origin. Such large fractions of biogenic carbon present in ambient aerosols indicate the importance of biogenic VOCs in modeling atmospheric organic aerosols in both urban and remote areas.

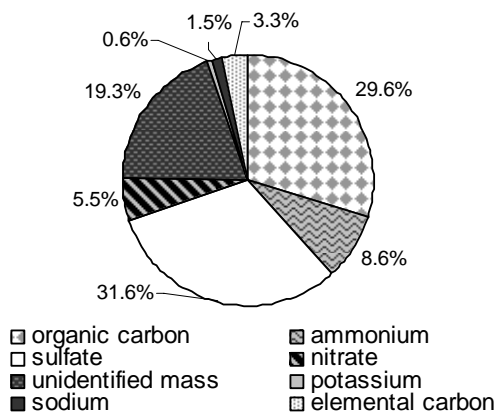


Figure 1.2a, Average daily PM2.5 aerosol composition in Queens, NY Drewnick et al, 2004a.

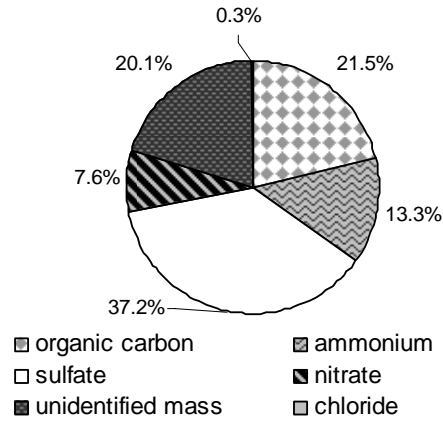


Figure 1.2b, Average daily PM2.5 aerosol composition in Houston TX Russell et al, 2004.

1.1.2.1 SOA Formation from Thermodynamic Partitioning

The oxidized products from both biogenic and anthropogenic VOCs both partition to pre-existing aerosols and also self nucleate. Partitioning is a thermodynamically governed process which determines how much of a gas phase compound becomes incorporated into a liquid aerosol phase. The equilibrium is described by an absorptive thermodynamic partitioning coefficient ($K_{om,i}$) derived by Pankow (1994). Equation 1.1 provides a mathematical description of the expected ratio of gas phase to aerosol phase concentrations.

$$K_{om,i} = \frac{7.501RTf_{om}^i}{10^9 MW_{om}^i \gamma_{om}^i p_L^0} = \frac{C_{aerosol}}{C_{gas}} \quad (\text{m}^3/\mu\text{g}) \quad (1.1)$$

R is the ideal gas phase constant (8.314 J/mol K), T is the temperature, f_{om} is the fraction of organic matter present in the aerosol, MW_{om} is the average molecular weight of the aerosol phase organic matter, γ_{om}^i is the activity coefficient of the organic phase and p_L^0 is the saturated vapor pressure of

compound *i*. The absorptive partitioning coefficient is inversely proportional to the saturated vapor pressure of the compound of interest. Thus compounds with high vapor pressures have smaller partitioning coefficients, and compounds with lower vapor pressures have higher partitioning coefficients.

Thermodynamic partitioning theory describes the absorption of a molecule into a liquid particle, and assumes that once a product partitions it remains as a monomer and no further reactions occur in the particle phase. The assumption of no further reactions has been used to model the formation of ambient SOA mass (Chen and Griffin 2005; Griffin et al. 2005; Jenkin 2004; Pun et al. 2002). Atmospheric particulate models are used by the USEPA to be able to estimate how changes to emission regulations will affect the ambient aerosol load, with the goal of improving human health. One flaw in the sole use of thermodynamic partitioning to describe aerosol formation is that it excludes formation of SOA mass from other processes, which may cause underestimations, as well as failure to properly identify possible trends leading to increased aerosol mass. Particle phase reactions have been shown to be an additional process leading to SOA mass formation. Recent studies our lab (Jang et al. 2002; Jang et al. 2003; Jang et al. 2004; Northcross and Jang 2007), have shown that the concentration of aerosol mass formed through secondary processes is affected by the presence of inorganic aerosols. A better understanding of the processes occurring in mixed aerosols will allow atmospheric aerosol models to predict aerosol formation under conditions similar which are more representative of atmospheric conditions.

1.1.2.2 SOA Formation from Heterogeneous Reactions

Particle phase reactions have been hypothesized to occur through the carbonyl structures present on many of the organic oxidized products which partition to aerosols. Particle phase reactions have been shown to form oligomers (Kalberer et al. 2004; Tolocka et al. 2004) and organic sulfates (Iinuma et al. 2007; Liggió and Li 2006; Romero and Oehme 2005; Surratt et al. 2007). The formation of organic sulfates within atmospheric aerosols is a very new discovery; quantification and formation process are still being determined, organic sulfates are not considered in the research

presented here. Examples of the particle phase reactions responsible for oligomer formation may consist of but may not be limited to hydration, acetal/hemi-acetal formation, trioxane formation, adol condensation, and oligomer formation. The products have many names in the literature (humic like substances (HULIS), oligomers, polymers, and high MW structures); however they, all refer to the same processes and will be called oligomers in this work.

Particle phase reactions are catalyzed by the presence of inorganic acidity. Under acidic conditions free protons are able to protonate carbonyl species. Protonated carbonyls react more readily with hydrates, unprotonated carbonyls, water, and alcohols than carbonyls in their unprotonated form. Thus, acid acts as a catalyst and increases oligomer formation and SOA yields. Figure 1.3 shows hypothesized mechanisms for acid catalyzed heterogeneous reactions. Once organic carbonyls are transformed by particle phase reactions the previously formed thermodynamic equilibrium established between the aerosol and the gas phase is disturbed. Thus, the oxidized

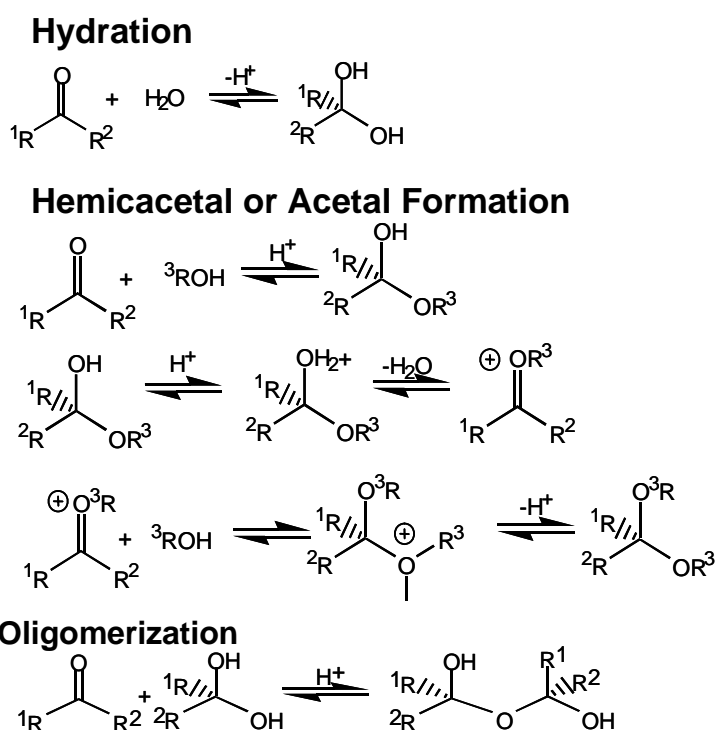


Figure 1.3 Hypothesized reaction mechanisms for acid catalyzed heterogeneous reactions

products continue to partition to the aerosol to compensate for the disturbance to the equilibrium aerosol concentrations. This process does not occur indefinitely. Increased oligomer formation changes the aerosol phase from a liquid phase to a more solid-like aerosol. The physical changes in aerosol affect the partitioning coefficient by altering the solubility of partitioning organics, and increasing the average molecular weight of the aerosol media.

Also, the formation of organic sulfate may lower the particle acidity also reducing oligomer formation.

It is important to note that oligomers are not formed exclusively in SOA created in the presence of inorganic aerosols. Kalberer et al. (2004) and other researchers have reported the presence of oligomers in aerosols created in smog chambers in the absence of inorganic seed aerosol. The formation of oligomers in the presence of inorganic aerosols is enhanced, and acidic conditions have larger SOA yields than neutral conditions (Czoschke et al. 2003; Jang et al. 2004; Northcross and Jang 2007).

Identification of oligomers in aerosols has been achieved by researchers (Gao et al. 2004; Gross et al. 2006; Bahreini et al. 2005). Tolocka et al. (2004) measured oligomers using MALDI mass spectrometry in SOA created from α -pinene ozonolysis in the presence of acidic seed aerosol. A repeating peak pattern containing molecular weights much higher than any of the expected products of α -pinene with ozone was reported. This pattern was typical of oligomers. Iinuma et al. (2004) showed a 40% increase in particle phase organics when α -pinene was reacted with ozone in the presence of preexisting acidic inorganic aerosols emphasizing the effect of an acid catalyst on heterogeneous reactions.

Studies of ambient aerosols have also shown oligomer presence. The characterization of ambient aerosol from the south-eastern United States by Zhang et al. (2006) showed an 18% increase in ambient aerosol mass when acidity, measured as the ratio of $\text{NH}_4^+/\text{SO}_4^{2-}$, increased. It is suggested that the increase in aerosol mass by aerosol acidity is due to acid catalyzed heterogeneous aerosol reactions. Brock et al. (2003) and Chu (2004) both measured increases in aerosol mass within air parcels at higher sulfuric acid and VOC concentrations. More direct evidence has been reported by Kiss et al. (2002) and Krivacsy et al. (2001) who measured an oligomeric fraction of the ambient aerosols comprising as much as 30%.

Field studies which evaluate the influence of particle acidity on SOA formation are extremely complicated due to interference from various factors such as light, emission profiles, meteorology, and changes in VOC compositions. In general, the trends of the relationships between acidity and aerosol mass have been shown by researchers. However, the specific responses of aerosol mass to the many variables present in the environment are not known. Thus, laboratory studies are necessary to systematically examine the effects of changing parameters and atmospheric environments on aerosols under controlled conditions.

1.2 Motivation

The formation of organic oligomers within SOA may alter the current explanation of the SOA atmospheric processes. The radiative balance of solar radiation may be very different for aerosol containing oligomers. Misclassifications of aerosol composition may also affect global climate change model results. Atmospheric aerosol concentrations are also modeled on the urban and regional scale. Currently in regional models inorganic and organic aerosol mass is modeled separately assuming that the no interaction occurs between the two groups. This assumption may not accurately represent the processes occurring by atmospheric aerosols. The formation of oligomers by acid catalyzed particle phase reactions within aerosols is a prime example of interaction between the inorganic and organic constituents of the aerosols. Ignoring this process may cause an underestimation of the total atmospheric mass predicted by aerosol models. Also important relationships between emitted gases and SOA mass formation may not be fully defined.

The description of how particles cause adverse health effects is strongly dependent on an accurate characterization of the chemical and physical processes of the particles. Because secondary organic aerosols have been assumed to be composed of monomers the current understanding of the interaction between particles and health effects is based on an inaccurate model. Particle phase reactions may influence change our understanding of the mechanism of injury.

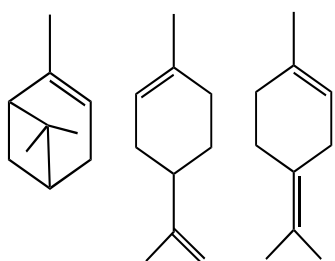
1.3 Objective

This dissertation aims to study oligomer formation in SOA from monoterpenes in the presence of inorganic aerosols through laboratory experimentation and by the use of mathematical models in order to better understand the formation of oligomers in particles by acid catalyzed particle phase reactions due to the presence of inorganic aerosols.

1.4 Project description

This study is divided into three separate studies which are presented in Chapters 2-4. The first study focused on quantifying the increase in aerosol mass formed by the ozonolysis of monoterpenes in the presence of inorganic aerosols. The second study developed a method using thermal gravimetric analysis to quantify the fraction of oligomer mass in aerosols samples of SOA and inorganic aerosols. The third study developed the modeling framework to estimate the particle phase oligomer mass as well as the total SOA mass from terpene ozonolysis in the presence of inorganic aerosols.

In order to confirm that a measurable increase in aerosol yield was observed in the presence of inorganic acidity, and to be able to determine the relevant parameters need to accurately model SOA mass mathematically a series of smog chamber reactions were carried out. Six monoterpenes were reacted individually with ozone in the absence and presence of inorganic aerosols of varying acidities and relative humidities in a 2m³ indoor Teflon smog chamber. The results confirmed that under the most acidic conditions the aerosol mass formed for each terpene system was the highest and the mass decreased as acidity decreases. Also as seed mass increased so did the aerosol mass formed,



α -pinene d-limonene terpinolene
Figure 1.4. Molecular structures for terpenes used in modeling study

thus aerosol yield (Y) is not constant for each terpene, and also shows that seed mass is important in determining SOA formation. The study is further discussed in Chapter 2.

The results from the aerosol yield study were used to choose three terpenes for further analysis and modeling: α -

pinene, terpinolene and d-limonene (Figure 1.4). α -Pinene was chosen due to the large amount of literature available. Also α -pinene is typically used as a surrogate for the terpene class in atmospheric regional scale models SAPRC (Carter 2000) and CAM (Andreani-Aksoyoglu et al. 2003)) and is the most emitted terpene in the monoterpene class. d-Limonene is emitted from citrus trees and forms the largest fraction of the monoterpene derived SOA. Limonene is also used as a compound in many cleaning products; thus it has consequences for indoor aerosol concentrations as well. Terpinolene composes the largest fraction of tea tree oil and comes from the tea tree. It was included in the modeling study due to the molecular structure. Although ozonolysis at the exocyclic double bond which has the largest reactivity will cause the loss of three carbons leading to products with higher vapor pressure than α -pinene and limonene the aerosol yields formed are comparable. This suggests that oligomer formation may be larger in terpinolene than α -pinene and limonene.

In Chapter 3 a method developed to quantify the fraction of oligomers within an aerosol experimentally is presented. Thermal gravimetric analysis (TGA) utilizes temperature to understand the bulk phase composition of a sample. By compensating for effects of the inorganic seed, aerosol monomer mass is volatilized leaving the oligomer fraction of the aerosol remaining. This method represents the first approach to quantify the oligomeric fraction in SOA. The experimental results are compared with the modeling results and reveal a model which is able to estimate oligomer aerosol mass within 25% of the measured oligomeric fraction.

The SOA model development and validation study is contained in Chapter 4. Three models were needed to estimate SOA mass; a gas phase model, a thermodynamic aerosol partitioning model, and an acid catalyzed particle phase oligomer formation model. The gas phase model used was the master chemical mechanism (MCM) developed by Jenkin et al. (2004) at the University of Leeds in England. MCM utilizes structural reactivity relationships to determine the reaction mechanisms. It provides a near explicit product distribution which allows the analysis of the products to be approached from both ability to partition and oligomer forming potential. A mechanism for α -pinene

had previously been published and was used as published. The mechanisms for terpinolene and d-limonene were developed using the MCM protocol. The product distribution estimated by MCM is lumped based on a protocol of vapor pressure and reactivity. Aerosol mass for each representative lumped group is estimated using two models.

Jang et al. (2006) developed a method to estimate oligomer mass which incorporates the effects of seed mass, acidity, relative humidity, partitioning and particle phase reactivity. Oligomer mass is estimated for each lumped product group. The mass attributable to only thermodynamic partitioning is estimated using a modified version of the secondary organic aerosol model (SOGRAM) model developed by Schell et al. (2001) at the University of California at Davis. This model uses a mass balance approach where the oligomer mass and gas phase concentration are subtracted from the total product group formed with the remaining mass being the aerosol mass formed solely from thermodynamic partitioning. The eloquence of this approach is that it divides the aerosol mass into monomers and oligomers which may have different chemical and physical properties, as well as different health effects.

Conclusions are contained in Chapter 5 which provides a summary of results and highlights the interesting and important results of this research project.

1.5 References

Andreani-Aksoyoglu, S., Keller, J., Dommen, J., and Prevo, A. S. H. (2003). Modeling of air quality with CAMx: A case study in Switzerland. *Water, Air, & Soil Pollution: Focus*. 3: 281-296.

Bahreini, R., Keywood, M.D., Ng, N. L., Varutbangkul, V., Gao, S., Flagan, R. C., Seinfeld, J. H., Worsnop, D. R., and Jimenez, J. L. (2005). Measurements of secondary organic aerosol from oxidation of cycloalkenes, terpenes, and m-Xylene using an aerodyne aerosol mass spectrometer. *Environmental Science and Technology*. 39: 5674-5688.

Brock, C.A., Trainer, M., Ryerson, T.B., Neuman, J. A., Parrish, D.D., Holloway, J.S., Nicks, D.K., Frost, G.J., Huebler, G., Fehsenfeld, F.C., Wilson, J.C., Reeves, J. M., Lafleur, B.G., Hilbert, H., Atlas, E.L., Donnelly, S.G., Schauffler, S.M., Stroud, V.R., Wiedinmyer, C. (2003). Particle growth in urban and industrial plumes in Texas. *Journal of Geophysical Research [Atmospheres]*. 108:1-12.

Carter, W. P. L. 2000. Development and evaluation of the SAPRC-99 chemical mechanism. EPA/600/R-00/076, proceedings sixth US/Germany workshop on ozone/fine particle science, 1999.

Chen, J. and Griffin, R. J. (2005). Modeling secondary organic aerosol formation from oxidation of α -pinene, β -pinene, and d-limonene. *Atmospheric Environment*. 39: 7731-7744.

Chu, S.H. (2004) PM2.5 episodes as observed in the speciation trends network. *Atmospheric Environment*. 38: 5237-5246.

Czoschke, N.M., Jang, M., and Kamens, R.M. (2003). Effect of acidic seed on biogenic secondary organic aerosol growth. *Atmospheric Environment*. 37: 4287-4299.

Drewnick, F., Jayne, J.T., Canagaratna, M., Worsnop, D.R., and Demerjian, K.L. (2004). Measurement of ambient aerosol composition during the PMTACS-NY 2001 using an aerosol mass spectrometer. Part II: Chemically speciated mass distributions. *Aerosol Science and Technology*. 38: 104-117.

Fitzgerald, J.W. and Spyers-Duran, P.A. (1973). Changes in cloud nucleus concentration and cloud droplet size distribution associated with pollution from St. Louis. *Journal of Applied Meteorology* 12: 511-15.

Gao, S., Ng, N.L., Keywood, M., Varutbangkul, V., Bahreini, R., Nenes, A., He, J., Yoo, K.Y., Beauchamp, J.L., Hodyss, R.P., Flagan, R.C., and Seinfeld, J.H., 2004. Particle phase acidity and oligomer formation in secondary organic aerosol. *Environmental Science and Technology*. 38: 6582-9.

Ghan, S.J. and Easter, R.C. (2007). Impact of cloud-borne aerosol representation on aerosol direct and indirect effects. *Atmospheric Chemistry and Physics*. 6: 4163-4174.

Griffin, R.J., Dabdub, D., and Seinfeld, J.H. (2005). Development and initial evaluation of a dynamic species-resolved model for gas phase chemistry and size-resolved gas/particle partitioning associated with secondary organic aerosol formation. *Journal of Geophysical Research, [Atmospheres]*. 110: D05304-1-D05304/16.

Gross, D.S., Galli, M.E., Kalberer, M., Prevot, A.S.H., Dommen, J., Alfarra, M.R., Duplissy, J., Gaeggeler, K., Gascho, A., Metzger, A., and Baltensperger, U. (2006). Real-time measurement of oligomeric species in secondary organic aerosol with the aerosol time-of-flight mass spectrometer. *Anal. Chem.* 78:2130-37.

Iinuma, Y., Boge, O., Gnauk, T., and Herrmann, H. (2004). Aerosol-chamber study of the α -pinene/O₃ reaction: influence of particle acidity on aerosol yields and products. *Atmospheric Environment*. 38: 761-773.

Iinuma, Y., Mueller, C., Berndt, T., Boege, O., Claeys, M., and Herrmann, H. (2007). Evidence for the existence of organosulfates from β -Pinene ozonolysis in ambient secondary organic aerosol. *Environmental Science & Technology*. 41: 6678-6683.

Jang, M., Czoschke, N.M., and Northcross, A.L. (2004). Atmospheric organic aerosol production by heterogeneous acid-catalyzed reactions. *Chemphyschem* 5:1-16.

Jang, M.S., Czoschke, N.M., Lee, S., and Kamens R.M. (2002). Heterogeneous atmospheric aerosol production by acid-catalyzed particle-phase reactions. *Science* 298:814-817.

Jang, M., Lee, S., and Kamens, R.M. (2003). Organic aerosol growth by acid-catalyzed heterogeneous reactions of octanal in a flow reactor. *Atmospheric Environment*. 37: 2125-2138.

Jang, M., Czoschke, N.M., Northcross, A., Cao, G., 2006. SOA Formation from partitioning and heterogeneous reactions: model study in the presence of inorganic species. *Environmental Science and Technology*. 40:3013-22.

Jenkin, M.E. (2004). Modeling the formation and composition of secondary organic aerosol from α - and β -pinene ozonolysis using MCM v3. *Atmospheric Chemistry and Physics*. 4: 1741-1757.

Kalberer, M., Sax, M., and Samburova, V. (2006) Molecular size evolution of oligomers in organic aerosols collected in urban atmospheres and generated in a smog chamber. *Environmental Science and Technology*. 40:5917-5922.

- Kaufman, Y.J. (2007). Satellite observations of natural and anthropogenic aerosol effects on clouds and climate. *Space Science Reviews*. 125: 139-147.
- Kiss, G., Varga, B., Galambos, I., and Ganszky, I. (2002). Characterization of water-soluble organic matter isolated from atmospheric fine aerosol. *Journal of Geophysical Research, [Atmospheres]*. 107: ICC1-1-ICC1/8.
- Kogan, Z.N., Kogan, Y.L., and Lilly, D.K. (1997). Cloud factor and seasonality of the indirect effect of anthropogenic sulfate aerosols. *Journal of Geophysical Research, [Atmospheres]*. 102: 25927-25939.
- Krivacsy, Z., Gelencser, A., Kiss, G., Meszaros, E., Molnar, A., Hoffer, A., Meszaros, T., Sarvari, Z., Temesi, D., Varga, B., Baltensperger, U., Nyeki, S., and Weingartner, E. (2001). Study on the chemical character of water soluble organic compounds in fine atmospheric aerosol at the Jungfraujoch. *Journal of Atmospheric Chemistry*. 39: 235-259.
- Laden F.N.L., Dockery D.W., and Schwartz J. (2000). Association of fine particulate matter from different sources with daily mortality in six US cities. *Environmental Health Perspectives* 108:941-947.
- Lathiere, J., Hauglustaine, D.A., Friend, A.D., De Noblet-Ducoudre, N., Viovy, N., and Folberth, G.A. (2006). Impact of climate variability and land use changes on global biogenic volatile organic compound emissions. *Atmospheric Chemistry and Physics*. 6: 2129-2146.
- Lewis, C.W., Klouda, G.A., and Ellenson, W.D. (2004). Radiocarbon measurement of the biogenic contribution to summertime PM-2.5 ambient aerosol in Nashville, TN. *Atmospheric Environment*. 38: 6053-6061.
- Liggio, J. and Li, S.M. (2006). Organosulfate formation during the uptake of pinonaldehyde on acidic sulfate aerosols. *Geophysical Research Letters* . 33: L13808-1-L13808/4.
- Neuberger, M., Schimek, M.G., Horak, F., Moshhammer, H., Kundi, M., Frischer, T., Gomiscek B., Puxbaum, H., and Hauck H. (2004). Acute effects of particulate matter on respiratory diseases, symptoms and functions: epidemiological results of the Austrian Project on Health Effects of Particulate Matter (AUPHEP). *Atmospheric Environment* 38:3971-3981.
- Northcross, A.L. and Jang, M. (2007). Heterogeneous SOA yield from ozonolysis of monoterpenes in the presence of inorganic acid. *Atmospheric Environment*. 41: 1483-1493.
- Pankow, J.F. (1994). An absorption-model of gas-particle partitioning of organic-compounds in the atmosphere. *Atmospheric Environment* 28:185-188.

Pope, C.A., Hansen, M.L., Long, R.W., Nielsen, K.R., Eatough, N.L., Wilson, W.E., and Eatough, D.J. (2004). Ambient particulate air pollution, heart rate variability, and blood markers of inflammation in a panel of elderly subjects. *Environmental Health Perspectives*. 112:339-345.

Pun, B. K., Griffin, R.J., Seigneur, C., and Seinfeld, J.H. (2002). Secondary organic aerosol 2. Thermodynamic model for gas/particle partitioning of molecular constituents. *Journal of Geophysical Research, [Atmospheres]*. 107: AAC4-1-AAC4/15.

Romero, F. and Oehme, M. (2005). Organosulfates - A New component of humic-like substances in atmospheric aerosols? *Journal of Atmospheric Chemistry*. 52: 283-294.

Russell, M., Allen, D.T., Collins, D.R., and Fraser, M.P. (2004). Daily, seasonal, and spatial trends in PM_{2.5} mass and composition in southeast Texas. *Aerosol Science and Technology*. 38: 14-26.

Sakulyanontvittaya T., Duhl T., Wiedinmyer C., Helmig D., Matsunaga S., Potosnak M., Milford J., and Guenther A. (2007) Monoterpene and sesquiterpene emission estimates for the United States. *Environmental Science and Technology*, es-2007-02274e.R1.

Schell, B., Ackermann, I.J., Hass, H., Binkowski, F.S., Ebel, A. (2001) Modeling the formation of secondary organic aerosol within a comprehensive air quality model system. *Journal of Geophysical Research, [Atmospheres]*. 106, p. 28275-93.

Schulz, M., Textor, C., Kinne, S., Balkanski, Y., Bauer, S., Bernsten, T., Berglen, T., Boucher, O., Dentener, F., Guibert, S., Isaksen, I. S. A., Iversen, T., Koch, D., Kirkevåg, A., Liu, X., Montanaro, V., Myhre, G., Penner, J. E., Pitari, G., Reddy, S., Seland, O., Stier, P., and Takemura, T. (2007). Radiative forcing by aerosols as derived from the AeroCom present-day and pre-industrial simulations. *Atmospheric Chemistry and Physics*. 6:5225-5246.

Surratt, J.D., Kroll, J.H., Kleindienst, T. E., Edney, E.O., Claeys, M., Sorooshian, A., Ng, N.L., Offenberg, J.H., Lewandowski, M., Jaoui, M., Flagan, R.C., and Seinfeld, J.H. (2007). Evidence for organosulfates in secondary organic aerosol. *Environmental Science & Technology*. 41:517-527.

Szidat, S., Jenk, T.M., Synal, H.A., Kalberer, M., Wacker, L., Hajdas, I., Kasper-Giebl, A., and Baltensperger, U. (2006). Contributions of fossil fuel, biomass-burning, and biogenic emissions to carbonaceous aerosols in Zurich as traced by ¹⁴C. *Journal of Geophysical Research, [Atmospheres]*. 111: D07206-1-D07206/12.

Tolocka, M. P., Jang, M., Ginter, J. M., Kamens, R. M., and Johnston, M. V. (2004). Formation of oligomers in secondary organic aerosol. *Environmental Science and Technology* 38:1428-1434.

Zhang et al. 2006 (AAAR International Aerosol Conference).

Chapter 2

Heterogeneous SOA Yield from Ozonolysis of Monoterpenes in the Presence of Inorganic Acid

Amanda L. Northcross and Myoseon Jang*

* Department of Environmental Sciences and Engineering

CB# 7431, Rosenau Hall, The University of North Carolina at Chapel Hill

Chapel Hill, North Carolina, 27599

Tel: 919-966-9010, Fax: 919-966-7911

email: mjang@email.unc.edu

Published in Atmospheric Environment
41 (2007) 1483–1493

ABSTRACT

The secondary organic aerosol (SOA) yield of a series of monoterpenes was investigated to determine the relative amounts of organic mass which can be attributed to mass produced by heterogeneous acid catalyzed reactions. Five monoterpenes (α -pinene, terpinolene, d-limonene, Δ^2 -carene, β -pinene) were studied using a 2m³ indoor Teflon chamber and SOA was created in the presence of both acidic and neutral inorganic seed aerosol. The relative humidity was varied to create differing acidic seed environments. The heterogeneous aerosol production was influenced by the seed mass concentration, the acidity of the inorganic seed aerosol, and also molecular structure of the monoterpene ozonolysis products. This study also can be incorporated with our previously presented model of the kinetic expression for SOA mass production from heterogeneous acid catalyzed reactions.

Keywords: Monoterpenes, SOA, Heterogeneous Reactions, Acid Catalyst, Ozonolysis

2.1. Introduction

Terpenes are ever-present atmospheric organic compounds of biogenic origin (Rasmussen 1972), which are susceptible to oxidation by OH radicals, as well as ozone in the atmosphere because of the unsaturated carbon-carbon double bonds present in these compounds (Atkinson and Arey 2003; Calogirou et al. 1999; Hakola et al. 1994). Due to the large amounts of biogenics emitted into the atmosphere (Müeller 1992; Guenther 1995), the secondary organic aerosol (SOA) burden on the total organic aerosol mass may be significant (Andreae and Crutzen 1997).

The formation of SOA has often been attributed to the partitioning of oxidation products of a VOC to existing aerosols (Colville and Griffin 2004; Griffin et al. 1999; Kamens et al. 1999; Odum et al. 1996) and to a lesser extent, from the new particle formation *via* nucleation of oxidation products (Kavouras and Stephanou 2002). Recently aerosol growth through particle phase heterogeneous reactions has been proposed (Gao et al. 2004; Jang et al. 2006; Jang and Kamens 2001; Kalberer et al. 2004; Tolocka et al. 2004) as another pathway for the formation of SOA. Atmospheric acidic particle surfaces can accelerate heterogeneous reactions of secondary organic products created from the gas-phase oxidation reactions of reactive volatile organic carbons (VOCs). Atmospheric particles have been measured to have pH values as low as 0.25 (Pathak et al. 2004), which falls within the range of particle acidity used to study acid catalyzed heterogeneous reactions. Thus it is extremely important to understand the contributions of heterogeneous acid catalyzed reactions on SOA flux, as the occurrence of these reactions in the atmosphere is accelerated due to the acidity of atmospheric particles.

This study aims to further our understanding of the aerosol yield increases by heterogeneous acid catalyzed reactions through determining how this increase varies with the initial terpene structure. Terpenes, which produce products that are more reactive for heterogeneous reactions in aerosols, should have higher increases in SOA when in the presence of acidic seed as compared to neutral seed as acid acts a catalyst increasing oligomer formation (Jang et al. 2002; Czoschke et al. 2003).

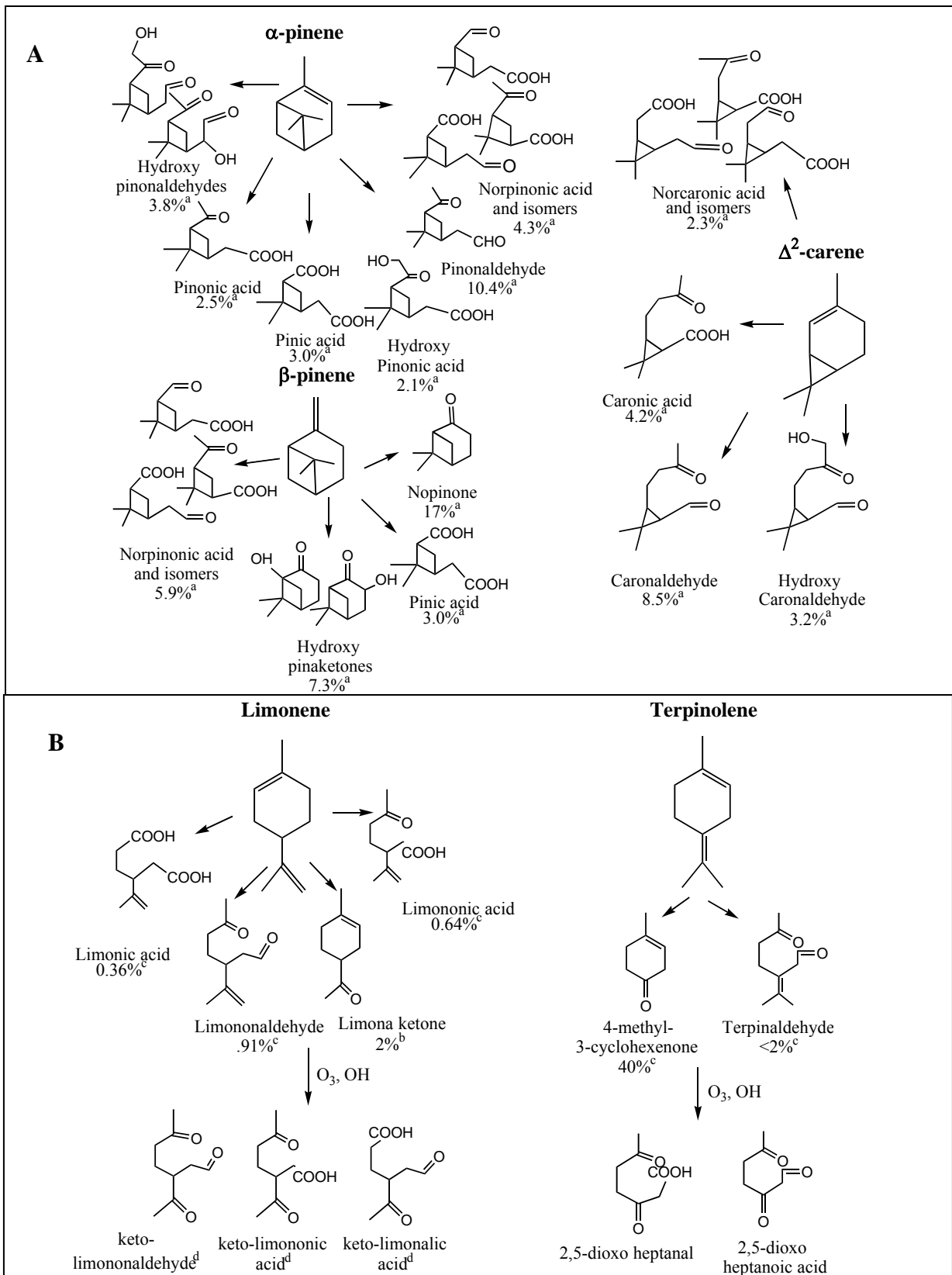
The major goals of this study were threefold: 1) investigate the relationship between the molecular structures of a series of monoterpenes that took place in ozonolysis reactions and the subsequent SOA yield due to heterogeneous acid catalyzed reactions; 2) determine the influences of preexisting seed aerosols on SOA yields; and 3) quantify the SOA yield increase for various monoterpenes at a range of different humidities and acidities of seed aerosols.

2.2. Experimental Section

The SOA yield study was carried out in an indoor 2.16 m³ chamber constructed of Teflon. All experiments were conducted in the dark to prevent photochemical reactions of VOCs. The chamber was filled with clean air from two clean air generators: a Whatman FT-IR purge gas generator (model 75-52) and an Aadco 737 pure air generator. The percent relative humidity (%RH) was controlled by bubbling clean air through distilled water and was measured by a Hanna instruments thermo hygrometer HI 9160C, which was also used to measure temperature. Seed aerosol was generated using a TSI constant output Atomizer model 3076. The acidic seed solution was composed of a 2:3 volume ratio of H₂SO₄ to NH₄HSO₄ of 0.01M aqueous solutions. The neutral seed solution was composed of a 1:1 volume ratio of 0.01M (NH₄)₂SO₄ solution to H₂O. The particle concentration and population was monitored by a TSI scanning mobility particle sizer (SMPS) (Model 3080) in series with a TSI condensation nuclei counter (CNC) (Model, 3025A). The scanning time of aerosol through the internal plumbing column of the SMPS was three minutes with a sheath flow rate of 2 L/min. The SMPS measured particle size data over a size range of 20 nm to 835 nm.

Ozone was added to the chamber by passing clean air past a Jelight UV lamp model 600, before entering the chamber. Ozone levels were measured using a Thermo Electron Instruments UV Photometric O₃ analyzer model 49. The terpenes used in this investigation are shown in Figures 2.1A and 2.1B, they were purchased from Sigma Aldrich with a purity of >98%. The terpenes were injected into the chamber by volatilization using a gentle stream of clean air through a heated

manifold. The concentration of terpene in the chamber was measured using a gas chromatograph with a flame ionization detector. Table 2.1 tabulates the experimental conditions used for the experimental data presented here. More detailed information about the experimental methods is contained in Appendix A.



ROG	[ROG] ($\mu\text{g}/\text{m}^3$)	initial $[\text{O}_3]^a$ (ppm)	%RH	[initial seed] ($\mu\text{g}/\text{m}^3$)	\bar{Y}_{acid}^c 20% RH	$\bar{Y}_{neutral}^d$ 20% RH	\bar{Y}_{acid}^c 40% RH	$\bar{Y}_{neutral}^d$ 40% RH
α -pinene ^b	325(avg.)	0.22	16-19	125-443	n.a.	n.a.	n.a.	n.a.
α -pinene	995.4	0.34-0.43	22-53	91-226	0.23 \pm 0.032	0.14 \pm 0.008	0.22 \pm 0.017	0.13 \pm 0.006
β -pinene	995.4	0.32-0.59	21-48	109-207	0.14 \pm 0.013	0.10 \pm 0.027	0.11 \pm 0.016	0.14 \pm 0.007
Δ 2-carene	497.7	0.32-0.48	21-46	102-310	0.46 \pm 0.001	0.25 \pm 0.001	0.35 \pm 0.054	0.30 \pm 0.015
terpinolene	697.8	0.31-0.45	19-46	180-181	0.44 \pm 0.013	0.25 \pm 0.005	0.37 ^e	0.33 \pm 0.073
d-limonene	697.8	0.30-0.49	20-48	73-183	0.49 \pm 0.054	0.36 \pm 0.095	0.55 \pm 0.04	0.49 \pm 0.061

Table 2.1. Experimental Conditions and average SOA yields for neutral ($\bar{Y}_{neutral}$) and acidic seed (\bar{Y}_{acid}) experiments at 20% and 40% RH. [ROG] is the mass concentration of reactive oxygenated gas (terpene) reacted.

a: Initial ozone concentrations.

b: α -pinene data used to determine relationship between seed mass and aerosol yield. Figure 2.2.

c. Average Y of acidic seed experiments for a given relative humidity.

d. Average Y of neutral seed experiments for a given relative humidity.

e. One experiment was conducted

n.a.: not applicable

2.3. Results and Discussion

2.3.1 Aerosol yields

The most common way to determine the SOA yield has been defined by Odum et al. (1996) as, $Y = \Delta M / \Delta HC$ measuring the change in aerosol mass ΔM ($\mu\text{g}/\text{m}^3$) and dividing by the amount of hydrocarbons reacted ΔHC ($\mu\text{g}/\text{m}^3$). In our study, the SOA yields for the neutral particles are consistent with yields from previous studies (Grosjean et al. 1993; Hakola et al. 1994; Keywood et al. 2004) where reactions were conducted under excess ozone conditions. In this study the highest yield in the neutral system was limonene followed in order by terpinolene, Δ^2 -carene, α -pinene, and β -pinene (Table 2.1). This order was consistent at both 20%RH and 40%RH showing that the partitioning processes were similar at the various %RH in systems where heterogeneous reactions are not acid-catalyzed. The neutral seeded experiments are used as a standard to measure effects of particle acidity on SOA formation in acidic seeded experiments.

In order to investigate the aerosol mass contribution from acid catalyzed heterogeneous reactions, we define the heterogeneous acid catalyzed yield aerosol yield (ΔY^*), equation 2.1.

$$\Delta Y^* = \frac{Y_{acid} - \bar{Y}_{neutral}}{M_{seed_acid}} \quad (2.1)$$

where Y_{acid} is the aerosol yield in the acidic system and $\bar{Y}_{neutral}$ is the average aerosol yield in the neutral system. ΔY^* is calculated by dividing the difference between Y_{acid} and $\bar{Y}_{neutral}$ for each terpene system by the amount of acidic seed aerosol (M_{seed_acid}) ($\mu\text{g}/\text{m}^3$) present at the beginning of the experiment, at a given %RH and terpene. This difference of yields can be used to estimate the SOA mass increase (OM_{H-A}) due to heterogeneous acid catalyzed reactions (Jang et al 2006). Mass formed by heterogeneous reactions can also take place in neutral inorganic seeded experiments (Jonsson et al 2006; Kalberer et al. 2004; Tolocka et al. 2004), to a lesser extent. Our focus in this study, is to

quantify the additional yield increase due to the presence of acid, so heterogeneous reactions without an acid catalyst are not included in ΔY^* .

Unlike the common method for reporting SOA yield (Y), ΔY^* (equation 2.1) contains a normalization of the acid/neutral yield difference by M_{seed_acid} . The normalization is required to compensate for experimental differences in seed mass. Higher concentrations of M_{seed_acid} at a given humidity and seed composition increases the amount of available protons. This study shows that the amount of heterogeneous acid catalyzed mass formed is dependant on acidity as well as M_{seed_acid} . In Figure 2.2 as the M_{seed_acid} increases the SOA yield increases despite the fact the ozone and terpene (α -pinene) concentrations are held constant.

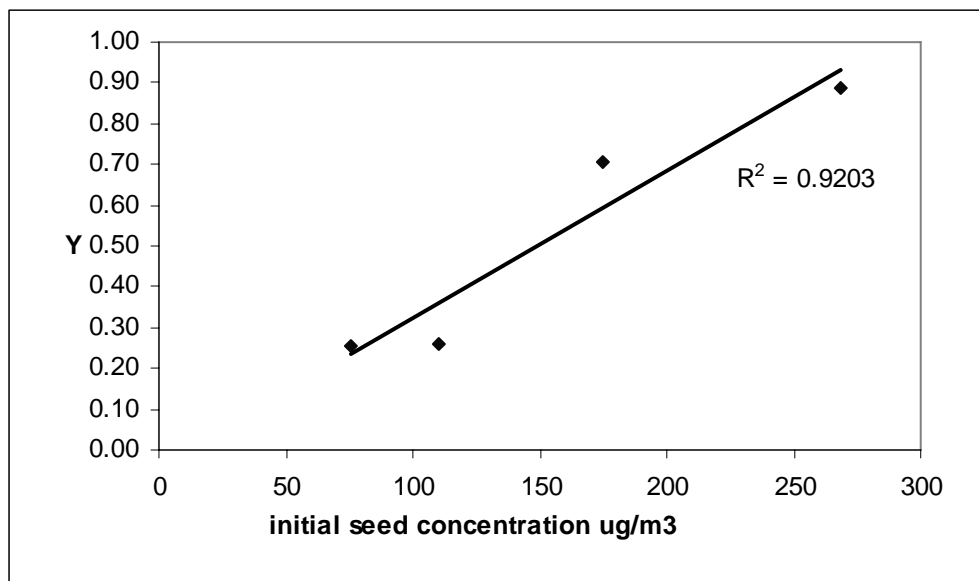


Figure 2.2 SOA aerosol yield (Y) from ozonolysis of α -pinene in the presence of inorganic acidic seed aerosol vs. inorganic seed aerosol mass (M_{seed_acid}). $Y = \Delta M / \Delta HC$ measuring the change in aerosol mass ΔM ($\mu\text{g}/\text{m}^3$) and dividing by the amount of hydrocarbons reacted ΔHC ($\mu\text{g}/\text{m}^3$). %RH = 16-19 and temperature = 297 K.

In order to have an accurate comparison between acidic and neutral seeded experiments the inorganic seed particles should be liquid. Thus, we have chosen to use the yield of neutral seeded experiments at %RH = 40 for all calculations using equation 2.1 to ensure that the neutral seed is liquid: the efflorescence point of ammonium sulfate is 34%RH (Wise et al. 2005). All acidic seed systems are liquid in our experimental conditions.

The concentrations for ozone and the initial terpene are held constant for both non-acidic and acidic experiments allowing comparison of the yields between the neutral and the acidic environments without large variation in either the gas phase oxidation reactions or the composition of secondary products. Increased %RH may lead to variations in the product distribution for products formed through the stabilized Criegee Intermediate (CI) reactions with water (Jonsson et al. 2006). Products formed through the CI include aldehydes, ketones and organic acids and their formation may be influenced by higher %RH (Calvert et al. 2000). The difference in products formed at different relative humidities may cause an underestimation of the enhanced yield formation due to the presence of acid catalyzed reactions.

2.3.2 Acidity and Inorganic Aerosols

Seed particle acidity can be quantified using the mass percent of proton concentration, $[H^+]_{\text{mass\%}}$ which is estimated using an inorganic thermodynamic computational algorithm (e.g., ISORROPIA Nenes et al. 1998). The variation in the seed particle acidity with respect to H_2SO_4 can also be described using excess acidity (X), as expressed in our previous studies (Jang et al. 2006; Jang et al. 2002). Both X and the $[H^+]_{\text{mass\%}}$ describes the effect of acidity in different ways.

X describes the ability of a weak base (e.g., carbonyl) to be protonated by a strong acid, and takes into consideration the non-ideality of the system due to non-dilute conditions. The focus of X is the activity coefficient of the protonated carbonyl, which becomes an intermediate species in the acid catalyzed heterogeneous reaction in the formation of oligomers. In comparison pH assumes an activity of 1 (ideal conditions) for the proton. The inorganic seed aerosols in this study have a small water concentration possibly causing non-ideal conditions, thus both X and $[H^+]_{\text{mass\%}}$ are needed to fully describe the particle acidity.

2.3.3 Acidity Effect on SOA Yields

All terpenes tested had a higher yield for the acidic seeded experiments in comparison to the neutral seeded experiments at 20% RH and 21-26°C (Table 2.1). The additional mass formed in the experiments using acidic seed can be attributed to acid catalyzed heterogeneous reactions. Similar to

previous studies (Czoschke et al. 2003; Jang et al. 2006) the yield of the acidic seed experiments was largest for the most acidic seed aerosol.

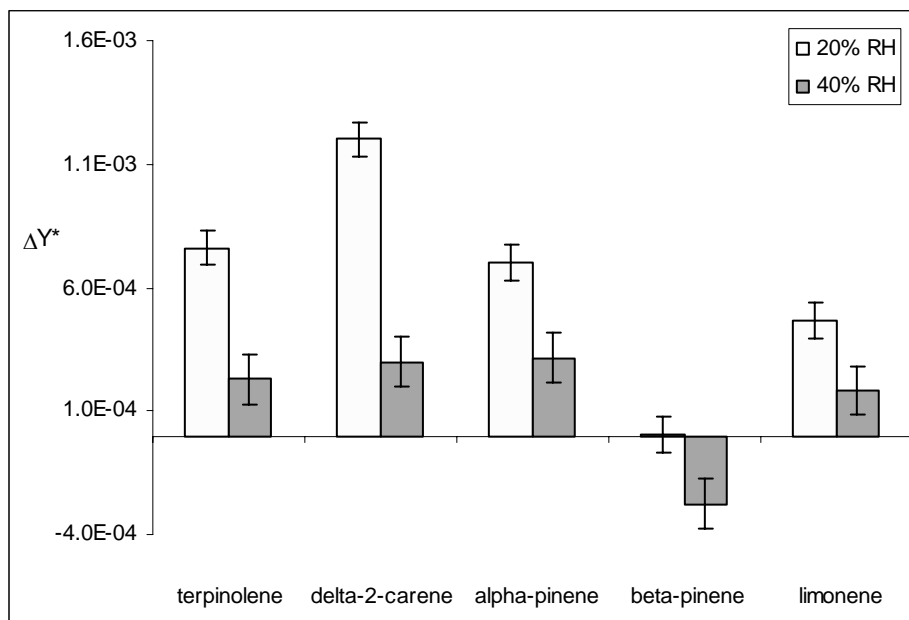


Figure 2.3. Normalized SOA yield difference (ΔY^*) between acid and neutral at %RH = 20 and 40.

$$\Delta Y^* = \frac{Y_{acid} - \bar{Y}_{neutral}}{M_{seed_acid}}$$
, where Y_{acid} is the SOA yield with acidic seed and $\bar{Y}_{neutral}$ is the average SOA yield with neutral seed at %RH = 40. Errors were calculated using standard deviation from experimental SOA data.

Figure 2.3 shows the ΔY^* resulting from differences in OM_{H-A} production for the studied terpenes at differing %RH. Larger values for ΔY^* indicate that more mass is being produced from heterogeneous acid catalyzed reactions. The values for ΔY^* were different for each system. At 20 %RH, the Δ^2 -carene system produced the most mass from acid catalyzed heterogeneous reactions followed in order by terpinolene, α -pinene, d-limonene and lastly β -pinene. The amount of acid catalyzed heterogeneous SOA produced at 40 %RH was less than that at 20 %RH. β -Pinene has a negative ΔY^* value. A possible explanation for the negative value of β -pinene has not been determined.

ΔY^* for Δ^2 -carene, terpinolene, and α -pinene are very close in value at 40 %RH. At more acidic conditions (20 %RH) the terpenes produce differing amounts of OM_{H-A} suggesting that for weakly acidic aerosols the acid catalyst effect is more dependent on the acidity and not strongly dependent on the structure of the partitioned product (see Section 2.3.4). This result could possibly

be important on aerosol models. The answer to the question- Should heterogeneous acid catalyzed reactions be included in aerosol models?- is not a direct yes or no answer, but may depend on the acidity of the particles.

The high acidity results are also supported by the work of Jang et al. (2005) which showed that SOA yield attributed to heterogeneous acid catalyzed reactions (ΔY^*) is proportional to the apparent reaction rate constant for oligomerization through polyacetal formation and aldol condensation. The rate of formation for heterogeneous yields occurs through a second order reaction expressed as $\Delta Y^* = \sum k'_{app,i} t [B_i] / (1 + \sum k'_{app,i} t [B_i])$, where t is time, $[B_i]$ is the concentration of the various oxidation products and k'_{app} is the rate constant. We have assumed that the $\log(\Delta Y^*)$ is directly proportional to the $\log(k'_{app})$. This assumption is only valid when the \log of the denominator varies much less with acidity than the \log of the numerator. This is a reasonable assumption under these experimental conditions. The rate constant (k'_{app}) for compound i as shown in equation 2.2, is dependant on X and the concentration of the proton (C_{H^+}) (Jang et al. 2005; Jang et al. 2006).

$$\log k'_{app,i} = \log(K_{hyd}/K_{BH^+}) + m' m^* X + \log C_{H^+} + \log a_w \quad (2.2)$$

Three of the terms in equation 2.2, C_{H^+} , X , and a_w , are associated with the inorganic seed aerosol and the relative humidity. These environmental terms are fixed for given experimental conditions, while K_{hyd} and K_{BH^+} depend on the gas phase oxidation product (i). The protonation equilibrium constant (K_{BH^+}) of a simple base (B) is commonly given by, where a_B , a_{BH^+} , and a_{H^+} are the activity of the base (B), protonated base (BH^+), and proton (H^+) in a given inorganic medium.

$$K_{BH^+} = \frac{a_B a_{H^+}}{a_{BH^+}} \quad (2.3)$$

The hydration equilibrium constant (K_{hyd}) of a carbonyl is described by $K_{hyd} = a_{hydrate} / (a_B a_w)$ where $a_{hydrate}$, a_B and a_w are the activities of a hydrate, a carbonyl, and water. The K_{hyd}/K_{BH^+} ratio represents the reliance of the rate constant on the concentration of the hydrated and protonated carbonyls, as K_{hyd} is directly proportional to the activity of the hydrated carbonyl and K_{BH^+} is the inversely proportional

to the activity of the protonated carbonyl. The coefficients m^*m' are compound and reaction specific variable which describe how X changes with different reaction systems. C_{H^+} and X are directly related to the particle acidity.

The change in acid catalyzed heterogeneous SOA yield due to the acidity of the seed particles is different for each system. Equation 2.2 predicts that aerosol yield will increase as acidity increases given that the other variables are constant. Figure 2.4 plots $\log(\Delta Y^*) - \log(a_w)$ to illustrate the relationship between acid catalyzed SOA yield and particle acidity. a_w is subtracted from ΔY^* to isolate the variables which represent particle acidity as the independent variables in the linear regression. The activity of water does not vary widely within this study. The particle acidity is mostly represented by $[m^*m'X + (\log C_{H^+})]$.

Figure 2.4 shows that $\log(\Delta Y^*) - \log(a_w)$ increases as excess acidity increases which is accomplished in this study by lowering the %RH while the acidic seed composition remains constant.

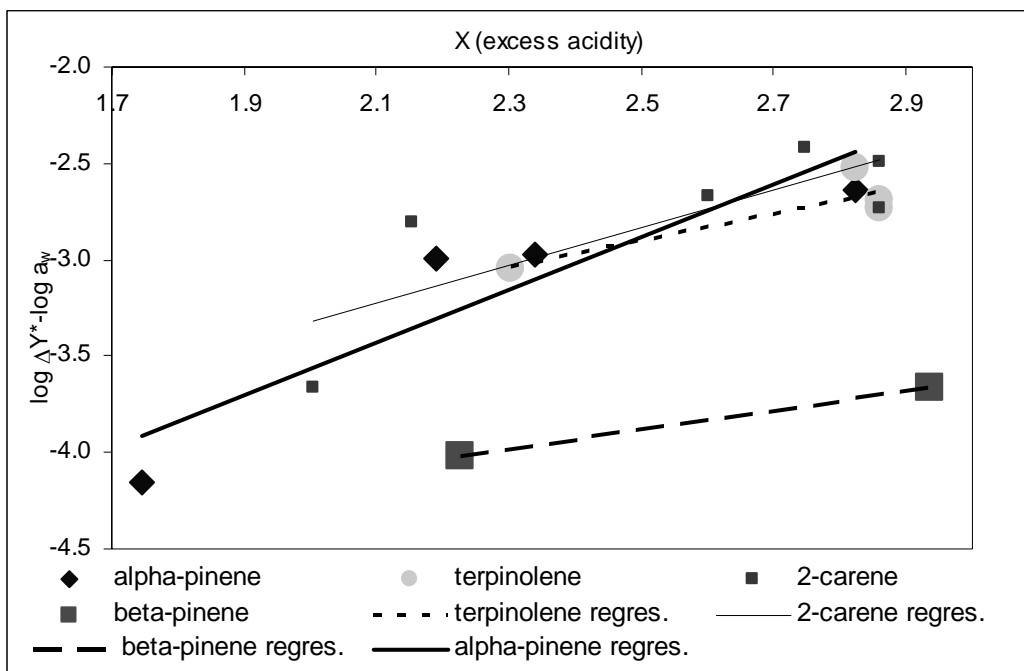


Figure 2.4. ($\log \Delta Y^* - \log a_w$) vs. X (excess acidity) for ozonolysis of various terpenes in the presence of an acid catalyst. Inorganic seed composition was 2:3 mole ratio of H_2SO_4 to NH_4HSO_4 . Regression line equations: β -pinene = $0.50X - 5.13$, α -pinene = $1.37X - 6.31$ ($R^2 = 0.84$), Δ^2 -carene = $0.99X - 5.30$ ($R^2=0.66$), terpinolene = $0.70X - 4.65$ ($R^2= 0.79$). a_w (water activity) was calculated using ISORROPIA (1998).

It appears that a strong correlation occurs between X and the subsequent heterogeneous acid catalyzed SOA yield which is expected as predicted by equation 2.2. The correlation coefficients for the shown regression curves vary between 0.75 and 0.87. Excess acidity is strongly correlated to the proton concentration, so it is expected that a similar trend would exist for $\log(\Delta Y^*) - \log(a_w)$ versus C_{H^+} .

The reactivity of the SOA's components for acid catalyzed heterogeneous reactions corresponds to the y-intercept of Figure 2.4. Equation 2.2 shows that for a constant seed aerosol composition the y-intercept varies only by $\log(K_{hyd}/K_{BH^+})$. Each terpene has a unique value for $\log(K_{hyd}/K_{BH^+})$. This value is the sum of the individual $\log(K_{hyd}/K_{BH^+})$ for each terpene ozonolysis product which partitions to the aerosol. The overall value gives a measure of which ozonolysis systems are more sensitive for acid catalyzed heterogeneous reactions. For example Δ^2 -carene and terpinolene are the most sensitive followed by α -pinene and β -pinene as demonstrated by their intercept values in Figure 2.4 and also the ΔY^* values in Figure 2.3. The correlations in Figure 2.4 are not perfectly linear, but do show a strong correlation. The deviation from linearity can be attributed to experimental error associated with SMPS data, the transition of organic matter from a liquid like to a solid like phase, and changes in the water content of the aerosol. Another source of error is the assumption that acid catalyzed yield is directly proportional to the rate constant. A more complete model estimation for the heterogeneous aerosol yield will include the full reaction rate. Due to nucleation the results for d-limonene is not included in Figure 2.4.

2.3.4 Molecular Structure of Oxidation Products and Reactivity

The increase in ΔY^* depends upon the acidity of the aerosol (X and C_{H^+}), molecular structures of oxidation products (K_{HYD} and K_{BH^+}), and the ratio of ΔHC to inorganic seed. The ability for the oxidized products (e.g., carbonyl) to be transformed into the hydrated or the protonated carbonyl forms in the particle phase directly affects ΔY^* , as the concentration of the hydrate and protonated carbonyl in the aerosol phase determine the rate constant for the formation of acid catalyzed oligomer mass. The formation of such hydrated and protonated species of an oxidized product is reliant on the

molecular structure of the oxidized product. For example, $K_{hyd}=0.85$ for propionaldehyde (Guthrie 1975), while acetone, which has the same molecular formula, has $K_{hyd}=0.008$ (Guthrie 1975). In general K_{hyd} for aldehydes is higher than those of ketones. A similar trend holds for protonation of the carbonyl structures. Thus products containing aldehydes produce higher heterogeneous SOA production than ketones (Jang et al. 2003).

Our experimental results (Table 2.1) show significant differences in the overall SOA yields between the different terpenes systems. We assert that the varying yields are caused by the differences in the gas phase ozonolysis products which partition to the preexisting aerosols to form SOA. Unlike aldehydes and ketones, carboxylic acid products strongly partition to existing aerosols but react less for acid catalyzed heterogeneous reactions. Reported molar yields for the major oxidation products of the terpenes studies are shown in Figures 2.1A and 2.1B. The molecular structures of oxidation products are directly related to the structure of the terpenes. Although only a portion of the total products produced by ozonolysis are shown in Figures 2.1A and 2.1B, these are the major products, and additional products should be analogous to these with the exception of the addition of an OH radical to some of the products. Possible acid catalyzed heterogeneous reactions include the hydration of aldehydes, hemiacetal/acetal formation, aldol condensation, and polymerization of hydrated aldehydes. Equation 2.2 assumes that the hydration and basicity constants represent the ability of a carbonyl to undergo hydration, hemiacetal/acetal formation, and aldol condensation. In addition to these reactions which form high molecular weight structures, three and four membered exo-carbonyl products also result from cis/trans isomerizations, and structural rearrangement by ring opening reactions in the presence of an acid catalyst.

2.3.4.1 α -pinene vs. β -pinene

α -pinene and β -pinene have similar structures in that both are bicyclic alkenes (Figure 2.1A). However, α -pinene has an endocyclic double bond while β -pinene has an exocyclic double bond. Table 2.1 shows that α -pinene produces larger SOA yield in both the neutral and acidic seed

conditions as compared to β -pinene. The difference in total aerosol yields for the neutral aerosol is mainly due to differences in partitioning. In the case of acid catalyzed reactions, the reactivity of partitioned products to oligomers, in part, determines the organic mass formed by heterogeneous acid catalyzed reactions.

The differences in ozonolysis products result from the location of the reactive double bonds. The ozonolysis of the endocyclic double bond in α -pinene retains all ten carbons of the monoterpene and produces aldehydes among other carbonyl compounds, while the exocyclic double bond in β -pinene leads to the loss of carbons from the original terpene structure and also creates exocyclic ketones as shown in Figure 2.1A.

Figure 2.1A shows that nopinone, an exocyclic-ketone, is by far the most abundant ozonolysis product of β -pinene with yields of 15.8%, and 17.0% reported in the gas phase (Yu et al. 1999), and trace amounts measured in the aerosol phase. Overall nopinone from ozonolysis of β -pinene does not strongly partition to the aerosol phase, nor does it strongly react for heterogeneous acid catalyzed reaction once this product is present in the particle phase. In comparison α -pinene produces ring opening structures which have lower vapor pressures due to the presence of carboxylic acid groups in comparison to β -pinene products. One of major ozonolysis products from the α -pinene system is pinonaldehyde with yields of 5.7%-19.0% in the gas phase and 0.3% to 1.1% in the aerosol phase (Yu et al. 1999). Pinonaldehyde, an aldehyde is reactive for heterogeneous acid-catalyzed reactions.

2.3.4.2 α -pinene vs. Δ^2 -carene

α -pinene and Δ^2 -carene have similar structures in that both are bicyclic endo-alkenes (Figure 2.1A). The major difference is the bicyclic structure: Δ^2 -carene has a cyclo-propane ring while α -pinene has a cyclo-butane ring. In comparing the products from ozonolysis of α -pinene and Δ^2 -carene (it was assumed that the products of Δ^2 -carene are analogous to Δ^3 -carene's products, due

to the lack of product information available for Δ^2 -carene), the products are similar except for the cyclobutane ring in the α -pinene products and the cyclopropane ring of the Δ^2 -carene products.

Although the ozonolysis products of α -pinene and Δ^2 -carene are both cyclic and oxygenated, significant differences are observed between the average SOA yield in the presence of acid (\bar{Y}_{acid}) and neutral seeds ($\bar{Y}_{neutral}$) as well as for ΔY^* (Table 2.1). The large differences can be partially explained by the difference of the ring size in these systems, and the location of the carbonyl groups in relation to the rings.

The rings present in the oxidized products help to delocalize the positive charge of the protonated carbonyl through ring opening reactions which help to push the equilibrium towards the protonated carbonyl. In general, a three membered ring is more reactive for ring opening reactions through carbocation rearrangement than a four membered ring (Scheme 2.1) due to its double bond character, which increases ring opening reactions through protonation of carbonyl next to the ring (Scheme 2.1). The smaller cyclopropane ring present in Δ^2 -carene products also has a higher ring strain energy than the cyclobutane ring in many of the α -pinene products, 28.1 kcal/mol and 26.3 kcal/mol respectively (Carey and Sundberg, 2000) which also aids to the ring opening reactions. Although the ring size difference may not account for all of the difference in the acid catalyzed heterogeneous mass formation it does help to explain the large difference in the response to the acid catalyst.

2.3.4.3 Terpenes with two double bonds.

Both terpinolene and d-limonene have two double bonds and potentially consume more ozone than α -pinene, β -pinene, and Δ^2 -carene. The first generation ozonolysis products of terpinolene and d-limonene can be further oxidized when the excess amounts of ozone are injected to the chamber in our experimental conditions as shown Figure 2.1A. For example, the first generation ozonolysis products of terpinolene are mostly 4-methyl-3-cyclohexenone (40% of the gas products) (Hakola et al.1994). This major product is not enough to explain the significant SOA aerosol yield

increases in the presence of an acid catalyst. The gas phase yield of reactive terpenaldehyde for the heterogeneous acid catalyzed reaction (*via* aldehyde protonation and tautomerization) is also too low to cause the observed SOA yield increases. The large secondary yield for terpinolene in our experimental conditions is explained by reaction of two double bonds with excess amounts of ozone, as well as the OH radicals which are byproducts from ozonolysis. Thus the secondary organic products create 2,5-dioxo-heptanal as a major product. This 2,5-dioxo-heptanal is much more reactive than 4-methyl-3-cyclohexenone for heterogeneous reactions. Similarly, the secondary oxidation products of d-limonene (Figure 2.1B) can better explain the high increase in SOA yield in acidic conditions.

The increase in SOA yield for d-limonene is not as sensitive to the presence of acidic seed as terpinolene. This may be attributable to particle nucleation in the limonene system. The relative order of ΔY^* for the different terpenes tested should be the same at different %RH, however this is not the case for d-limonene (Table 2.1). The experimental condition of excess concentrations of ozone may be the cause of this inconsistency.

d-Limonene reacts much faster than α -pinene due to high reaction rate with ozone. The increased sites for oxidation (2 double bonds) and the fast reaction rate produce a large concentration of low vapor pressure products quickly, leading to increased nucleation. This decreases the products available for heterogeneous reactions on inorganic seed aerosol, and subsequently affects the amount of mass created by acid catalyzed reactions. The amount of nucleation differs between acid and neutral experiments, with more nucleation in the neutral experiments. This difference in nucleation creates uncertainty in the determination of ΔY^* .

Terpinolene, which also has two double bonds, (both an exo and an endo double bond), reacts faster than limonene due to the highly substituted exo-double bond. However, in terpinolene oxidation of the exo-double bond, which is more reactive than the endo-double bond causes the loss of three carbons which decreases the vapor pressures of the products, and much less nucleation is

seen in the terpinolene system as compared to the d-limonene system. Experiments at lower ozone mixing ratios and at a higher initial seed concentrations help to minimize nucleation in d-limonene. Thus the SOA yield of terpenes with more than one double bond is also dependant on the ratio of ozone to terpenes, and the comparison of yield data should be conducted with caution.

The d-limonene data presented here illustrates that both Y and ΔY^* is strongly dependent on partitioning. Despite the fact that the products produced from d-limonene should be very reactive for heterogeneous acid catalyzed reactions, their partitioning and subsequently nucleation ability proceed in importance for our experimental conditions. However the results from d-limonene shown here still demonstrate that the presence of acid increases the SOA mass in comparison to neutral compositions regardless of the mass formed by nucleation.

2.4. Conclusion

This study has shown that the amount of SOA associated with heterogeneous reactions is directly related to particle acidity, amounts of inorganic seed aerosol, and the molecular structure of the oxidation products of the terpenes studied here. We have also demonstrated the usefulness of both partitioning theory and kinetics of heterogeneous acid catalyzed reactions (Jang et al. 2005) to quantify the SOA yield for various monoterpenes in the presence of inorganic acid. Further study needs to be done to better understand the fraction of the particle that becomes polymerized and how other atmospheric VOCs participate in these processes and is linked to SOA production.

2.5. Acknowledgments

This work was supported by a grant from the National Science Foundation (ATM-0314-128). We would also like to thank Research Education Support Program - UNC at Chapel Hill sponsored by National Science Foundation- AGEP (#HRD-0450099).

2.6 References

Andreae M.O.; Crutzen P.J. 1997 Atmospheric aerosols: biogeochemical sources and role in atmospheric chemistry. *Science (Washington, D. C.)*. 276 (5315), 1052-1058.

Atkinson, R. and Arey, J. (2003). Gas-phase tropospheric chemistry of biogenic volatile organic compounds: a review. *Atmospheric Environment*. 37: S197-9.

Calogirou, A., Larsen, B.R., and Kotzias, D., 1999. Gas-phase terpene oxidation products: a review. *Atmospheric Environment* 33:1423-39.

Calvert, J.G., Kerr, J.A., Madronich, S., Moortgat, G.K., Wallington, T.J., and Yarwood, G., 2000. The mechanisms of atmospheric oxidation of the alkenes. 560 pp.

Carey, F.A. and Sundberg, R.J., 2000. Advanced Organic Chemistry Part A: Structure and Reactivity. New York, NY: Kluwer Academic.

Colville, C.J. and Griffin, R.J., 2004. The roles of individual oxidants in secondary organic aerosol formation from Δ^3 -carene: 2. SOA formation and oxidant contribution. *Atmospheric Environment*. 38: 4013-23.

Czoschke, N.M., Jang, M., and Kamens, R.M., 2003. Effect of acidic seed on biogenic secondary organic aerosol growth. *Atmospheric Environment*. 37: 4287-99.

Gao, S., Ng, N.L., Keywood, M., Varutbangkul, V., Bahreini, R., Nenes, A., He, J., Yoo, K.Y., Beauchamp, J.L., Hodyss, R.P., Flagan, R.C., and Seinfeld, J.H., 2004. Particle phase acidity and oligomer formation in secondary organic aerosol. *Environmental Science and Technology*. 38: 6582-9.

Glasius, M., Lahaniati, M., Calogirou, A., Di Bella, D., Jensen, N.R., Hjorth, J., Kotzias, D., and Larsen, B.R., 2000. Carboxylic acids in secondary aerosols from oxidation of cyclic monoterpenes by ozone. *Environmental Science and Technology*. 34: 1001-10.

Griffin, R.J., Cocker, D.R., Flagan, R.C., and Seinfeld, J.H., 1999. Organic aerosol formation from the oxidation of biogenic hydrocarbons. *Journal of Geophysical Research* 104:3555-67.

Grosjean, Daniel, Williams, Edwin L. II, Grosjean, Eric, Andino, Jean M., and Seinfeld, John H., 1993. Atmospheric oxidation of biogenic hydrocarbons: reaction of ozone with β -pinene, d-limonene and trans-caryophyllene. *Environmental Science and Technology*. 27: 2754-8.

Guthrie, J.P., 1975. Carbonyl addition reactions. Factors affecting the hydrate-hemiacetal and

hemiacetal-acetal equilibrium constants. *Canadian Journal of Chemistry*. 53: 898-905.

Guenther, A., Hewitt, C.N., Erickson, D., Fall, R.G.C., Gradel, T., Harley P., Klinger L., Lerdau M., McKay W.A., Pierce, T., Scholes B., Steinbrecher R., Tallamraju R., Taylor J., Zimmerman P. 1995. A global model of natural volatile organic compound emissions. *J. Geophys. Res.* 100 8873-92.

Hakola, H., Arey, J., Aschmann, S.M., and Atkinson, R., 1994. Product formation from the gas-phase reactions of OH radicals and O₃ with a series of monoterpenes. *Journal of Atmospheric Chemistry*. 18: 75-102.

Jang, M., Czoschke, N.M., Northcross, A., Cao, G., 2006. SOA Formation from partitioning and heterogeneous reactions: model study in the presence of inorganic species. *Environmental Science and Technology*. 40:3013-22.

Jang, M., Czoschke N.M., and Northcross A.L., 2005. Semiempirical model for organic aerosol growth by acid-catalyzed heterogeneous reactions of organic carbonyls. *Environmental Science and Technology*. 39:164-74.

Jang, M., Carroll, B., Chandramouli, B., and Kamens, R.M., 2003. Particle growth by acid-catalyzed heterogeneous reactions of organic carbonyls on preexisting aerosols. *Environmental Science and Technology*. 37: 3828-37.

Jang, M., Czoschke, N.M., Lee, S., and Kamens, R.M., 2002. Heterogeneous atmospheric aerosol production by acid-catalyzed particle-phase reactions. *Science* 298:814-7.

Jang, M. and Kamens, R.M., 2001. Atmospheric secondary aerosol formation by heterogeneous reactions of aldehydes in the presence of a sulfuric acid aerosol catalyst. *Environmental Science and Technology*. 35: 4758-66.

Jang, M. and Kamens, R.M., 1999. A predictive model for adsorptive gas partitioning of SOCs on fine atmospheric inorganic dust particles. *Environmental Science and Technology*. 33:1825-31.

Jonsson, A.M., Hallquist, M., and Ljungstrom, E., 2006. Impact of humidity on the ozone initiated oxidation of limonene, delta3-carene, and alpha-pinene. *Environmental science & technology*. 40: 188-94.

Kalberer, M., Paulsen, D., Sax, M., Steinbacher, M., Dommen, J., Prevot, A.S.H., Fisseha, R., Weingartner, E., Frankevich, V., Zenobi, R., and Baltensperger, U., 2004. Identification of polymers as major components of atmospheric organic aerosols. *Science* 303: 1659-62.

Kamens, R., Jang, M., Chien, C.J., and Leach, K., 1999. Aerosol formation from the reaction of

alpha-pinene and ozone using a gas-phase kinetics aerosol partitioning model. *Environmental Science and Technology* 33:1430-38.

Kavouras I.G., and Stephanou E.G., 2002. Direct evidence of atmospheric secondary organic aerosol formation in forest atmosphere through hetero-molecular nucleation. *Environmental Science & Technology*. 36: 5083-91.

Keywood, M.D., Varutbangkul, V., Bahreini, R., Flagan, R.C., and Seinfeld, J.H., 2004. Secondary organic aerosol formation from the ozonolysis of cycloalkenes and related compounds. *Environmental Science and Technology*. 38: 4157-4164.

Muller, J.F. 1992. Geographical distribution and seasonal variation of surface emissions and deposition velocities of atmospheric trace gases. *Journal of Geophysical Research*. 97 3787-3804.

Nenes, A., Pandas, S.N., Pilings, C., 1998. ISORROPIA. A new thermodynamic equilibrium model for multiphase multi component inorganic aerosols. *Aquatic Geochemistry*. 4:123-52.

Odum, J.R., Hoffmann, T., Bowman, F., Collins, D., Flagan, R.C., and Seinfeld, J.H., 1996. Gas/particle partitioning and secondary organic aerosol yields. *Environmental Science and Technology*. 30: 2580-85.

Pathak, Ravi Kant, Louie, Peter K. K., and Chan, Chak K., 2004. Characteristics of aerosol acidity in Hong Kong. *Atmospheric Environment*. 38: 2965-74.

Rasmussen, R.A., 1972. What do the hydrocarbons from trees contribute to air pollution? *Journal of Air Pollution Control Association* 22:537-43.

Tolocka, M.P., Jang, M., Ginter, J.M., Kamens, R.M., and Johnston, M.V., 2004. Formation of oligomers in secondary organic aerosol. *Environmental Science and Technology* 38:1428-34.

Wise, M., Biskos, G., Martin, S., Russell, L., and Buseck, P., 2005. Phase transitions of single salt particles studied using a transmission electron microscope with an environmental cell. *Aerosol Science and Technology*. 39: 849-56.

Yu, J., Cocker, D.R. III, Griffin, R.J., Flagan, R.C., and Seinfeld, J.H., 1999. Gas-phase ozone oxidation of monoterpenes: gaseous and particulate products. *Journal of Atmospheric Chemistry*. 34: 207-5.

Chapter 3

Quantifying the nonvolatile fraction of biogenic secondary organic aerosols formed in the presence of inorganic aerosols through thermal analysis.

Amanda L. Northcross[#], and Myoseon Jang^{*}

[#]Department of Environmental Sciences and Engineering
The University of North Carolina at Chapel Hill

^{*} corresponding author
Department of Environmental Engineering Science
The University of Florida
P.O. Box 116450
Gainesville, FL 32611-6450
Tel: 352-846-1744
email: mjang@ufl.edu

In preparation for submission to Atmospheric Environment

ABSTRACT

Secondary organic aerosols are composed of hundreds of oxidized products from the gas phase reactions of volatile organic carbons. The aerosol phase oxidized products are not inert and are able to react within the particle phase to form oligomers. The particle phase reactions are catalyzed by the presence of inorganic acidity which is ubiquitous in the ambient atmosphere. The presence of oligomer mass within SOA can alter the chemical and physical properties from those of a theoretically inert particle.

Quantifying the fraction of oligomer mass formed within SOA under differing inorganic acidities is essential for SOA formation models, estimating radiative forcing, and better understanding the implications of SOA on health. This study quantifies the oligomer fraction in produced from the ozonolysis of terpenes (α -pinene and terpinolene) in the presence of inorganic seed aerosols (ammonium sulfate, ammonium bisulfate, and sulfuric acid) using an indoor Teflon chamber. The change in mass of SOA samples as a function of temperature was measured using a thermal gravimetric analyzer (TGA). By exploiting the relationship between vapor pressure and structural properties of the organic compounds in SOA, the mass fraction of oligomers present in the SOA was determined by analysis of TGA data.

The measured oligomer fraction is used to describe the relationship between SOA increases due to the presence of inorganic aerosols, as well as describe the impact of varying inorganic acidities on oligomer formation from α -pinene and terpinolene SOA. The effect of charring on the determination of the fraction of oligomers in SOA was also studied.

KEYWORDS: SOA, thermal gravimetric analysis, oligomers, particle phase reactions, particle acidity

3.1. Introduction

Secondary organic aerosols (SOA) traditionally have been described using the thermodynamic partitioning theory under the assumption that the particle phase organics are inert. However in the presence of inorganic acidic aerosols, which are ubiquitous to the ambient atmosphere, molecules in the particle phase react through acid catalyzed heterogeneous reactions. Researchers have proposed possible mechanisms (Iinuma et al. 2004; Tolocka et al. 2004; Jang et al. 2003), elucidated chemical structures of oligomers (Gao et al. 2004a; Kalberer et al. 2004), and have measured SOA yields influenced acid catalyzed oligomer formation (Czoschke et al. 2003; Jang et al. 2002). However the exact process of oligomer formation has not been determined, but the presence of inorganic acidity has been shown to catalyze the formation of oligomers.

Oligomers have different chemical and physical properties than the unreacted organics. For example particle phase molecules in the monomer form within an aerosol are semi-volatile, while oligomers are nonvolatile due to their very low vapor pressures. Oligomers are less soluble in water as monomers suggesting that particles with larger fractions of oligomers may be less likely to act as cloud condensation nuclei. Also the oligomers and monomers may have very different optical properties which are used to determine the radiative forcing of atmospheric aerosols. Finally the thermal properties of oligomers and monomers are very different. The boiling points of oligomers are much higher than monomers making them distinguishable through thermal analysis.

The limitations of the current characterization techniques for the quantification of oligomer mass within SOA requires the development of a method which directly quantifies the fraction of the oligomers in the aerosol bulk phase as opposed to analyzing each individual compound. In this study thermal gravimetric analysis (TGA) is used to determine the fraction of semi-volatile organic and oligomeric matter associated with SOA. TGA exploits the differences in the physical properties of oligomers, inorganic constituents, and organic monomers to measure the oligomeric fraction in the aerosol. TGA has been used in other fields to study fuels, polymers, catalysts, pyrolysis, and chemical synthesis.

Thermal denuders are another analytical technique which exploit the varying volatility of aerosol constituents to investigate the composition of aerosols and determines the nonvolatile fraction of an aerosol. Aerosols are passed through a heated tube, and the aerosol volume changes are measured before and after the heated tube. By changing the temperature valuable information is gained as to the content of the aerosol composition. The use of temperature to volatilize components from aerosols is similar to the TGA technique. The major difference between the two techniques is that thermal denuders are an online process which provides information about the change in volume of the aerosol passing through the denuder with respect to a fixed denuder temperature. TGA is an offline method which directly measures the mass changes of aerosol as a function of temperature and allows for the study of the thermal behavior of individual components (e.g., inorganics, semi-volatiles, and nonvolatile organic matter) within a mixed organic/inorganic aerosol.

The large difference in the molecular weights between the oligomers and monomers within SOA make these particles a prime candidate for a TGA study. Studies analyzing SOA generated from the ozonolysis of α -pinene using single particle mass spectrometers (Bahreini et al. 2005), report that the majority of monomers in terpene systems have molecular weights which fall into the range of 150-230 g/mol (Yu et al. 1999). In general, oligomers have much higher molecular weights than monomers. For example, Tolocka et al. (2004) showed the presence of oligomers in SOA from ozonolysis of α -pinene with mass units ranging from 200-900 mass units. The oligomers identified by Iinuma et al. (2004) in SOA from α -pinene ozonolysis had molecular weights of 354 and 370 mass units and those identified by Gao et al. (2004b) had molecular weights which ranged from 250–1600 mass units. Oligomers and semi-volatile organics within SOA formed from the ozonolysis of terpenes have molecular weight differences of at least 100 mass units causing them to volatilize or decompose at different temperatures.

This study analyzed SOA created from the ozonolysis of α -pinene and terpinolene using an indoor Teflon film chamber. We hypothesize that the oligomeric fraction in the aerosol is influenced

by the differing responses to particle acidity by the two different terpene systems. For example, a recent study by Northcross and Jang (2007) has shown that terpinolene has larger increases than α -pinene in SOA mass when formed in the presence of inorganic acidic aerosols as compared to neutral inorganic aerosol strongly suggesting that oligomer formation is larger in the terpinolene system in comparison to the α -pinene system.

3.2. Experimental Methods

3.2.1 Chamber Operation

Terpene	# of experiments	Terpene Conc. ppm	M_{seed} $\mu\text{g}/\text{m}^3$	O_3 ppm	%RH	$M_{\text{seed}}/\Delta\text{HC}$	Yield (Y)
α -pinene	3	0.43	neutral, 850	0.49	58	0.35	0.79
α -pinene	2	0.76	no seed	0.72	15	N/A	0.61
α -pinene	2	0.43	acidic, 180	0.56	20	0.07	0.62
α -pinene	2	0.43	acidic, 600	0.72	23	0.25	1.32
terpinolene	3	0.43	acidic, 243	0.46	26	0.10	0.61
terpinolene	3	0.43	acidic, 253	0.55	21	0.11	0.65

Table 3.1. Experimental Conditions for TGA analysis of SOA T constant at 23°C. All values are average for experimental conditions.

A 2 m³ indoor Teflon film chamber was used to conduct all SOA experiments. The chamber has been described in previous studies (Northcross and Jang 2007, Czoschke and Jang 2006). Neutral and acidic seed aerosols were created from aqueous solutions. The acidic seed solution was composed of 0.01M of sulfuric acid (H₂SO₄) (Sigma Aldrich, 95-98%) and 0.01M ammonium bisulfate (NH₄HSO₄) (Aldrich, 98%) in a 2:3 mole ratio. The neutral seed solution was composed of 0.01M of ammonium sulfate (NH₄)₂SO₄) (Sigma Aldrich, \geq 99%). Seed aerosol was produced using a TSI constant output Atomizer (model 3076).

SOA was produced from the ozonolysis of α -pinene (Sigma Aldrich, > 98%) and terpinolene (Sigma Aldrich, > 98%). Ozone was added to the chamber using an ozone generator (Jelight UV lamp model 600), and measured using an ozone monitor (Thermo Electron Instruments UV Photometric O₃ analyzer model 49). Ozone concentrations ranged from 0.49 to 0.72 ppm (Table 3.1).

The terpene was volatilized into the chamber using a gentle stream of clean air (Whatman FT-IR purge gas generator (model 75-52); Aadco 737 pure air generator) through a heated manifold. All experiments were conducted in the dark to prevent photochemical reactions.

The particle concentration and population was monitored by a scanning mobility particle sizer (SMPS) (TSI, Model 3080) in series with a condensation nuclei counter (TSI, Model, 3025A) during the course of the experiments the particle size ranged from 19.8 nm to 835.4 nm. The aerosol data was corrected for particle losses to the chamber walls using a first order wall loss model based on the number of particles (McMurray and Grosjean 1985).

3.2.2 Aerosol Sampling

Once the ozonolysis reactions were completed, the aerosol mass in the chamber was collected on 13 mm diameter Pallflex tissuquartz 2500 QAT-UP 25mm quartz fiber filters. The small filter size was used due to size restrictions of the TGA sampling pan. Prior to use each filter was baked at 400°C for 60 minutes to remove any contaminants. Filters were weighed before and after sampling to determine the mass collected on the filter and ensure enough sample mass was present to increase the accuracy of the analysis. A pump (Gast, DOA-P704-AA) was used to sample SOA from the chamber. The collected aerosol mass varied from 400µg to 1mg (Table 3.1). Gas phase adsorption to the filter is minimized by the using a small filter which decreases the available surface area for adsorption.

3.2.3 Thermal Gravimetric Analysis

SOA filter samples, inorganic aqueous solutions which represent the inorganic seed aerosols, and pure organics compounds were analyzed using TGA. Inorganic aerosol solutions were spiked onto filters and analyzed using TGA (Pyris 1, Perkin Elmer). SOA filter samples were immediately analyzed after sampling. The organic model compounds and inorganic aqueous aerosol solutions were placed directly in TGA Pt sample pan for analysis. Samples were analyzed with a TGA heating rate of 10°C/minute from 25°C to 600°C, as well as at isothermal conditions where temperature was

held at 70°C for 80 minutes and then ramped to 600°C at 10°C/min. 600°C as a final temperature was found to be excessive, most data produced from the analysis was used at temperatures lower than 300°C. Dry nitrogen (99.998%, National Welders) flowed past the sampling boat at 20L/min throughout the run. Mass measurements were taken at a rate of at least 1 per second.

3.2.4 FTIR Analysis of TGA Samples

Fourier Transform Infrared (FTIR) spectroscopy analysis was performed for samples of pure pinonic acid and mixtures of pinonic acid and seed solutions composed to represent strongly acidic and mildly acidic aerosols equilibrated at 20%RH conditions as estimated by the Aerosol Inorganic Model developed by Clegg et al. (1998). The mildly acidic seed contained 16g NH₄HSO₄, 8mL H₂O and 5mL of H₂SO₄, the sample was composed of 2.3mg pinonic acid and 9.4mg of seed solution. The strongly acidic sample contained 4.8mg of pinonic acid and 8.5 mg of the strongly acidic seed solution, which was made of 1g of NH₄HSO₄, 1mL of H₂O, and 1.5mL of H₂SO₄ (95%, Sigma Aldrich). FTIR samples were taken using a Nicolet Magna-IR 560 Spectrometer equipped with a magnetic circular dichroism (MCD) detector. The instrument was operated in the reflectance mode, the signal to noise ratio was 3. The purpose of the FTIR analysis was to identify changes in the chemical structure of the sample components and not measure concentrations of the components. The mixture samples containing pinonic acid and the inorganic seed solutions were analyzed using FTIR both before and after TGA. The TGA temperature program increased from 25°C to 250°C at a rate of 10°C/min.

3.3. Theory

3.3.1. Classification of Chemical Species in Aerosols

The temperature increase during TGA causes the compounds in the sample to volatilize and/or thermally decompose leading to decreases in the sample mass. The temperature at which volatilization occurs is dependent on the boiling point of the compound. However, mass loss during TGA typically occurs before the boiling point due to the vapor pressure increasing with sample

temperature as well as the nitrogen stream blowing over the sample which prevents the volatilized molecule from being reabsorbed to the sampled aerosol.

TGA data interpretation requires knowledge of the compound classes present within the sampled SOA. The aerosol components are divided into four classes of chemical compounds: inorganic compounds, organic semi-volatiles, organic sulfate and oligomers. Organic semi-volatiles are oxidized products of the precursor terpene which partition to an aerosol but are not transformed into oligomers through particle phase reactions. A complete chemical characterization of the ozonolysis products of either α -pinene or terpinolene has not been conducted. Structural reactivity relationships (Saunders et al., 2003) have been used to estimate a near explicit distribution for the ozonolysis α -pinene and terpinolene. The average boiling point temperature was estimated (Joback and Reid 1987; Stein and Brown 1994) for the products and to be lower than 330°C for α -pinene and 400°C for terpinolene although volatilization will occur at much lower temperatures.

In this study $(\text{NH}_4)_2\text{SO}_4$, NH_4HSO_4 and H_2SO_4 are used to represent ambient inorganic species and are referred to as inorganic seed aerosols. The third class of compounds is organic sulfate which is produced from the reaction of sulfuric acid and organic species within an aerosol and is an identified constituent of SOA (Liggio et al. 2005; Surratt et al. 2007; Iinuma et al. 2007). Organic oligomers are compounds that are formed from two or more organic monomers due to particle phase reactions. Oligomer mass is increased when SOA is formed in the presence of acidic seed aerosols by acid catalyzed reactions. For example, Tolocka et al. (2004) measured oligomers in SOA formed from α -pinene ozonolysis in the presence of both acidic and neutral aerosols. The mass to charge ratio was ten times higher in the presence of acidic seed aerosols than those with neutral seed aerosols. Estimated boiling points of the dimers present in SOA formed from the α -pinene ozonolysis (Iinuma et al. 2004) range from 440°C to 500°C using the group combination method of Joback and Reid (1987) with modified parameters by Stein and Brown (1994). The theoretical boiling point of dimers formed from the aldol condensation of the major semi-volatile SOA products

from terpinolene ozonolysis would be higher than 500°C. The estimations indicate that boiling points of high molecular weight oligomers are distinguishable from those of semi-volatile organics and that the masses will evolve at different temperatures.

3.3.2 TGA Data Analysis

A TGA thermogram shows the weight percent wt%(T) (eq. 3.1) (Figure 3.1) of an aerosol

$$\text{wt\%(T)} = \frac{\text{TGA measured sample mass (T)}}{\text{initial sample mass}} \quad (3.1)$$

sample as a function of temperature. The shape of the thermogram depends on the thermal properties of products, the volume of a sample, the temperature program, and the sample gas (N₂) flow rate.

The characteristic temperature for vaporization or thermal decomposition of a specific species is visible in the thermogram as an inflection point, the point where the curvature changes signs. The wt%(T) at an inflection point is used to determine the fraction of components remaining at a given temperature. The position and the number of inflection points in a TGA thermogram can be detected by differential temperature analysis (DTA), which is the first order derivation of the TGA thermogram and defines the volatilization rate of compounds leaving the sample. A peak in a DTA thermogram corresponds to the inflection points in a TGA thermogram, making it easier to determine the temperature of maximum volatilization.

The volatilization rate of each component is fastest at its characteristic inflection point. The aerosol has characteristic inflection points associated with water vaporization, semi-volatile organic vaporization, and decomposition of organic sulfate and the inorganic seed aerosol. This specific pattern of a thermogram is a “fingerprint” and present for each component in the sample. As the compound begins to volatilize change in the slope and curvature of the thermogram create the fingerprint. For example, in Figure 3.1 the thermogram of pure (NH₄)₂SO₄ and the thermograms of SOA from the ozonolysis of α-pinene in the presence and absence of (NH₄)₂SO₄ are shown.

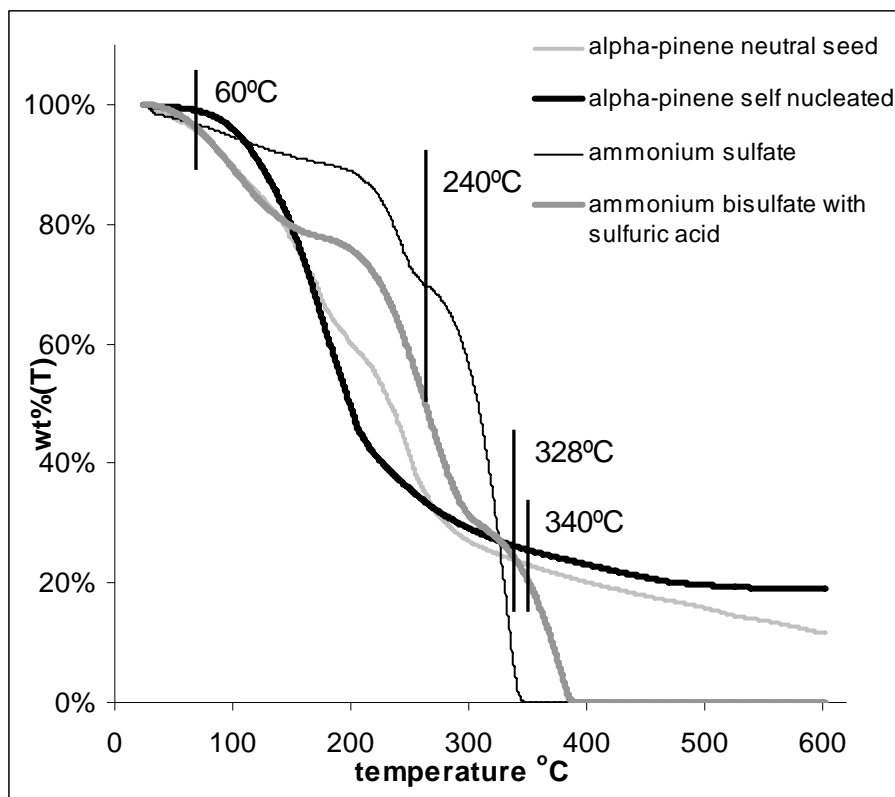


Figure 3.1. Thermograms of simulated $(\text{NH}_4)_2\text{SO}_4$ seed, $\text{NH}_4\text{HSO}_4\text{-H}_2\text{SO}_4$ aqueous solution, neutral seeded α -pinene SOA, self-nucleated α -pinene SOA. The temperatures for inflection points are shown for each system. Inflection points at 240°C and 340°C are for $(\text{NH}_4)_2\text{SO}_4$ seed. Inflection points at 60°C, 240°C, and 328°C are for aqueous acidic seed solution ($\text{H}_2\text{SO}_4:\text{NH}_4\text{HSO}_4 = 2:3$).

The fingerprint of $(\text{NH}_4)_2\text{SO}_4$ thermogram is visible in the SOA seeded with $(\text{NH}_4)_2\text{SO}_4$. When the thermogram of SOA from α -pinene ozonolysis without seed is compared to the seeded SOA, the $(\text{NH}_4)_2\text{SO}_4$ fingerprint becomes even more recognizable, illustrating the characteristic temperatures of SOA compounds and $(\text{NH}_4)_2\text{SO}_4$.

The TGA thermogram of a mixture can be decoupled into the thermogram of each component when the original thermogram is additive for the components. Although the fingerprints of the components in the thermogram are distinguishable, the characteristic temperatures in the thermogram of each pure component may appear to be shifted in a mixture. Temperature shifts occur due to sulfonation reactions when $(\text{NH}_4)_2\text{SO}_4$ is physically mixed with polystyrene (Zhu et al. 1997). The shift of the characteristic temperatures in thermogram can be also detected by DTA thermograms.

3.3.3 Thermogram of Inorganic Seed Aerosol

The first step in analyzing SOA thermograms is decoupling the total aerosol mass into the organic and inorganic fractions. In order to properly decouple the aerosol mass, it is essential to understand the thermal properties of pure inorganic aerosol. Thermograms were observed for 10 μ L of aqueous inorganic solutions spiked on to a filter to simulate the inorganic species of the seed aerosols (Figure 3.1).

The acidic aqueous solution (H₂SO₄-NH₄HSO₄) and the neutral aqueous solution ((NH₄)₂SO₄) presented very different thermograms as shown in Figure 3.1. The thermogram of the neutral solution follows the decomposition mechanism as described by Kiyoura and Urano (1970). The thermogram of (NH₄)₂SO₄ has two major inflection points at 240°C and 340°C (Figure 3.1) corresponding to the thermal decomposition. (NH₄)₂SO₄ decomposes into NH₄HSO₄ with the loss of ammonia gas. Next, NH₄HSO₄ decomposes into water and sulfamic acid which then immediately further decomposes into various volatile gases. The temperatures at which the inflections points occur slightly differ from the literature values. This is attributed to the difference of the ratio of sample volume to N₂ flow rate.

The thermogram of the aqueous acidic seed solution has three major inflection points at temperatures of 60°C, 240°C, and 328°C (Figure 3.1). At 60°C water is volatilizing from the sample. The inflection point at 240°C is due to the NH₄HSO₄ decomposition, as well as the decomposition of H₂SO₄ to SO₂ and water. The inflection point at 328°C is caused by sulfamic acid reacting with excess NH₄HSO₄ to form ammonium pyrosulfate, which undergoes a host of reactions leading ultimately to decomposition and the release of volatile gases including NH₃, SO₃, H₂SO₄, hydrogen, nitrogen, and water vapor (Kiyoura and Urano 1970).

3.3.4 Thermograms of Organics in the Presence of Inorganics

The effects of temperature and inorganic species on organic stability, oligomer formation, organic sulfate formation, and charring have been studied using nonanol and pinonic acid. Pinonic acid is one of the major identified SOA products from α -pinene ozonolysis. Nonanol was chosen to

study the thermal behavior of aerosol organic sulfate; a recent study has reported the formation of organic sulfate from the reaction of alcohol and sulfuric acid in aerosols (Inuma et al. 2007). Figure 3.2 shows the thermograms for a series of pinonic acid experiments where pinonic acid is mixed with nonanol, acidic seed solution, or water.

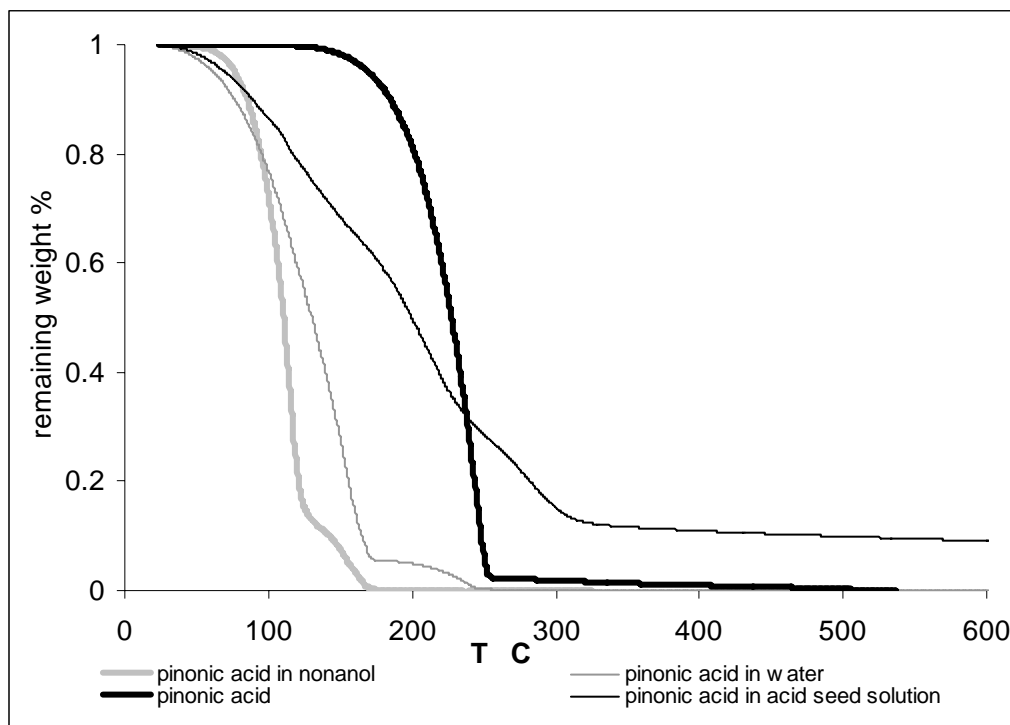


Figure 3.2. Thermograms of pinonic acid (2.2mg), and pinonic acid (0.5 mg) with nonanol (3.0 μL), water, and acid seed solution (207mg NH_4HSO_4 , 2mL H_2SO_4 , 2ml H_2O).

The thermogram of pure pinonic acid (boiling point = $\sim 300^\circ\text{C}$) shows volatilization at 257°C (Figure 3.2). However when pinonic acid is mixed with water or nonanol it volatilizes at a temperature much lower than 257°C . The volatilization of pinonic acid at lower temperatures in mixtures than the pure compound occurs due to the physical state of compounds. Solubilized pinonic acid in a liquid mixture requires less energy to volatilize as opposed to the crystalline form of pure pinonic acid. Pinonic acid is more soluble in nonanol than in water, and correspondingly volatilizes at lower temperatures in nonanol as opposed to water. The bimodal nature of both the pinonic acid–nonanol and the pinonic acid–water thermograms occurs due to the volatilization of nonanol in the first mode and non-crystalline pinonic acid in the latter. Nonanol (boiling point = 215°C) volatilizes

by 150 °C and liquid-like pinonic acid, by 172 °C (section 3.3.1). Low temperature volatilization will also occur in the SOA samples which are multi component systems comprising carboxylic acids, carbonyls, alcohols, and water.

Pinonic acid in the acid seed solution did not completely volatilize illustrating the formation of oligomers in the sample. Both pinonic acid and the acid seed solution (Figure 3.1) completely volatilize when analyzed separately. However the mixture of pinonic acid and the acid seed solution have remaining mass that is nonvolatile. The nonvolatile mass is due to the formation of higher molecular weight oligomers that formed through acid catalyzed reactions.

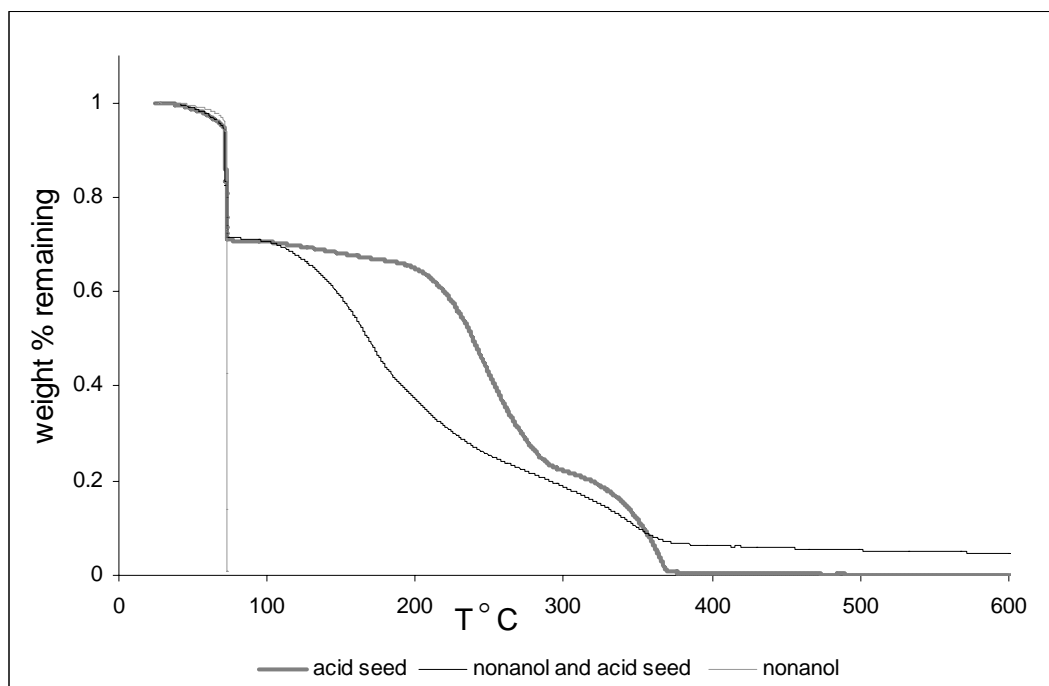


Figure 3.3. Isothermal analysis thermograms of nonanol (1.7 mg), acid seed solution (composition: 207 mg NH_4HSO_4 , 2 mL H_2SO_4 , 2 ml H_2O), and nonanol (1.71mg) with acid seed solution (7.4 mg) Isothermal temperature program was 80 minutes at 70°C and then ramped from 70°C to 600°C at 10°C/min.

Isothermal analysis using pure nonanol, acidic seed solution, and nonanol with acidic seed solutions were conducted to ensure that oligomers were not formed by compounds at elevated temperatures which do not form oligomers at room temperatures. Figure 3.3 shows that when held at 70°C nonanol completely volatilizes. The mass lost during the isothermal temperature analysis for the acidic seed solution can be mostly attributed to the water evaporation. The water content was 34% and the mass lost during the isothermal analysis was 30%. The water content in the mixture of

nonanol and acidic seed was about 28%. Figure 3.3 shows that the mass loss in the isothermal analysis of this mixture is mainly by water evolution. It is assumed that most nonanol was converted into organic sulfate in the presence of excess amounts of highly acidic sulfuric acid, as suggested by Inuma et al. (2007). More importantly, the resulting organic sulfate is decomposed before 200°C. The thermogram of nonanol with acidic seed solution also shows only 2% of mass is not volatile which slightly increases the error of the oligomer mass determination.

In comparison a set of experiments was conducted with a mixture of pinonic acid-aqueous acidic seed solution. Pinonic acid is a crystal at room temperature and not volatile therefore an isothermal analysis of the pure compound was not conducted. Unlike nonanol the pinonic acid system produced oligomers in the acidic environment, which is expected due to the presence of a ketone on the molecule.

The differences between two different systems can be seen in the DTA for the two systems (Figure 3.4) which highlights the temperatures where the maximum volatilization occurred as peaks.

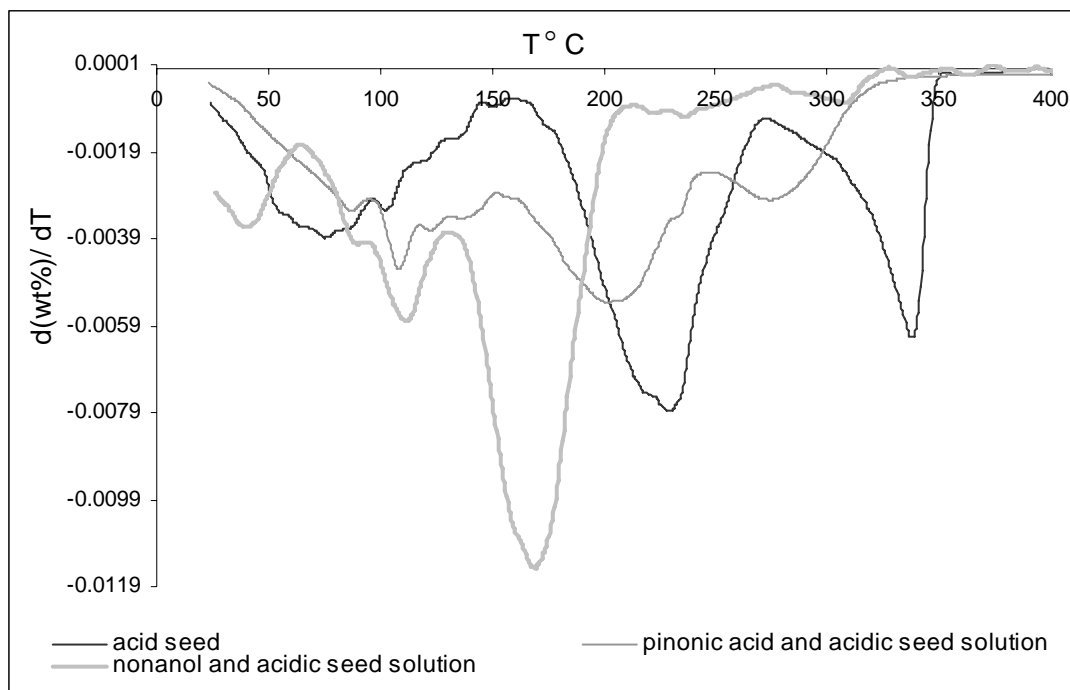


Figure 3.4. DTA thermograms of acidic seed solution and nonanol (65%_{wt}), and acid seed solution and pinonic acid (15%_{wt}), and acidic seed solution.

The nonanol-acid seed system shows a large peak between 130°C and 200°C, which corresponds to the volatilization of nonanol and the decomposition of organic sulfate. The thermal evolution of semi-volatile organics, sulfuric acid and organic sulfate is at 155°C-240°C for the pinonic acid-acid seed system. The shift in the peak temperature is consistent with the difference in volatilization temperatures for the solubilized compounds. The peak between 240°C and 325°C corresponds to the decomposition of the oligomers in the pinonic acid-acid seed system. The final peak (270-356°C) in the acid seed thermogram is the decomposition of inorganic species.

As the temperature increases the organic compounds in the absence of inorganics volatilized completely. Unlike samples without inorganic seed, in the presence of acidic inorganics both pinonic acid and nonanol produced char. Nonanol only formed 2% of the total mass as char (Figure 3.3), while this fraction was higher for the pinonic acid system.

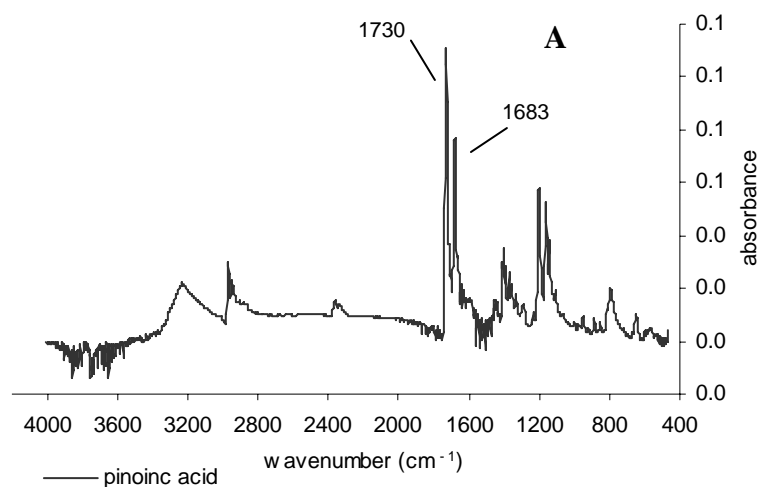
3.3.5 FTIR Spectral Analysis of TGA Samples

In order to further investigate changes in the composition of a sample due to the increasing temperature of TGA, pinonic acid mixed with acid seed solution was analyzed by TGA followed by FTIR spectrometry. Samples composed of pinonic acid with mildly acidic and strongly acidic seed solutions were analyzed. The C=O bond is used to identify pinonic acid, which contains both a ketone and a carboxylic acid functional group. The C=O of carboxylic acid absorbs sharply at 1730 cm⁻¹ and the C=O of the ketone stretches at 1683 cm⁻¹ (Figure 3.5A). The inorganic fraction of the sample also contains strong characteristic peaks. NH₄ in ammonium hydrogen sulfate stretches appear at 3240, 3090, 2890, and 1420 cm⁻¹ and SO₄²⁻ stretches near 1200, 1090, 850, and 588 cm⁻¹.

The FTIR spectra of samples containing both pinonic acid and acidic seed solution are shown in Figures 3.5B and 3.5C. The FTIR spectra taken prior to TGA analysis reveal the presence of both the inorganic seed solution and the organic acid in both the mildly acidic and strongly acidic samples. Initially the mixture samples have FTIR spectra peaks for the organics which are broader than the pure pinonic acid due to hydrogen bonding, oligomerization, and the formation of new products associated through various reaction pathways such as aldol condensation, ring opening, and

carbocation rearrangement. Comparing the spectra taken before TGA analysis to the spectra taken after the sample was heated to 250°C confirms the volatilization of semi-volatiles (e.g., pinonic acid and ring rearrangement products) as well as additional organic oligomeric mass remaining in the sample. The sample after heating was a thick dark tar like substance. The sharp peaks corresponding to the C=O bonds of the carboxylic acid and ketones at 1730 and 1680 cm^{-1} are no longer present while a peak centered near 1705 cm^{-1} remained (Figure 3.5D). The carboxylic OH stretching ranged from 2400 to 3700 cm^{-1} in the sample after TGA, although the absorbance was smaller compared to the original mixture before TGA. Thus after TGA pinonic acid has volatilized confirmed by the mass loss by TGA and the remaining organic mass is concluded to be due to oligomers remaining in the sample.

Direct quantitative comparison of the mildly acidic and strongly acidic spectra is difficult as the ratio of organic to inorganic compounds varies between the two samples. However, the FTIR spectra taken after TGA analysis are very similar, implying that the sample composition remaining at 250°C is very comparable. Overall the FTIR analysis and TGA data (Figure 3.4) support our claim that semi-volatile organics will volatilize below 250°C. Changes to the sample above 250°C does not effect interpretation of thermograms as the goal is to measure to semi-volatile fraction of aerosols and the oligomeric mass determined through a mass balance.



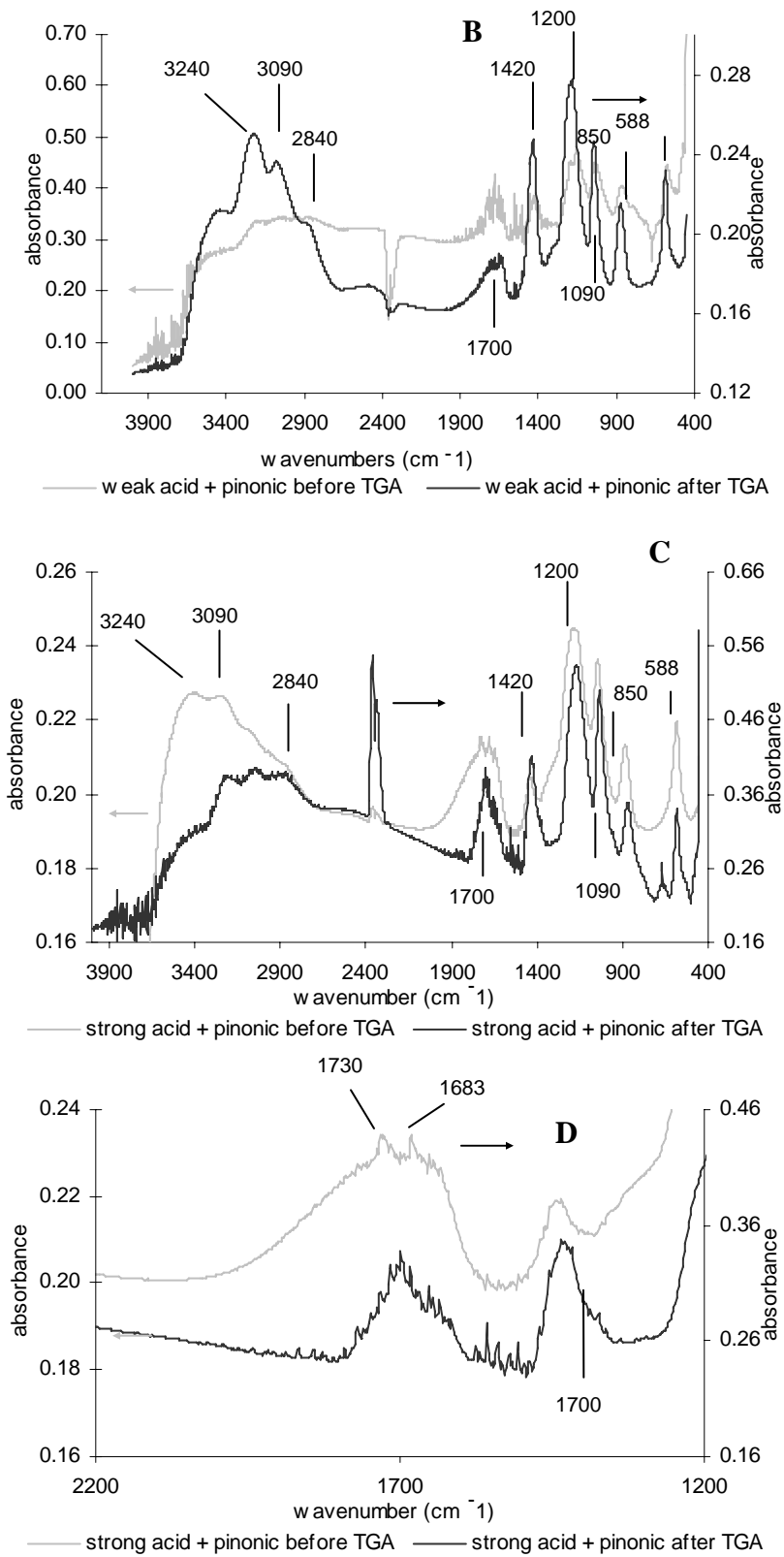


Figure 3.5. FTIR spectra of pinonic acid and mixtures of pinonic acid with acidic seed solutions before and after TGA analysis. **A.** pure pinonic acid **B.** Mildly acidic mixture: 2.3 mg pinonic acid and 9.4 mg mildly acidic seed solution (16 g NH_4HSO_4 , 8 mL H_2O and 5 mL of H_2SO_4) **C.** Strongly acidic mixture: 4.8 mg of pinonic acid and 8.5 mg of strongly acidic seed solution (1.0 g NH_4HSO_4 , 1 mL H_2O and 1.5 mL of H_2SO_4). **D.** Enlarged section of **C.**

3.3.6 Decoupling Organic and Inorganic Aerosol Mass

The total aerosol mass (M_{TOT}) is composed of four components as shown in equation 3.1:

$$M_{TOT} = M_{seed} + M_{soc} + M_{olig} + M_{org-sul} \quad (3.1)$$

M_{soc} is the mass of semi-volatile organic compounds (SOC), $M_{org-sul}$ is the mass of organic sulfate, M_{olig} is the mass of organic oligomers, and M_{seed} is the mass of inorganic seed. The total organic mass (OM) in the aerosol is the sum of M_{soc} , M_{olig} , and the organic portion of $M_{org-sul}$. In order to determine the oligomeric fraction in the SOA of the aerosol, the OM portion of the thermogram is separated from the total aerosol thermogram by subtracting the inorganic seed mass (M_{seed}) thermogram from the thermogram of the total aerosol. The separated OM thermogram is then used to determine M_{olig} . Estimation of M_{olig} is based on the assumption that M_{soc} and $M_{org-sul}$ decompose and volatilize before the oligomers begin to decompose. This assumption may not hold exclusively as 2% of the total mass remains as char in the alcohol-acid seed system, which forms $M_{org-sul}$, increasing the uncertainty in the oligomer mass estimation.

M_{seed} is estimated using the volume concentration of the inorganic seed from the SMPS data multiplied by the seed aerosol density, which is determined, estimated using a method developed by Semmler et al. (2006). The water content of the seed aerosols at a given %RH was determined using ISORROPIA (Nenes et al. 1998) and further used for the density estimation of seed aerosols.

OM is determined by multiplying the organic aerosol density by the volume difference between inorganic seed mass and the total aerosol assuming an organic aerosol density of 1.4g/mL. This assumed density is an average between the density of highly oxidized oligomers of similar chemical structure as expected in the sampled aerosol at 1.5g/mL (Rothe and Rothe 1989) and the reported SOA density for terpinolene of 1.29 and 1.19 for α -pinene (Bahreini et al. 2005) respectively which are the lower limits for the SOA density.

$$wt\%_{org}(T) = \frac{M_{TOT} wt\%_{TOT}(T) - M_{seed} wt\%_{seed}(T)}{OM} \quad (3.2)$$

The OM thermogram is decoupled from the total aerosol TGA thermogram using equation 3.2, where the weight percent of the organic fraction with respect to temperature is $wt\%_{\text{org}}(T)$ and $wt\%_{\text{TOT}}(T)$ represents the weight percent at a given temperature for the total aerosol mass.

It is essential that $wt\%_{\text{seed}}(T)$, the weight percent with respect to temperature for the inorganic seed, represents the same volatilization rates as the inorganic seed core at a given temperature. Subtraction of the inorganic aerosol thermogram signal from the total aerosol thermogram is complicated by changes to the inorganic volatilization when in the presence of organic compounds. As previously mentioned in the presence of organic compounds, the thermal decomposition of the inorganic seed occurs at temperatures lower than the characteristic temperature of a pure sample. In order to confirm that temperature shifts occurred for the seeded SOA, inorganic and organic mixed samples, thermograms for samples of $(\text{NH}_4)_2\text{SO}_4$ were compared to an aqueous mixture of aqueous $(\text{NH}_4)_2\text{SO}_4$ and pinonic acid, which is one of the major SOA products from the ozonolysis of α -pinene. Figure 3.6A shows the resultant DTA thermograms. A temperature shift of 80°C occurred when pinonic acid was mixed with $(\text{NH}_4)_2\text{SO}_4$. After shifting the thermogram, the two plots track each other closely (Figure 3.6B). The degree of the temperature shift was determined by matching the temperature of the final peak in the DTA plot for the pure inorganic and the final peak in SOA seeded systems.

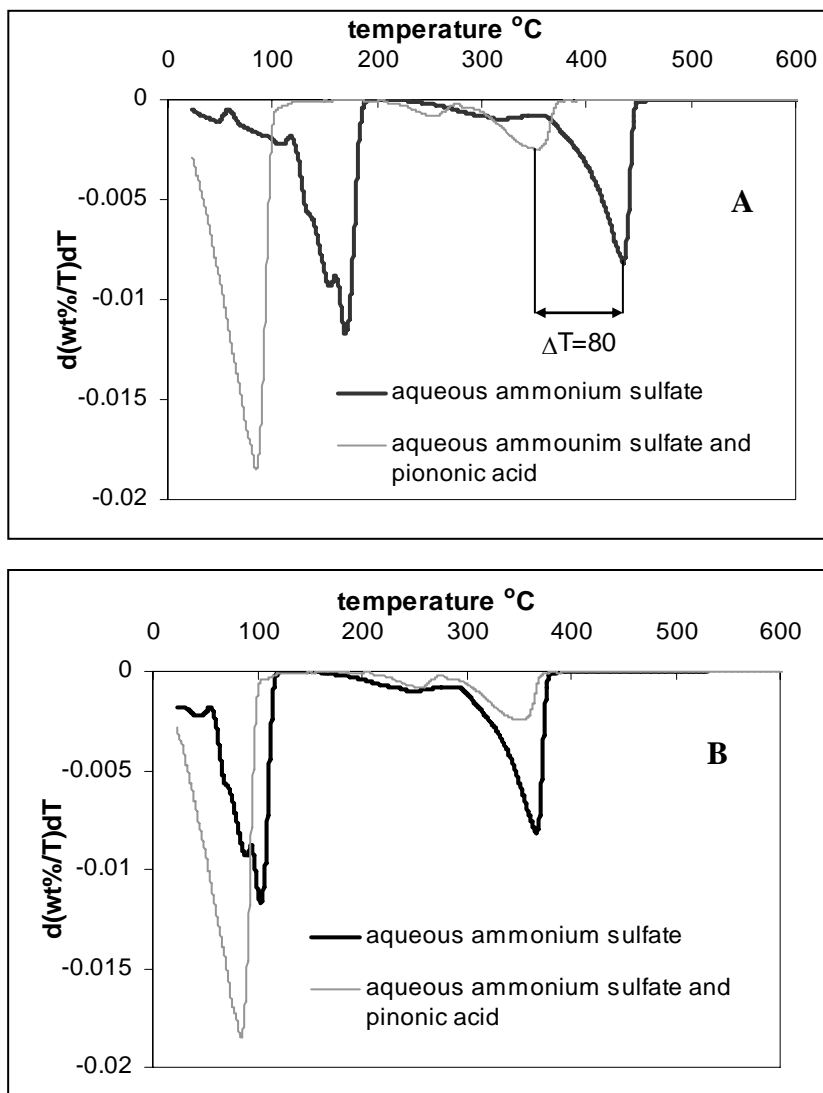


Figure 3.6. DTA thermograms. **A:** aqueous $(\text{NH}_4)_2\text{SO}_4$ solution and aqueous solution containing both $(\text{NH}_4)_2\text{SO}_4$ (16%_{wt}) and pinonic acid (13%_{wt}). **B:** T shifted ($\Delta T=80^{\circ}\text{C}$) aqueous $(\text{NH}_4)_2\text{SO}_4$ solution and aqueous solution containing both $(\text{NH}_4)_2\text{SO}_4$ (16%_{wt}) and pinonic acid (13%_{wt}).

Figures 3.7A and 3.7B show the temperature shift for the SOA from the ozonolysis of α -pinene in the presence of inorganic seed aerosol. The inorganic aerosol thermogram is shifted by reconfiguring the thermogram so the temperature for the weight percent is lower than reorder by the TGA. Once the thermogram of the inorganic seed aerosol is adjusted for the temperature shift, equation 3.2 is then used to generate the OM thermogram comprising of monomers and oligomers.

The evaporation or condensation of organics is assumed to follow a Gaussian mode. The DTA curve for self-nucleated SOA (no seed aerosol, Figure 3.7C) shows the presence of a large peak centered at 150°C which has a tail beginning at 209°C. At this temperature SOC volatilization is near completion. Both thermograms in Figure 3.7C show that the curve starts to deviate from the Gaussian distribution near 209 °C. The start of the tail is the end of the SOC volatilization. All mass beyond this point is attributed to oligomer mass. The tail corresponds to the decomposition and volatilization of oligomers which occur at higher temperatures. The slow decomposition of the oligomers is in keeping with typical polymeric thermal decomposition (Kiyoura and Urano 1970) which progresses gradually as temperature increases. The range of the characteristic temperatures for the SOC fraction in each SOA system was narrow as $\Delta T = 15^\circ\text{C}$. This range is mainly due to differences in the organic aerosol composition of the different terpenes (Table 3.1).

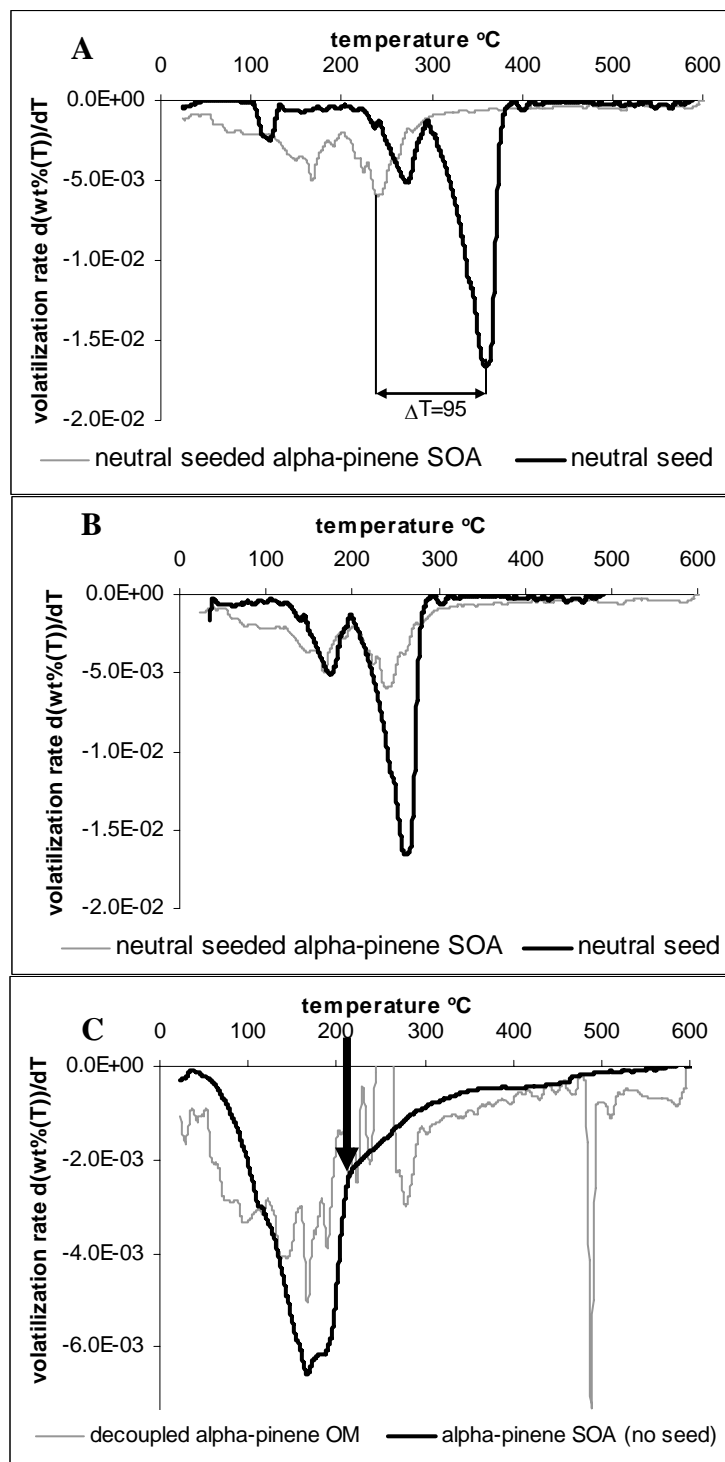


Figure 3.7. DTA thermograms. **A:** aqueous neutral seed solution and neutral seeded α -pinene SOA; **B:** T shifted ($\Delta T=100^\circ\text{C}$) neutral seed solution and neutral seeded α -pinene SOA; **C:** OM only decoupled from neutral seeded α -pinene SOA using equation 2 and self nucleated α -pinene SOA (no seed used). The arrow shows the slope change used to determine the monomer T_f .

3.4. Results

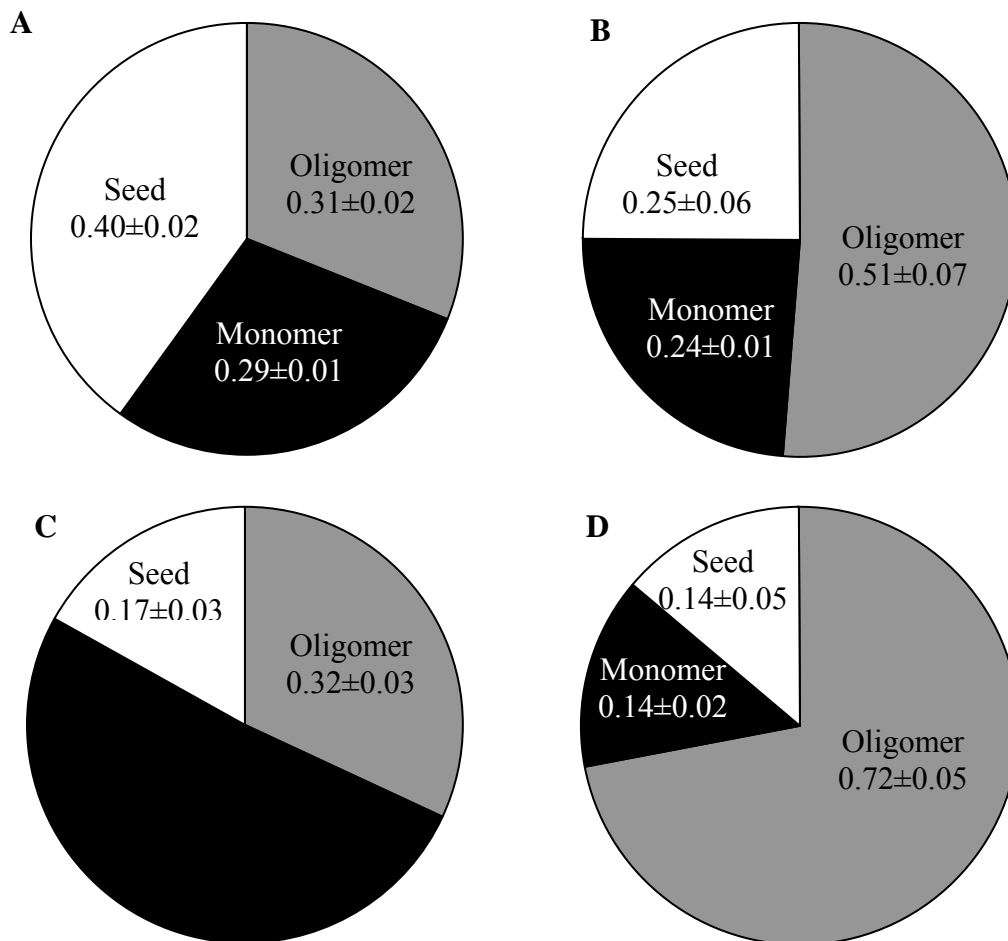


Figure 3.8 Composition of aerosol. **A:** neutral seeded α -pinene SOA, $M_{\text{seed}}/\Delta\text{HC} = 0.5$; **B:** acidic seeded α -pinene SOA, $M_{\text{seed}}/\Delta\text{HC} = 0.25$; **C:** acidic seeded α -pinene SOA, $M_{\text{seed}}/\Delta\text{HC} = 0.1$; **D:** acidic seeded terpinolene SOA, $M_{\text{seed}}/\Delta\text{HC} = 0.15$.

3.4.1 Experimental Yield

The most common way to determine the SOA yield has been defined by Odum et al. (1996) and described by equation 3.

$$Y = \frac{OM}{\Delta\text{HC}} \quad (3.3)$$

The SOA yield (Y) is determined by OM dividing by the amount of hydrocarbons reacted (ΔHC).

OM ($\mu\text{g}/\text{m}^3$) is estimated by the difference between the initial M_{seed} and the final M_{TOT} measured in the chamber (equation 1). The larger M_{seed} can cause larger aerosol yields. In Figures 3.8B and 3.8C,

as the fraction of M_{seed} increases the aerosol yield increases, as well as the fraction of oligomer present at %RH = 22-23. The resulting Y were 0.63 and 1.32 at $M_{\text{seed}}/\Delta\text{HC} = 0.1$ ($M_{\text{seed}} = 180 \mu\text{g}/\text{m}^3$) and $M_{\text{seed}}/\Delta\text{HC} = 0.25$ ($M_{\text{seed}} = 600\mu\text{g}/\text{m}^3$), respectively. SOA formed in the presence of neutral inorganic seed has a higher Y as compared to the self nucleated SOA (Table 3.1). It appears that the presence of inorganic seed aids oligomer formation and increases the SOA yield. This enhancement of oligomer formation can be explained by the presence of water contained in the inorganic seed aerosol as well as the slightly acidic nature of $(\text{NH}_4)_2\text{SO}_4$. The yield enhancement in neutral systems due to the presence of inorganic seed may be limited as $M_{\text{seed}}/\Delta\text{HC}$ increases because organic solubility may decrease by the presence of inorganics.

3.4.2 Effect of Particle Acidity on SOA Formation

The effect of particle acidity on the oligomeric fraction of seeded SOA was investigated for the ozonolysis of α -pinene in the presence of neutral and acidic inorganic seed aerosols. Figures 3.8A and 3.8B show the resulting aerosol compositions of the SOC, oligomer, and inorganic fractions. The SOA formed in the presence of acidic seed (Figure 3.8B) has a much higher mass fraction of oligomer than the neutral seeded SOA (Figure 3.8A). This observation is similar to the results of previous studies which have found higher SOA yields in the presence of acidic aerosols (Czoschke et al. 2003; Jang et al. 2006; Czoschke and Jang 2006; Northcross and Jang 2007). More than half of the OM of the acidic aerosols in this study is composed of oligomers as shown in Figure 3.8B. Oligomeric matter is also found in neutral aerosols (Figure 3.8A) although the oligomeric fractions are much smaller compared to SOA formed in the acidic environment.

3.4.3 Types of Terpenes

The subsequent reactivity for particle phase acid catalyzed reactions of the products formed from ozonolysis of terpenes is partially dependant on the initial structure of the terpene being oxidized. It is hypothesized that highly oxidized SOA products created from the ozonolysis of terpinolene are likely to be more reactive for particle phase reactions as compared to α -pinene-ozone

SOA (Northcross and Jang 2007). The two double bonds in terpinolene can be completely oxidized in excess ozone concentrations creating more oxidized products than α -pinene. Such multifunctional carbonyls in the terpinolene system increase oligomer formation (Jang et al., 2006) through the particle phase reactions in the aerosol, leading to a larger increase of mass formed in the acidic seed experiments in comparison to the neutral seed experiments.

Figure 3.8D presents the fractional composition of SOA produced from ozonolysis of terpinolene with acidic seed aerosol ($M_{\text{seed}}/\Delta\text{HC} = 0.10$). Comparison of α -pinene SOA (Figure 3.8C, $M_{\text{seed}}/\Delta\text{HC} = 0.1$) and terpinolene SOA (Figure 3.8D) demonstrates the influence of different terpenes on the M_{olig} fraction in SOA. The M_{olig} fraction is 0.72 for the total aerosol formed from the terpinolene SOA and 0.32 for α -pinene SOA. Baker et al. (2004) reported a larger fraction of aldehyde products from terpinolene ozonolysis, suggesting that the product distribution is partially responsible for the aerosol mass differences. The aldehyde products are more reactive for particle phase reactions than ketones and carboxylic acids (Jang et al., 2006).

3.5. Conclusion

This study demonstrated the ability of TGA to measure the oligomeric fraction of an aerosol composed of both inorganic and organic compounds. The methodology presented here is quantitative and practical for laboratory generated SOA. This method is limited to experimentally formed SOA and is not yet applicable to ambient SOA due to the necessity of the prior knowledge of the organic and inorganic compositions. However, if TGA is used in conjunction with current ambient aerosol characterizations techniques for analyses of major inorganic species and source apportionment methods for major primary particulate sources (Bhave et al, 2001), a reasonable estimate of the oligomeric fraction may be obtainable. Future studies should focus on the thermal decomposition of mixed inorganic compositions (e.g. $\text{NH}_4\text{-SO}_4\text{-NO}_3\text{-Na-Cl}$) which are ubiquitous in the ambient atmosphere.

The effect of heating the SOA may influence the formation of oligomers producing uncertainty in this technique and needs to be further studied through the studies of model compounds. Our study suggests that the heating effect is also expected to occur within OC/EC analysis adding another layer to the uncertainty of that technique as well. The effect of charring on the quantified oligomeric fraction has been tentatively measured, but should be further explored in future studies which will also help to decrease the uncertainty of this technique. However, the successful use of thermal denuders, which face many of the same uncertainties, to measure the nonvolatile fraction of both ambient and laboratory generated aerosols implies that this technique is applicable to filter collected SOA and will be useful to the aerosol community.

3.6 Acknowledgments

This work was supported by a grant from the National Science Foundation (ATM-0314128 and ATM-0703941). We would also like to thank Dr. Joseph DeSimone and Benjamin Pierce (Department of Chemistry at UNC-Chapel Hill) for analytical assistance.

3.7 References

- Baker, J., Arey, J., Atkinson, R. (2004). Kinetics of the gas-phase Reactions of OH radicals, NO₃ radicals and O₃ with three C7-carbonyls formed from the atmospheric reactions of myrcene, ocimene and terpinolene. *J. Atmos. Chem.* 48:241-60.
- Bahreini, R., Keywood, M.D., Ng, N.L., Varutbangkul, V., Gao, S., Flagan, R.C., Seinfeld, J.H., Worsnop, D.R., and Jimenez, J.L. (2005). Measurements of secondary organic aerosol from oxidation of cycloalkenes, terpenes, and m-xylene using an aerodyne aerosol mass spectrometer. *Environ. Sci. & Tech.* 39: 5674-88.
- Bhave, P.V., Ferguson, D.P., Prather, K.A., Cass, G. R. (2001) Source Apportionment of Fine Particulate Matter by Clustering Single-Particle Data: Tests of Receptor Model Accuracy. *Environ. Sci. & Tech.* 39: 2060-72.
- Clegg, S.L., Brimblecombe, P., and Wexler, A.S. (1998). Thermodynamic model of the system H⁺-NH₄⁺-Na⁺-SO₄²⁻-NO₃⁻-Cl⁻-H₂O at 298.15 K. *J. of Phys. Chem. A.* 102: 2155-71.
- Czoschke, N.M., Jang, M., and Kamens, R.M. (2003). Effect of acidic seed on biogenic secondary organic aerosol growth. *Atmos. Environ.* 37:4287-99.
- Czoschke, N.M. and Jang, M. (2006). Acidity effects on the formation of α -pinene ozone SOA in the presence of inorganic seed. *Atmos. Environ.* 40: 4370-80.
- Gao, S., Keywood, M., Ng, N.L., Surratt, J., Varutbangkul, V., Bahreini, R., Flagan, R.C., and Seinfeld, J.H. (2004a). Low-molecular-weight and oligomeric components in secondary organic aerosol from the ozonolysis of cycloalkenes and α -pinene. *J. of Phys. Chem. A.* 108: 10147-64.
- Gao, S., Ng, N.L., Keywood, M., Varutbangkul, V., Bahreini, R., Nenes, A., He, J., Yoo, K., Beauchamp, J.L., Hodyss, R.P., Flagan, R.C., and Seinfeld, J.H., (2004b). Particle phase acidity and oligomer formation in secondary organic aerosol. *Environ. Sci. & Tech.* 38:6582-89.
- Gross, D.S., Galli, M.E., Kalberer, M., Prevot, A.S.H., Dommen, J., Alfarra, M.R., Duplissy, J., Gaeggeler, K., Gascho, A., Metzger, A., and Baltensperger, U. (2006). Real-time measurement of oligomeric species in secondary organic aerosol with the aerosol time-of-flight mass spectrometer. *Anal. Chem.* 78:2130-37.
- Iinuma, Y., Boge, O., Gnauk, T., and Herrmann, H. (2004). Aerosol-chamber study of the α -pinene/O₃ reaction: Influence of particle acidity on aerosol yields and products. *Atmos. Environ.* 38:761-73.

- Iinuma, Y., Müller, C., Böge, O., Gnauk, T., and Herrmann, H., (2007). The formation of organic sulfate esters in the limonene ozonolysis secondary organic aerosol (SOA) under acidic conditions. *Atmos. Environ* 41:6678-83..
- Jang, M., Czoschke, N.M., Lee, S., and Kamens, R.M. (2002). Heterogeneous atmospheric aerosol production by acid-catalyzed particle-phase reactions. *Science* 298:814-17.
- Jang, M., Carroll, B., Chandramouli, B., and Kamens, R.M. (2003). Particle growth by acid-catalyzed heterogeneous reactions of organic carbonyls on preexisting aerosols. *Environ. Sci. & Tech.* 37:3828-37.
- Jang, M., Czoschke, N.M., Northcross, A.L., Cao, G., and Shaof, D. (2006). SOA formation from partitioning and heterogeneous reactions: Model study in the presence of inorganic species. *Environ. Sci. & Tech.* 40:3013-22.
- Joback, K.G. and Reid, R.C. (1987). Estimation of pure-component properties from group contributions. *Chem. Engin. Comm.* 57: 233-43.
- Kalberer, M., Paulsen, D., Sax, M., Steinbacher, M., Dommen, J., Fisseha, R., Prevot, A.S.H, Frankevich, V., Zenobi, R., Baltensperger, U. (2004). Identification of polymers as major components of atmospheric organic aerosols. *Science* 303: 1659-62.
- Kiyoura, R. and Urano, K. (1970). Mechanism, kinetics, and equilibrium of thermal decomposition of ammonium sulfate. *Ind. & Engin. Chem. Proc. Des. & Devel.* 9:489-94.
- Liggio J., Li, S.-M., McLaren, R. (2005). Heterogeneous Reactions of Glyoxal on Particulate Matter: Identification of Acetals and Sulfate Esters. *Environ. Sci. & Tech.* 39: 1532-1541.
- McMurray, P.H. and Grosjean, D. (1985) Gas and aerosol wall losses in Teflon film smog chambers. *Environ. Sci. & Tech.* 19:1176-82.
- Nenes, A., Pandis, S.N., and Pilinis, C. (1998). ISORROPIA: A new thermodynamic equilibrium model for multiphase multicomponent inorganic aerosols. *Aqua. Geochem.* 4:123-52.
- Northcross, A.L., and Jang, M. (2007). Increases in SOA Yield from Heterogeneous Acid Catalyzed Reactions. *Atmos. Environ.* 41:1483-93.
- Odum, J.R., Hoffmann, T., Bowman, F., Collins, D., Flagan, R.C., and Seinfeld, J.H. (1996). Gas/Particle partitioning and secondary organic aerosol yields. *Environ. Sci. & Tech.* 30:2580-85.

Rothe, M. and Rothe, I. (1989). Chapter 4, Physical properties of oligomers. in *Polymer Handbook*, eds. J. Brandrup and E. H. Immergut, New York: John-Wiley and Sons.

Saunders, S.M., Jenkin, M.E., Derwent, R.G., and Pilling, M.J. (2003). Protocol for the development of the master chemical mechanism, MCM v3 (part A): tropospheric degradation of non-aromatic volatile organic compounds. *Atmos. Chem. and Phys.* 3: 161-180.

Semmler, M., Luo, B.P., and Koop, T. (2006). Densities of liquid $\text{H}^+ / \text{NH}_4^+ / \text{SO}_4^{2-} / \text{NO}_3^- / \text{H}_2\text{O}$ solutions at tropospheric temperatures. *Atmos. Environ.* 40:467-83.

Stein, S.E. and Brown, R.L. (1994). Estimation of normal boiling points from group contributions. *J. Chem. Inform. & Comp. Sci.* 34:581-7.

Surratt, J.D., Kroll, Jesse H., Kleindienst, Tadeusz E., Edney, E. O., Claeys, M., Sorooshian, A., Ng, Nga L., Offenberg, J. H., Lewandowski, M., Jaoui, M., Flagan, R. C., Seinfeld, J. (2007). Evidence for Organosulfates in Secondary Organic Aerosol. *Environ. Sci. & Tech.* 41: 517-27.

Tolocka, M., Jang, M., Ginter, J.M., Kamens, R.M., and Johnston, M. (2004). Formation of oligomers in secondary organic aerosol. *Environ. Sci. & Tech.* 38:1428-34.

Yu, J., Cocker, D.R., Griffin, R.J., Flagan, R.C., and Seinfeld, J.H. (1999). Gas-phase ozone oxidation of monoterpenes: gaseous and particulate products. *J. of Atmos. Chem.* 34: 207-58.

Zhu, X., Elomaa, M., Sundholm, F., and Lochmuller, C. H. (1997). Thermal and thermo-oxidative degradation of polystyrene in the presence of ammonium sulfate. *Macro. Chem. and Phys.* 198: 3137-48.

Chapter 4

Modeling Formation of SOA from Thermodynamic Partitioning and Heterogeneous Acid Catalyzed Reactions in the Presence of Inorganic Aerosols

Amanda L. Northcross[#], and Myoseon Jang^{*}

[#]Department of Environmental Sciences and Engineering
The University of North Carolina at Chapel Hill

^{*}corresponding author

Department of Environmental Engineering Science

The University of Florida

P.O. Box 116450

Gainesville, FL 32611-6450

Tel: 352-846-1744

email: mjang@ufl.edu

In preparation for submission to Environmental Science and Technology

4.1 Introduction

In the ambient atmosphere aerosols are composed of both inorganic and organic compounds (Drewnick et al. 2004; Russell et al. 2004; Morishita et al. 2006), originating from primary and secondary sources (Zhao and Hopke 2006; Kleeman et al. 2007; van Donkelaar et al. 2007; Bae et al. 2006; Pekney et al. 2006). Primary aerosols are emitted directly into the atmosphere and are much easier to quantify in comparison to secondary aerosols which are formed in the atmosphere. The total atmospheric aerosol composition can be modeled to estimate the concentration of various pollutants in the atmosphere, as well as to understand the effects of emission regulations a priori. Regional atmospheric models are typically composed of modules which simulate the concentration of constituents, such as inorganic and organic aerosols, and also simulate atmospheric processes such as gas phase chemical reactions, weather phenomena, and secondary organic aerosol (SOA) formation. Component modules are typically used to simplify complex ambient atmospheric system processes. This approach, although extremely practical can be flawed when atmospheric processes are able to be influenced by components which are not contained in the module. Secondary organic aerosol formation is one case when this occurs. Inorganic aerosols are currently modeled separately from organic aerosol formation, but are able to influence SOA formation. In other words the whole may be greater than the sum of the parts. A model which considers the interaction between inorganic and organic compounds to accurately describe SOA formation using atmospheric models is needed.

SOA formation has traditionally been described using the thermodynamic partitioning theory developed by (Pankow 1994). Thermodynamic partitioning describes SOA mass formation by the accommodation of oxidized gas phase products into preexisting particles and the establishment of a thermodynamic equilibrium between the gas and particle phases. However, ambient aerosols can contain both organics and inorganic acid. The inorganic acid constituents of ambient aerosols are able to catalyze particle phase reactions forming oligomers, altering the thermodynamic equilibrium, and causing further partitioning of gas phase products in order to reestablish the equilibrium. The overall result of particle phase reactions are increases in SOA mass beyond that attributable solely to

thermodynamic partitioning. The amount of particle phase acid catalyzed mass formed in SOA is affected by the inorganic compounds, the ability of the partitioned oxidized organic products to react within the particle phase, the relative fractions of inorganic and organic constituents, as well as the concentration of water in aerosol (Jang et al. 2002;Jang et al 2003).

This study presents an SOA model which attempts to the relative influences of thermodynamic partitioning as well as particle phase oligomer forming reaction on SOA formation. The proposed SOA model builds on the previous work (Czoschke and Jang 2006;Jang et al. 2005;Jang et al. 2004;Jang et al. 2002;Jang et al. 2003;Northcross and Jang 2007;Tolocka et al. 2004) which has focused on characterizing, quantifying and describing heterogeneous acid catalyzed SOA formation. The model presented here further expands a previous model (Jang et al. 2006), which described SOA formation from α -pinene in the presence of inorganic acidic aerosols to include limonene and terpinolene and also tests the model at concentrations which are atmospherically relevant.

α -Pinene, d-limonene, and terpinolene, the precursor VOCs, are biogenic terpenes. Biogenic terpenes are responsible for as much as 70% of the organic aerosol mass formed in the Southeast United States (Weber et al. 2007). This model is rigorously tested against experimental data produced using an indoor smog chamber. The model was tested using both the total aerosol mass formed from the ozonolysis of the terpenes in the presence of inorganic aerosols, as well as the measured organic oligomer fraction of the aerosols which was determined using thermal gravimetric analysis (TGA) (See Chapter 3). We are able to determine the expected SOA mass from the ozonolysis of three monoterpenes in the presence of both inorganic acidic and neutral aerosols and able to determine the fraction of oligomer mass formed at atmospherically relevant concentrations. The uniqueness of the model presented in this study is its ability to incorporate the influences pf both inorganic and organic compounds to estimate SOA mass.

4.2 Experimental Methods

The SOA yield study was conducted in the UNC indoor 2m³ Teflon film smog chamber. The monitoring equipment for the gas and particle concentrations includes: SMPS/CNC (TSI Model 3080 and Model, 3025A respectively) for particle number and sizes, GC/FID (Shimadzu) for terpene concentration, ozone monitor (Thermo Electron Instruments UV Photometric O₃ analyzer model 49), temperature and humidity probes. In depth analysis of aerosol samples were conducted using Fourier transform infrared spectroscopy (FTIR) (Nicolet Magna-IR 560 Spectrometer - MCD detector), and TGA (Pyris 1, Perkin Elmer).

Inorganic seed aerosol was added to the chamber by atomizing seed solutions of varying compositions. Ozone was added to the chamber using an ozone generator. Organic aerosol was formed by volatilizing terpenes into the chamber where they reacted with ozone. The aerosol formed was measured using a scanning mobility particle sizer in series with a condensation nuclei counter and the aerosol mass concentration was determined using the cumulative volume and an organic aerosol density of 1.4 g/m³ for SOA (Bahreini et al. 2005) and an estimated density for the inorganic aerosol from ISORRPIA (Nenes et al. 1998). Table 4.1 contains a summary of the experimental conditions.

Terpene	Terpene Conc. (ppm)	Acidity Level of Inorganic Aerosol	%RH	Inorganic Aerosol Mass Conc. (µg/m ³)	Ozone Conc. (ppm)	n
α-Pinene	0.05 - 0.25	Neutral	39-53%	399-511	0.3	18
α-Pinene	0.05 - 0.25	Mild Acid	22-53%	44-509	0.3	11
α-Pinene	0.05 - 0.25	Strong Acid	16-53%	124-600	0.3	21
d-Limonene	0.05 - 0.25	Neutral	38-54%	119-305	0.3	17
d-Limonene	0.05 - 0.25	Mild Acid	28-43%	117-372	0.3	11
d-Limonene	0.05 - 0.25	Strong Acid	20-48%	130-364	0.3	22
Terpinolene	0.05 - 0.25	Neutral	38-61%	178-396	0.3	21
Terpinolene	0.05 - 0.25	Mild Acid	24-43%	187-437	0.3	10
Terpinolene	0.05 - 0.25	Strong Acid	23-53%	123-320	0.3	14

Table 4.1 Experimental conditions for chamber generated SOA formed from the ozonolysis of α-pinene, d-limonene, and terpinolene in the presence inorganic aerosols. n is number of experiments conducted.

TGA was conducted on aerosols sampled on a quartz fiber filter taken at the conclusion of a chamber experiment. Due to the minimum mass requirements additional experiments were conducted at higher terpene and seed aerosol concentrations to increase the SOA mass formed and sampled. The fraction of inorganic to organic compounds in the aerosol was controlled to remain in the same range as the aerosol yield experiments. The analysis technique used is fully described in Chapter 3 of this document. TGA data interpretation of the inorganic/organic aerosols decouples and subtracts the inorganic fraction signal from the signal of the total aerosol. The remaining thermogram represents the organic fraction. The non-oligomer organic fraction of the aerosol is more volatile than the oligomer fraction. At ~230°C the non-oligomer organic mass has volatilized, and the remaining mass is attributable to the oligomer fraction. At temperatures higher the oligomer begins to decompose and at lower temperatures the non-oligomers are still present in the sample. The oligomer fraction measured is compared to the model estimated particle phase acid catalyzed mass formed.

4.3 Model Development

The proposed model is a compilation of three separate modules: gas phase chemistry, thermodynamic partitioning, and particle phase heterogeneous reactions. The gas phase terpene ozonolysis mechanism and reaction products are modeled using the Master Chemical Mechanism (MCM) (Jenkin 2004) and protocol (Saunders et al. 2003). The ozonolysis products formed are lumped into twenty groups based on thermodynamic partitioning, and acid catalyzed particle phase reactions. The particle phase oligomer mass (OM_H) and the mass attributable solely to thermodynamic partitioning (OM_P) are modeled for each product group using separated modules. The total organic mass (OM) formed is estimated by adding OM_P and OM_H (equation 4.1).

$$OM = OM_P + OM_H \quad (4.1)$$

4.3.1 Gas Phase Mechanism

A prediction of the gas phase organic products from the ozonolysis of the reactive organic gas (ROG) is fundamental to model SOA formation. An explicit gas phase kinetic model using the master chemical mechanism version 3 (MCM v.3) (Saunders et al. 2003; Jenkin 2004) was used in

this study. MCM produces a near explicit product distribution for the reaction of ozone and α -pinene (Jenkin 2004) based on reactant structural reactivity. The MCM protocol (Saunders et al. 2003b) was used to develop the gas phase model for ozonolysis of d-limonene and terpinolene. The model predicted ozone and terpene decays of the ozonolysis of α -pinene, limonene and terpinolene are compared to experimentally observed chamber data in Figures 4.1 A, B, C. Both ozone and terpene decays predicted by the MCM model reasonably agree with experimental data.

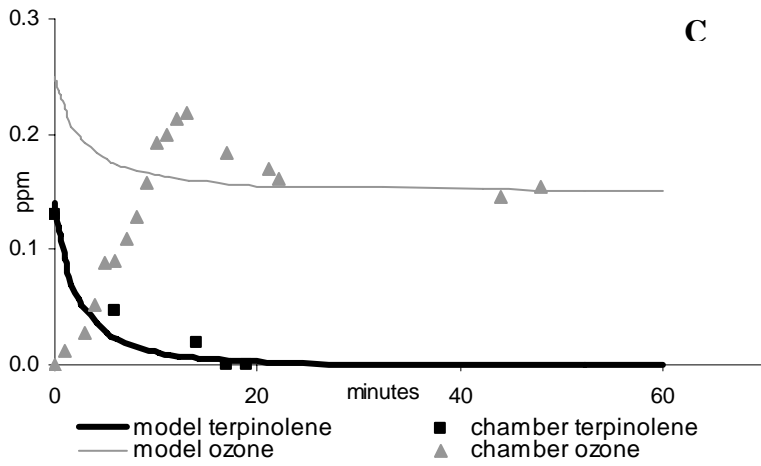
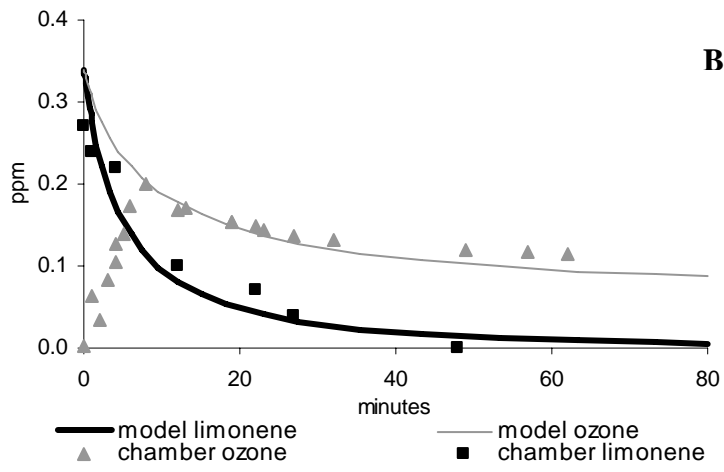
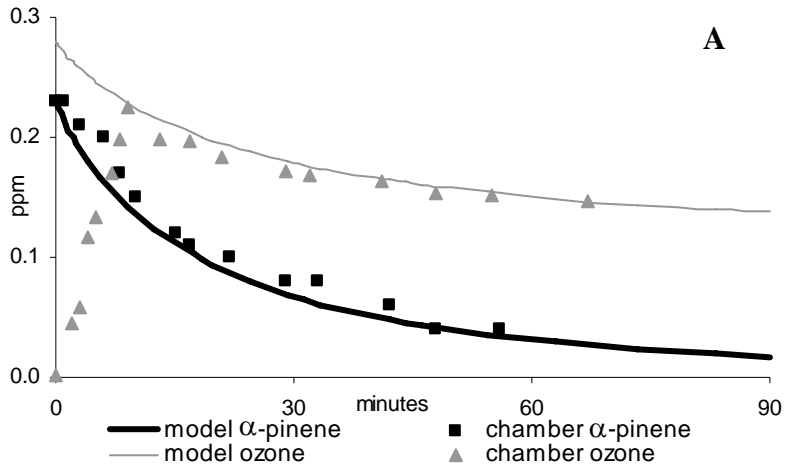


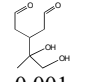
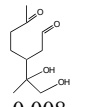
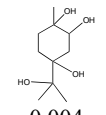
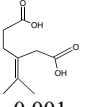
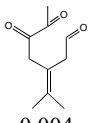
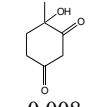
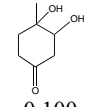
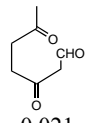
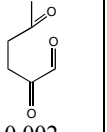
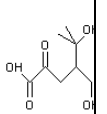
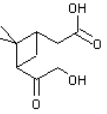
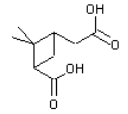
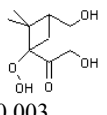
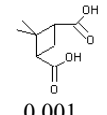
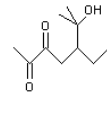
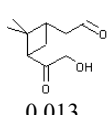
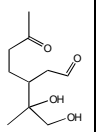
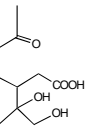
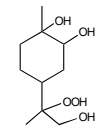
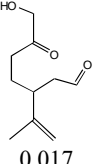
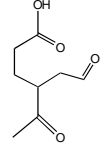
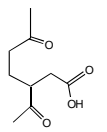
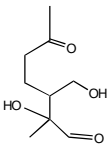
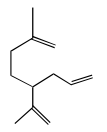
Figure 4.1 Gas phase terpene ozonolysis model estimation and smog chamber data. MCM model and protocol simulation for the decay of α -pinene, limonene and terpinolene with ozone and smog chamber experimental data for terpene and ozone decays. Terpene concentrated measured using GC/FID, ozone concentration measured using ozone monitor. Started adding ozone at time=0.

The explicit model produces over 100 products in the gas phase. Products estimated to have concentrations higher than 1×10^6 ppm were used in this study. The products were classified based on estimated vapor pressures and their reactivity for heterogeneous reactions. Vapor pressures of organic products are estimated using equation 4.2 (Schwarzenbach et al. 1992)

$$\ln^i p_L^o = \frac{\Delta S_{vap}(T_b)}{R} \left[1.8 \left(1 - \frac{T_b}{T} \right) + 0.8 \left(\ln \frac{T_b}{T} \right) \right] \quad (4.2)$$

The boiling point (T_b) is determined using a group contribution method (Joback and Reid 1987) modified by (Stein and Brown 1994). The entropy of vaporization ($\Delta S_{vap}(T_b)$) is estimated using a method developed by Zhao et al. (1999). Products are lumped into one of five vapor pressure groups labeled based on the partitioning coefficient which is inversely proportional to vapor pressures: VLP ($10^{-8} < \text{kPa}$), LP ($10^{-8} - 10^{-6}$ kPa), MP ($10^{-6} - 10^{-3}$ kPa), HP ($10^{-3} - 10^{-1}$ kPa) and VHP ($< 10^{-1}$ kPa). Each vapor pressure group is further segmented into four groups representing their heterogeneous reactivity: High (HR), medium (MR), weak (WR), and no reactivity (NR). These groups are determined by the product structure and the chemical functional group heterogeneous reactivity using the ranking system: multifunctional aldehydes > aldehydes > ketones > carboxylic acids (Carey and Sundberg 2000; Jang et al. 2005). For example, highly reactive products include α -carbonyl aldehydes, dialdehydes, or aldehydes with an alcohol group. Medium reactivity products contain only one aldehyde group. Low reactivity products contain ketones and carboxylic acids. Products which are inert to particle phase reactions do not contain carbonyl groups. Table 4.2 shows the representative structures for the lumped product groups for α -pinene, terpinolene, and limonene ozonolysis based on the estimated vapor pressures and reactivity.

The model was run for three terpenes of this study varying ozone concentrations. The resulting product distribution is described with stoichiometric coefficients (α_i), which remains almost constant when ozone is in excess. The average value for α_i is used in the model.

	VHP HR	VHP MR	VHP LR	VHP NR	HP HR	HP MR	HP LR	HP NR	MP HR	MP MR
terp	 0.001	 0.008	 0.004	 0.001	 0.004	 0.008	 0.100		 0.021	 0.002
α -pine	 0.002	 0.008	 0.020			 0.003	 0.001		 0.010	 0.013
d-lim	 0.036	 0.035	 0.005		 0.017	 0.029	 0.028		 0.006	 0.034

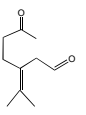
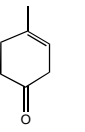
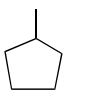
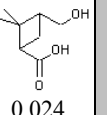
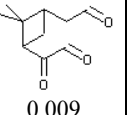
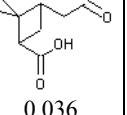
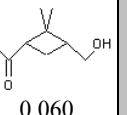
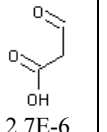
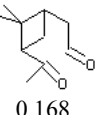
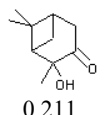
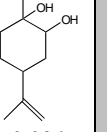
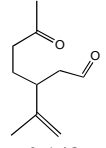
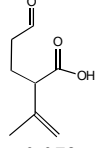
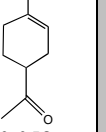
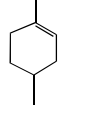
	MP LR	MP NR	LP HR	LP MR	LP LR	LP NR	VLP HR	VLP MR	VLP LR	VLR NR
terp	 0.002				 0.013					 0.070
α -pine	 0.024		 0.009	 0.036	 0.060		 2.7E-6	 0.168	 0.211	
d-lim	 0.094		 0.148	 0.073	 0.058					 0.047

Table 4.2 Stoichiometric coefficients and representative product group structures from the MCM product distribution for the ozonolysis of α -pinene, d-limonene, and terpinolene.

4.3.2 OM_H Model

Jang et al. developed the OM_H model (Jang et al. 2006) that estimates the formation of organic particle phase oligomer SOA mass. The heterogeneous particle phase reaction of partitioned oxidized organic products is described as a second order reaction, governed by the reaction rate constant k_H (equation 4.3) (Jang et al. 2005). Within the OM_H model, a sub-model calculates k_H using a semi-empirical equation developed by Jang et al. (2005).

$$k_{H,i} = rpK_{BH^+} + xX + z \log(a_{in,w} C_{H^+}) + sI \quad (4.3)$$

The rate constant accounts for both the structural influence of organic products on particle phase reactivity and the effect of the acidic inorganic aerosol. pK_{BH^+} describes the ability of a carbonyl to become protonated in acidic media and is determined using the representative structures for each product group. I is a structural indicator variable, used to classify the reactivity of the product groups for heterogeneous reactions. The affect of the acidic inorganic seed aerosol on OM_H is accounted for using the proton concentration (C_{H^+}), the activity coefficient ($a_{in,w}$) of the water in the inorganic aqueous aerosol and the excess acidity (X) of the acidic inorganic aerosol. The C_{H^+} and $a_{in,w}$ are estimated using an inorganic thermodynamic model, ISORROPIA, developed by Nenes et al. (1998). The X is determined based on the fraction of pure sulfuric acid in the aerosol, and the relative humidity in the system (Jang et al. 2004; Cox and Yates 1978) and compensates for the non-ideality of the acidity in the inorganic aerosols. r , x , z , and s , are the regression variables for the multi-variable regression (Jang et al. 2005).

The total aerosol mass formed by heterogeneous reactions for each product group ($OM_{H,i}$) is determined by equation 4.4 (Jang et al. 2006). The total mass is shown as the summation of the OM_H produced for products groups based on heterogeneous particle phase reactivity (i), and

thermodynamic partitioning (j).

$$OM_H = \sum_i \sum_j f_H \frac{\left(k_{H_j} t M_{seed} + k'_{oj} t \right) \left(\frac{10^3 \alpha_{i,Hj} \Delta ROG K_{om,i} \gamma_{om,i} V_{om} \rho_{om}}{MW_i \gamma_{w,i} V_w \rho_w} \right)^2}{1 + \left(k_{H_j} t M_{seed} + k'_{oj} t \right) \left(\frac{10^3 \alpha_{i,Hj} \Delta ROG K_{om,i} \gamma_{om,i} V_{om} \rho_{om}}{MW_i \gamma_{w,i} V_w \rho_w} \right) \left(\frac{MW_i \gamma_{w,i} V_w \rho_w}{10^3 K_{om,i} \gamma_{om,i} V_{om} \rho_{om}} \right)^2} \quad (4.4)$$

The derivation of equation 4.4 was performed by Jang et al. (2006) and a more in-depth description can be found in this reference. The important features of this model include: the partitioning of a product group to an existing inorganic aerosol using thermodynamic partitioning; the influence of the mass of inorganic seed aerosol (M_{seed}) present ; the heterogeneous rate constant of the organic products in the absence of inorganic seed aerosol ($k'_{oj} t$); the amount of terpene reacted by ozonolysis (ΔROG); the stoichiometric coefficient for each product group ($\alpha_{i,Hj}$); and the rate constant ($k_{H,i}$) of organic species for the heterogeneous reactions (equation 4.3).

The partitioning of an organic species into an aqueous inorganic aerosol is different than an organic species partitioning into an organic aerosol. The conversion of an organic species partitioning into aqueous inorganic aerosol is considered using the activity coefficients (γ) of the product group in water (_w) and semi-volatile organics (_{om}). γ_{om} are γ_w is estimated using the UNIFAC (Choy et al. 1996) group combination method, for each product group i . The aerosol mass differences are captured as the ratio molecular volume (V) and density (ρ) of water and organic monomer (_{om}).

4.3.3 OM_P Model

The aerosol mass formed solely by thermodynamic partitioning (OM_P) is estimated by modifying the preexisting secondary organic aerosol model (SOGRAM) developed by Schell et al. (2001). SOGRAM has been used for the estimation of SOA within regional scale atmospheric models. SOGRAM was modified (equation 4.5) in this study to include the contribution of

$$OM_p = \sum_i \left[C_{tot,i} - C_{H,i} - C_{sat,i}^* \frac{C_{aer,i} / m_i}{\sum_{a=1}^n (C_{aer,a} / m_a) + C_{init} / m_{init}} \right] \quad (4.5)$$

C_i is the concentration of a product group in the aerosol (_{aer}), the total product formed from the ozonolysis reactions (_{tot}), and the concentration of compound i which oligomerizes (_H). $C_{sat,i}^*$ is the saturation concentration of compound i in the gas phase as determined by thermodynamic

partitioning. The term $\sum_{a=1}^n (C_{aer,a} / m_a) + C_{init} / m_{init}$ represents the total aerosol mass available for partitioning, (Pankow, 1994) $C_{aer,a} / m_a$ is the total aerosol mass which is present in the aerosol by thermodynamic partitioning but does not include compound i and C_{init} / m_{init} is the preexisting aerosol mass, which we treat as OM_H . $C_{aer,a} / m_a$ is dependant on the compounds partitioning and is solved for iteratively using a combination of Newton's method and a globally convergent strategy for nonlinear systems (Odum et al. 1996). By summing OM_H and OM_p the total SOA mass is estimated. The remainder of this paper illustrates the modules ability to estimate the SOA from three different terpene species, three inorganic aerosol compositions, and relative humidity ranging from 20-50%RH.

4.4 Results and Discussion

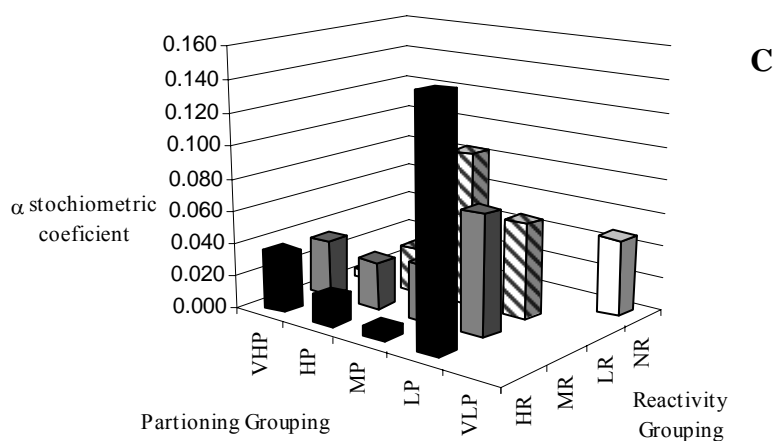
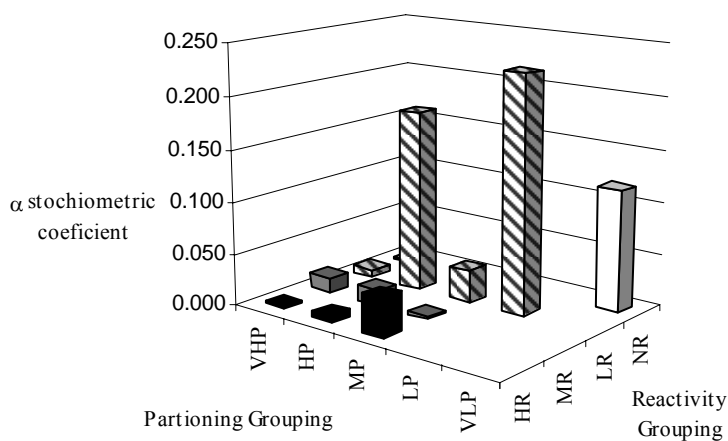
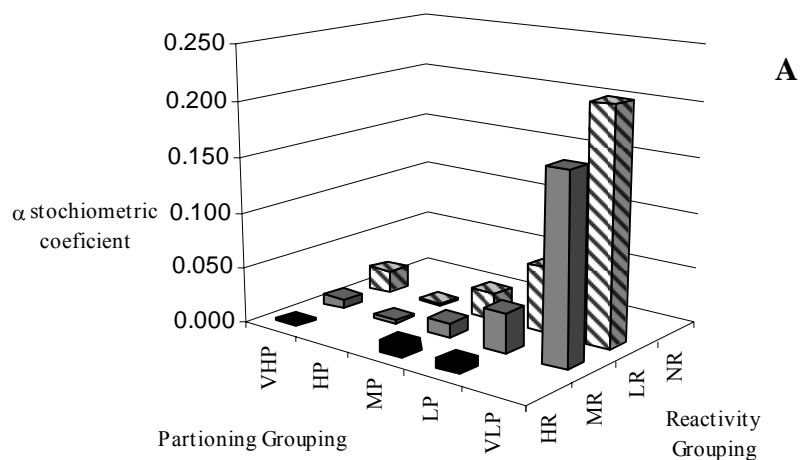


Figure 4.2 Stoichiometric coefficients from terpene ozonolysis, grouped based on thermodynamic partitioning: very high partitioning (VHP), high partitioning (HP), medium partitioning (MP), low partitioning (LP) and very low partitioning (VLP), and heterogeneous reactivity: highly reactive (HR), medium reactivity (MR), low reactivity (LR), and non-reactive (NR) **A**. α -pinene ozonolysis, **B** terpinolene ozonolysis, **C** d-limonene ozonolysis.

4.4.1 Product Distribution

The differences in the aerosol mass formed from the terpene systems are due to both the partitioning coefficients of the oxidized products as well as the particle phase reactivity. Figure 4.2 shows the stoichiometric coefficients for the gas phase oxidized products formed by MCM. The products for the three terpenes are ranked by partitioning and reactivity. Table 4.2 shows the representative structures for each of the product groups.

Comparing the product groups of the three terpenes shows that terpinolene and α -pinene have the most volatile products. The majority of the products formed in the α -pinene ozonolysis reactions are the low partitioning and very low partitioning groups. In comparison d-limonene has a product distribution which is more evenly spread over all of the partitioning groups.

The product grouping based on the heterogeneous reactivity is also shown in Figure 4.2. d-Limonene forms the largest concentration of highly reactive products, with very few products that do not react heterogeneously. Terpinolene has low and no reactivity products and the α -pinene ozonolysis products are mostly composed of medium and low reactivity products. The combination of high partitioning and high reactivity makes d-limonene less sensitive to changes in particle phase acidity. The d-limonene products readily react in the particle phase regardless of particle acidity compared to those of α -pinene and terpinolene. The largest fraction of terpinolene products which participate in particle phase reactions are grouped in the low reactivity group. Terpinolene derived SOA is more sensitive to changes in particle phase acidity (Northcross and Jang, 2007). For products which have a low reactivity for particle phase reactions, a strongly acidic particle will have more effect on the particle phase reactions by causing a large change to the reaction rate compared to more reactive products. High reactivity products also see an increase in the reaction rate due to increased particle acidity. However, the increase to the rate is not as large because these products are not as sensitive to inorganic acidity.

It is not possible to predict the total aerosol mass by only examining oligomerization through heterogeneous reactions or thermodynamic partitioning. For example, terpinolene has lower values for partitioning than α -pinene but produces more aerosol mass Figure 4.3. It may appear that particle phase reactivity drives SOA mass formation, but this assumption only holds in this specific study due to the similarity in the vapor pressure ranges of the gas phase reaction products. Isoprene a 5 carbon monoterpene species produces products with very high particle phase reactivity but very high vapor pressures that significantly reduce the SOA formation.

4.4.2 Total SOA Production

Figures 4.3 A, B and C show the total SOA mass estimated using the OM_P and OM_H models compared to the chamber produced SOA for each of the three terpenes. The total SOA production was tested against SOA formed in the presence of inorganic aerosols of neutral, mild and strong acidity and at two different relative humidities.

In previous studies (Jang et al. 2005; Czoschke and Jang, 2006; Northcross and Jang, 2007) we have shown that as the relative humidity increases the particle phase acidity decreases, as well as the acid catalyzed particle phase reactions rate. Figure 4.3 highlights the capability of the model to simulate the decrease in the production of particle phase organic aerosol mass. When the seed mass and chemical compositions are similar, the system with the higher humidity (~40%) produces less total aerosol mass, than the lower %RH systems (~20%RH). The model uses relative humidity to estimate the proton concentration, as well as the excess acidity, which quantify the acidity of the inorganic aerosol. Thus when the %RH is low the aerosol mass is higher due to increased heterogeneous aerosol mass being formed. Terpinolene and α -pinene both show larger responses to humidity do to their increased responsiveness to acidity as compared to limonene (section 4.4.1).

It is important to note that as OM_H increases, OM_P simultaneously increases as well because OM_H is treated as absorbing mass in the OM_P model. Thus the fraction of heterogeneous aerosol mass is less sensitive but the overall total aerosol mass changes. The increase in particle phase

oligomer formation due to a lower the humidity is the largest for terpinolene, followed by α -pinene and d-limonene respectively. The same order was also reported in the previous work by Northcross and Jang (2007).

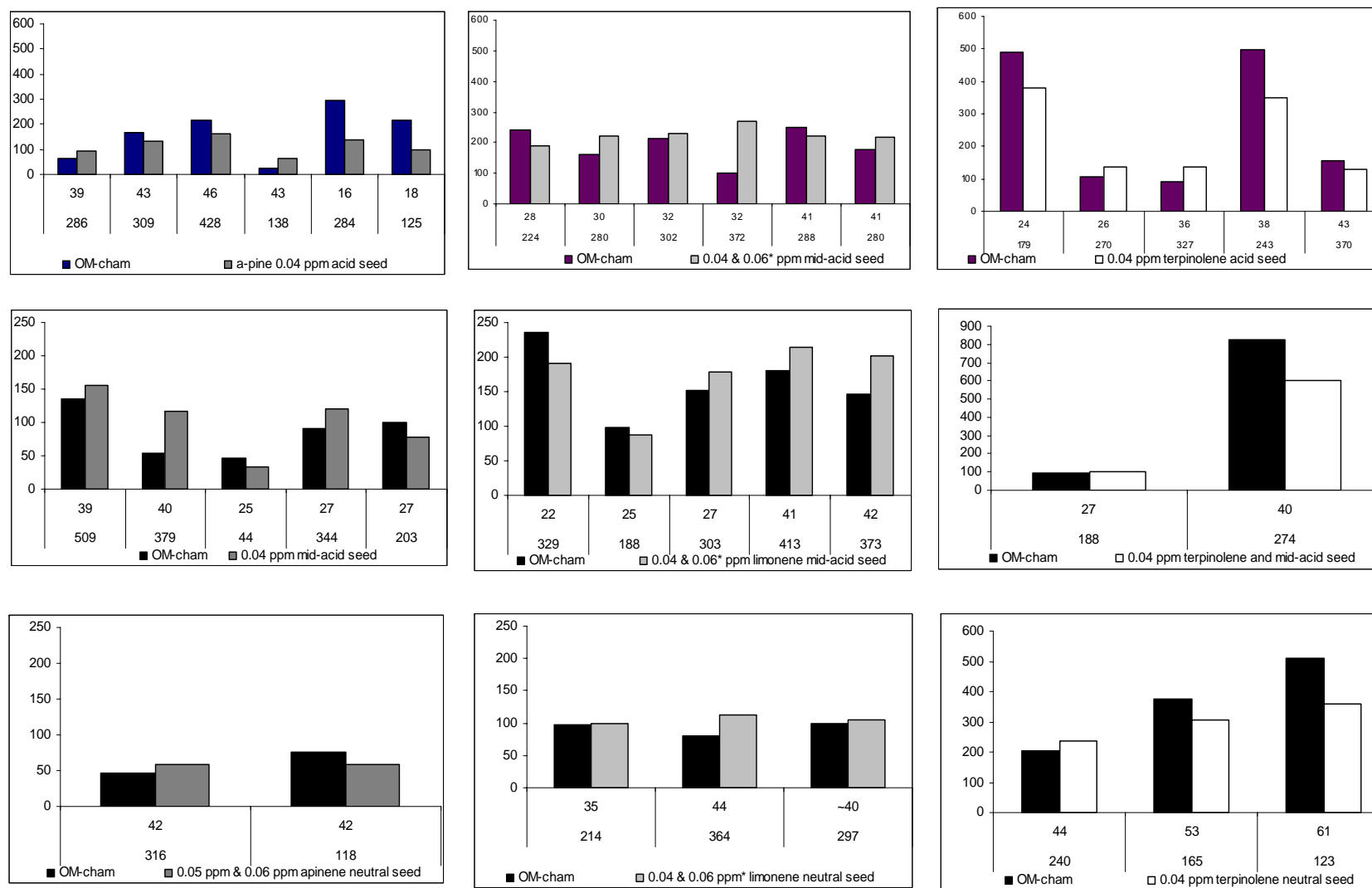


Figure 4.3 Total SOA mass from terpene ozonolysis in the presence of inorganic aerosols at low and high %RH. Acid seed: 2:3 $\text{H}_2\text{SO}_4/\text{NH}_4\text{HSO}_4$ Mid-acid seed 3:7 $\text{H}_2\text{SO}_4/\text{NH}_4\text{HSO}_4$, neutral seed $(\text{NH}_4)_2\text{SO}_4$. Black bar represent SOA from the smog chamber experiments, shaded bars are model results.

4.4.3 Oligomer Estimation

This model is distinct in that it is able to predict both total SOA mass as well as the SOA mass formed by heterogeneous reactions. The model oligomer mass estimation is compared the aerosol phase oligomer formed experimentally and measured using a TGA technique (see Chapter 3). The TGA method uses temperature to separate the semivolatile fractions from the oligomer mass which is less volatile. The maximum sample volume for the experimental setup was 1m^3 which limits the amount of aerosol mass which can be sampled. TGA, requires at least 1mg sample therefore, the TGA set of experiments were conducted at concentrations which are higher than atmospheric concentrations. We have maintained similar ratios of seed to SOA and assumed that the oligomer fractions will remain constant with higher aerosol mass concentrations; as long as the ratio of seed to SOA and ROG remains constant and all other parameters are similar. Figure 4.4 shows a comparison of the oligomer fraction of the chamber sampled SOA and the subsequent model estimated values. The module is able to estimate OM_H total mass within the uncertainty level.

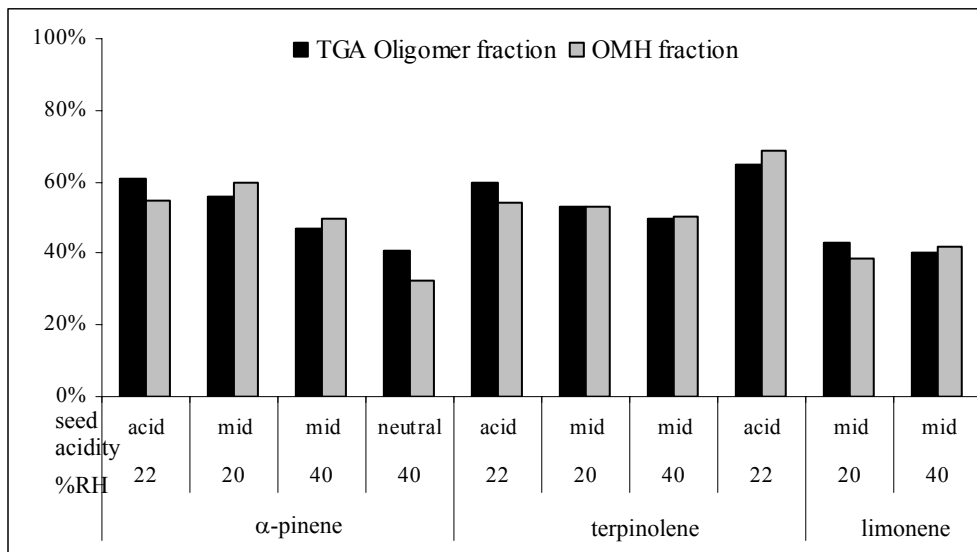


Figure 4.4 Comparison of oligomer fraction of the organic SOA. Oligomer fraction measured using TGA, OM_H estimated using equation 4.3. Black bars are experimentally measured TGA oligomer fractions, shaded bars are model results from oligomer fractions estimated using the shown acidity and relative humidity.

4.4.4 Acidic Inorganic Seed Concentration and SOA Mass

SOA mass formation is not only dependant on the amount of terpene reacted but is also dependant on the inorganic aerosol mass concentration (Northcross and Jang, 2007). As the concentration of inorganic aerosols increases, the subsequent SOA mass formed increases as well. Figures 4.2 A, B, and C, show that, as the concentration of inorganic seed aerosol increased, regardless of particle phase acidity, the observed aerosol mass increased. This suggests that the traditional method of estimating SOA based on the amount of reacted organic gas may not be an appropriate method for the estimation of SOA formed in the presence of inorganic aerosols. This model compensates for the presence of differing mass concentrations of inorganic aerosols using the f_H term, as defined by Jang et al (2006) in equation 4.5. The term a , is determined empirically using chamber data and ranges from 0.11 to 0.18 due to the variance of SOA produced by the different monoterpenes.

$$f_h = \frac{1}{1 + a \frac{M_{seed}}{ROG}} \quad (4.5)$$

The model is able to predict SOA mass when $\frac{M_{seed}}{ROG}$ is both large and small. When the seed mass is dominate in the system and $\frac{M_{seed}}{ROG}$ is large and this occurs in nature in areas of high inorganic aerosol production (*i.e.* coastal areas, live stock farming, and industrial processes with high SO₂ emissions). Small $\frac{M_{seed}}{ROG}$ values are representative of areas with high VOC emissions, such as agricultural areas and natural parks. The model performs well with both small and large values. At extremely small values equilibrium assumptions may not hold, and large values nucleation may become more important. The goal of this model was to predict the SOA mass formation from the ozonolysis of monoterpenes in the presence of inorganic aerosols at atmospherically relevant conditions.

4.4.5 Uncertainty Analysis

The model is a compilation of three separate models (gas phase explicit model, OM_P model, and OM_H model) which all have their own inherent uncertainty. In order to improve the confidence of this model it is imperative to be aware of the models limitations due to uncertainty. The gas phase model is tested against chamber data which used an ozone monitor and a GC/FID measure the ozone and terpene decays respectively. Both instruments were calibrated and only measurements above detection limits for the gas phase chamber data were used. However the estimated products are not measured. Many researchers have invested lots of time and energy to fully characterize the product distribution of the gas phase ozonolysis products from monoterpenes. However both the quantitative and qualitative analysis of SOA is very poor due to the unavailability of authentic standards and the instability of products in analytical procedure. Furthermore the complexity in SOA product characterization is increased through the potential of heterogeneous reaction in aerosol phase. The approach of the Master Chemical Mechanism focuses on a more theoretical approach to this problem. Thus, there is an uncertainty for the quality of the product distributions and concentrations. Such uncertainty can influence the quality of the model employed in this study.

Using the same product lumping scheme the measured products were grouped and compared to the products groups from the MCM model. Yu et al. (Yu et al. 1999) accounted for 30% of the total molar product yield by the sum of the gas and the particle products, and the products measured have the largest concentration in the lumped groups as predicted by MCM, so they can be used compare the product group and experimental data. Table 4.3 shows the comparison for the molar yield percents.

Product Group	MCM molar yield	Yu et al. (1999) Molar Yield
VHP NR	2.1%	3.0%
HP MR	0.3%	0.1%
MP LR	2.4%	2.5%
LP HR	0.9%	0.6%
LP MR	3.6%	3.8%
VLP MR	17.0%	11.6%

Table 4.3 Stoichiometric coefficients (α_i) for the product group from with the highest partitioning constant and highest reaction rate constant for α -pinene terpinolene and limonene.

The largest difference is 6% for group VLP MR, however this is also the largest product group for both MCM and Yu et al. (1999). The close accuracy to the measured value validates the product group values estimated from MCM. It is difficult to repeat this comparison for terpinolene since very little product analysis has been conducted for the terpinolene and limonene ozonolysis product concentrations.

The uncertainty in the alpha values can be estimated to be about 25% in terms of absolute values, however what is of more importance is the distribution of the products among themselves. There is little variation in the order of molar yields increasing the confidence of the alpha values and MCM products. The deviation the particle phase oligomer mass modeled and the actual oligomer mass can be determined by the difference between the TGA quantified oligomer fractions and the model estimated fractions. The modeled oligomer fraction within 25% of the TGA quantified fraction.

The fraction of SOA formed by the oxidized gas phase products, is estimated as the difference between the total oxidized product concentration minus the equilibrated gas phase concentration, and the mass concentration for products from the formation of particle phase oligomers (equation 4.5). The uncertainty in the estimation of OM_p can be estimated from the largest value of uncertainty in the terms used to determine OM_p . The uncertainty from the gas phase equilibrated

concentration is quantified by the error in the vapor pressure estimation. Mackay et al. (1982) estimated that the vapor pressure equation has a mean error of 1.25, or 25%. If the error in the vapor pressure is 25% this is the largest error in the estimation of K_p and subsequently the OM_p .

Finally the uncertainty in the particle phase oligomer estimation can be quantified using equation 4.1 and estimating the error for each of the parameters we have determined that the error in the equation is 30%. However when comparing the estimated values with the experimental values we find that this possible error is larger than the difference between experimental and model data suggesting that the difference may give a better estimation of the error in the model.

4.5 Conclusion

This study demonstrates the ability of a novel approach to estimate SOA mass from terpene ozonolysis formed in the presence of inorganic aerosols using both heterogeneous and partitioning. The model permits us to estimate SOA at ambient conditions, for a range of relative humidities, inorganic aerosol mass concentrations, and three separate terpenes. The model can be used to further investigate the effects of atmospheric conditions on the SOA formation, as well as the fractional composition of the SOA formed.

In the future the model frame work should be expanded for use with different reactive organic gases and condensed for the use with a regional scale model. Additional work should also be conducted which includes the photo irradiation of terpenes in the presence different levels of NO_x , as well as additional inorganic aerosols such as NaCl, $NaSO_4$, NH_4Cl and others.

4.6 References

- Bae, M., Schauer, J.J., and Turner, J.R. (2006). Estimation of the monthly average ratios of organic mass to organic carbon for fine particulate matter at an urban site. *Aerosol Science and Technology*. 40:1123-1139.
- Bahreini, R., Keywood, M.D., Ng, N.L., Varutbangkul, V., Gao, S., Flagan, R.C., Seinfeld, J.H., Worsnop, D.R., and Jimenez, J.L. (2005). Measurements of secondary organic aerosol from oxidation of cycloalkenes, terpenes, and m-xylene using an aerodyne aerosol mass spectrometer. *Environmental Science and Technology*. 39: 5674-5688.
- Carey, F.A. and Sundberg, R.J. (2000). *Advanced Organic Chemistry Part A: Structure and Reactivity*. New York, NY: Kluwer Academic.
- Choy, B.; Reible, D. D. *UNIFAC Activity Coefficient Calculator*, Version 3.0; September, 1996. <http://www.hsrb.org/hsrb/html/ssw/unifacal.exe>.
- Cox, R.A. and Yates, K. (1978). Excess acidities. A generalized method for the determination of basicities in aqueous acid mixtures. *Journal of the American Chemical Society*. 100:3861-3867.
- Czoschke, N.M. and Jang, M. (2006). Acidity effects on the formation of α -pinene ozone SOA in the presence of inorganic seed. *Atmospheric Environment*. 40: 4370-4380.
- Drewnick, F., Jayne, J.T., Canagaratna, M., Worsnop, D.R., and Demerjian, K.L. (2004). Measurement of ambient aerosol composition during the PMTACS-NY 2001 using an aerosol mass spectrometer. Part II: Chemically speciated mass distributions. *Aerosol Science and Technology*. 38:104-117.
- Jang M., Czoschke N.M., and Northcross A.L. (2004). Atmospheric organic aerosol production by heterogeneous acid-catalyzed reactions. *Chemphyschem* 5:1-16.
- Jang, M., Czoschke N.M., and Northcross A.L. (2005). Semiempirical model for organic aerosol growth by acid-catalyzed heterogeneous reactions of organic carbonyls. *Environmental Science and Technology*. 39:164-174.
- Jang M.S., Czoschke N.M., Lee S., and Kamens R.M. (2002). Heterogeneous atmospheric aerosol production by acid-catalyzed particle-phase reactions. *Science* 298:814-817.
- Jang, M., Carroll, B., Chandramouli, B., and Kamens, R.M. (2003). Particle growth by acid-catalyzed heterogeneous reactions of organic carbonyls on preexisting aerosols. *Environmental Science and Technology*. 37: 3828-3837.

- Jang, M., Czoschke, N.M., Northcross, A.L., and Cao, G. (2005). Semiempirical model for organic aerosol growth by acid-catalyzed heterogeneous reactions of carbonyls. *Environmental Science and Technology*. 39: 8110-8111.
- Jang, M., Czoschke, Nadine M., Northcross, A.L., Cao, G., and Shaof, D. (2006). SOA formation from partitioning and heterogeneous reactions: Model study in the presence of inorganic species. *Environmental Science & Technology*. 40: 3013-3022.
- Jenkin, M. E. (2004). Modeling the formation and composition of secondary organic aerosol from α - and β -pinene ozonolysis using MCM v3. *Atmospheric Chemistry and Physics*. 4: 1741-1757.
- Joback, K.G. and Reid, R.C. (1987). Estimation of pure-component properties from group contributions. *Chemical Engineering Communications*. 57: 233-43.
- Kleman, M.J., Ying, Q., Lu, J., Mysliwiec, M.J., Griffin, R.J., Chen, J., and Clegg, S. (2007). Source apportionment of secondary organic aerosol during a severe photochemical smog episode. *Atmospheric Environment*. 41: 576-591.
- Mackay, D., Bobra, A., Chan, D. W., and Shiu, W.Y. (1982). Vapor-pressure correlations for low-volatility environmental chemicals. *Environmental Science and Technology*. 16: 645-9.
- Morishita, M., Keeler, G.J., Wagner, J.G., and Harkema, J.R. (2006). Source identification of ambient PM_{2.5} during summer inhalation exposure studies in Detroit, MI. *Atmospheric Environment*. 40: 3823-3834.
- Nenes, A., Pandis, S.N., and Pilinis, C. (1998). ISORROPIA. A new thermodynamic equilibrium model for multiphase multicomponent inorganic aerosols. *Aquatic Geochemistry*. 4: 123-152.
- Northcross, A.L. and Jang, M. (2007). Heterogeneous SOA yield from ozonolysis of monoterpenes in the presence of inorganic acid. *Atmospheric Environment*. 41: 1483-1493.
- Odum, J.R., Hoffmann, T., Bowman, F., Collins, D., Flagan, R.C., and Seinfeld, J.H. (1996). Gas/Particle partitioning and secondary organic aerosol yields. *Environmental Science and Technology*. 30: 2580-2585.
- Pankow JF (1994). An absorption-model of gas-particle partitioning of organic-compounds in the atmosphere. *Atmospheric Environment* 28 :185-188.
- Pekney, N.J., Davidson, C.I., Robinson, A., Zhou, L., Hopke, P., Eatough, D., and Rogge, W.F. (2006). Major source categories for PM_{2.5} in Pittsburgh using PMF and UNMIX . *Aerosol Science and Technology*. 40: 910-924.

Russell, M., Allen, D.T., Collins, D.R., and Fraser, M. P. (2004). Daily, seasonal, and spatial trends in PM_{2.5} mass and composition in southeast Texas. *Aerosol Science and Technology*. 38: 14-26.

Saunders, S.M., Jenkin, M.E., Derwent, R.G., and Pilling, M.J. (2003). Protocol for the development of the master chemical mechanism, MCM v3 (part A): tropospheric degradation of non-aromatic volatile organic compounds. *Atmospheric Chemistry and Physics*. 3: 161-180.

Schell, B., Ackermann, I.J., Hass, H., Binkowski, F.S., and Ebel, A. (2001). Modeling the formation of secondary organic aerosol within a comprehensive air quality model system. *Journal of Geophysical Research, [Atmospheres]*. 106: 28275-28293.

Schwarzenbach, R.P., Gschwend, P.M., and Imboden, D.M. 1992. Environmental Organic Chemistry. 681 pp.

Stein, S.E. and Brown, R.L. (1994). Estimation of normal boiling points from group contributions. *Journal of Chemical Information and Computer Sciences*. 34: 581-7.

Tolocka, M P., Jang, M., Ginter, J.M., Kamens, R.M., and Johnston, M.V. (2004). Formation of oligomers in secondary organic aerosol. *Environmental Science and Technology* 38:1428-1434.

van Donkelaar, A., Martin, R.V., Park, R.J., Heald, C.L., Fu, ., Liao, H., and Guenther, A. (2007). Model evidence for a significant source of secondary organic aerosol from isoprene. *Atmospheric Environment*. 41: 1267-1274.

Weber, R.J., Sullivan, A.P., Peltier, R.E., Russell, A., Yan, B., Zheng, M., de Gouw, J., Warneke, C., Brock, C., Holloway, J.S., Atlas, E.L., and Edgerton, E. (2007). A study of secondary organic aerosol formation in the anthropogenic-influenced Southeastern United States. *Journal of Geophysical Research, [Atmospheres]*. 112: D13302-1-D13302/13.

Yu, J., Cocker, D.R., Griffin, R.J., Flagan, R.C., and Seinfeld, J.H. (1999). Gas-phase ozone oxidation of monoterpenes: gaseous and particulate products. *Journal of Atmospheric Chemistry*. 34: 207-258.

Zhao, L., Li, P., and Yalkowsky, S.H. (1999). Predicting the entropy of boiling for organic compounds. *Journal of Chemical Information and Computer Sciences*. 39: 1112-1116.

Zhao, W. and Hopke, P.K. (2006). Source investigation for ambient PM_{2.5} in Indianapolis, IN. *Aerosol Science and Technology*. 40: 898-909.

CHAPTER 5

Summary of Key Findings, Implications and Recommendation for Future Studies

5.1 Key Findings and Implications

The three studies presented in this dissertation have contributed to valuable information about secondary organic aerosol particle phase reactions and their relationship to ambient inorganic particulates in the atmospheric aerosol field. Using an indoor Teflon chamber, SOA mass formation in the presence of inorganic aerosols was investigated. The SOA mass formation study quantified the ability of a terpene to participate in particle phase reactions, and illustrated the connection between the chemical structure of the gas phase reactant, the subsequent oxidized products and the reactivity for particle phase acid catalyzed reactions. This study also showed that the quantity of aerosol mass formed from a specific reactive organic carbon is not only dependant on the concentration of reactant, but also the concentration of inorganic aerosol present in the system can influence the amount of aerosol mass formed. As the inorganic seed aerosol increases so does the SOA mass formed. The increase in SOA also depends on the acidity of the inorganic aerosol.

These findings have implications on the modeling of SOA, as well as how the aerosol community describes the chemical and physical processes that govern SOA formation. SOA mass is modeled in regional scale models using thermodynamic partitioning. This dissertation has shown that thermodynamic partitioning is a major contributor to SOA but not the only process which should be considered to model SOA mass formation. The SOA mass formation model has included both thermodynamic partitioning the as well as particle phase acid-catalyzed oligomer formation in the presence of inorganic aerosol. This approach more accurately represents the processes occurring during SOA formation. The oligomer fraction and total SOA aerosol mass both are estimated, which

provides additional information as to the composition of the aerosol. This model has been constructed to allow the framework to be used to model SOA from ROGs not included in this study. This can be achieved by simply adding the grouped stoichiometric coefficients for the ROG of interest. The mass balance approach of estimating total SOA allows for inclusion of additional SOA formation processes.

Beyond being able to model the fraction of oligomers formed due to the presence of inorganic aerosols, an experimental oligomer mass fraction estimation technique was developed using TGA which is targeted to bulk phase analysis of aerosols. The TGA method development study resulted in a new approach thermal analysis for aerosols. By subtracting the inorganic aerosol signal, the evolution of the particle phase organics with response to temperature increase is captured. The TGA study not only resulted in the development of a new analytical method, but also provide valuable information as to the how inorganics influence specific types of molecules. Under acidic conditions alcohols were found to only form organic sulfate, while pinonic acid which contains a carboxylic acid group and a ketone was able to form a small amount of oligomer. Also the TGA study revealed a possible flaw in the use of organic carbon, elemental carbon (OC/EC) thermal analysis. OC/EC analysis is a thermally based analysis technique which heats sampled aerosols, and analyzes the evolved gases. Typically organic carbon is quantified at temperatures as high as 500°C (Chow et al. 2004), and the charring of organics are assumed to occur in the presence of oxygen gas. The TGA study showed that at temperatures above 250°C the oligomer fraction of the aerosol begins to decompose and form char. This char is quantified as EC in OC/EC analysis causing a possible underestimation of the OC fraction of aerosols.

5.2 Recommendations for Future Studies

Acid catalyzed particle formation of organic oligomers in the presence of inorganic aerosols is a rapidly developing interest area within the atmospheric aerosol community. This study although narrow in focus has raised many questions which should be answered in future studies. These questions can be grouped into studies which are related to atmospheric and aerosol chemistry and

studies which focus on the impact of oligomer formation on human health as well as the broader environment.

5.2.1 Aerosol Chemistry Related Future Studies

5.2.1.1 Photolysis

This study focused solely on SOA formed from the ozonolysis of monoterpenes in the presence of inorganic aerosols. In the real atmosphere ozonolysis without photolysis mainly occurs at night, therefore additional studies are needed that focus on SOA from the photo-oxidation of reactive organic gases. The product distribution of photochemically reacted organics will contain species which are nitrogen containing and may have a different effect on oligomer formation than the oxygen containing products of ozonolysis reactions. NO_x a major component of ambient air pollution can also react photo-chemically to form nitric acid, which may also act as a catalyst for particle phase reactions and enhance oligomer formation.

5.2.1.2 Aromatics

Although monoterpenes are an important precursor of ambient SOA, there are other ROGs which should also be studied. In particular are aromatics. Aromatics react in photochemical reactions to produce highly oxidized products which can be very reactive for particle phase reactions. In the presence of inorganic aerosols these products may form SOA yields which are not negligible despite having high vapor pressures. An investigation of the SOA yield and particle oligomer fraction is needed to better understand the ability of aromatics to generate SOA. The highly reactive nature of these products may make them less sensitive to inorganic acidity, helping to further understand the point at which inorganic acidity fails to enhance SOA mass formation.

5.2.1.3 Inorganic Aerosols

The effect of the inorganic aerosol was quantified using sulfuric acid, ammonium bisulfate, and ammonium sulfate. Sodium, chloride, sulfate, and ammonium are the most prevalent atmospheric inorganic ions which can form salts from the various combinations of the ions, which

differ in acidity as well as hygroscopicity. The effect on SOA formation and particle phase reactions forming oligomers in the presence of different inorganic salts should be determined. Oligomer formation has been shown to be responsive to particle acidity, however what is unclear is if the response is dependent on the composition of the inorganic particle. Inorganics containing mixtures of various atmospherically relevant salts may help to explain further the relationship between inorganic particle phase acidity and the inorganic composition of the aerosol. An even more atmospherically relevant study would be to use inorganic gases (NO_2 , NH_3 , SO_2) which ultimately become inorganic aerosols, to quantify oligomer formation and SOA mass response to acidity.

5.2.1.4 Mixtures of Organics

Similar to the possibility of an inorganic aerosol of mixed composition affecting the formation of particle phase oligomers, mixtures of organic aerosols may also have varied effects on the formation of particle phase oligomers. For example the SOA produced from the ozonolysis of a 50:50 mixture of terpinolene and α -pinene in the presence of a strongly acidic inorganic aerosol would be difficult to predict. The α -pinene products have lower average vapor pressures and less responsivity to acidity, while terpinolene products have higher vapor pressures and are more responsive to acid-catalyzed particle formation. But an additional layer complexity is added to the puzzle because terpinolene is much more reactive with ozone than α -pinene, thus, the time at which products are partitioning and reacting may influence the subsequent SOA formation. As the reaction time progresses oligomer formation increases, which makes the organics become more solid like than liquid and decreases partitioning. α -Pinene products which may partition and possibly react through particle phase reactions in a system without terpinolene may not contribute as much to the SOA mass when terpinolene is present. This hypothesis should be tested as it may affect the SOA modeling of in realistic conditions.

5.2.1.5 Organic Sulfate

Oligomers are not the only product of particle phase reactions. Recently there have been studies (Iinuma et al., 2007; Surratt et al., 2007) which have identified the formation of organic-sulfate esters in SOA formed in the presence in ammonium sulfate-sulfuric acid inorganic aerosols. The identification of these compounds implies that an additional pathway of organic aerosol mass formation exists. It is crucial to be able to quantify organosulfate formation and furthermore to be able to determine the conditions which aide in the formation of these products. Modeling of organic sulfates may become important in the future if significant concentrations can be quantified.

5.2.2 Environmental Future Studies

The affect of oligomer presence in SOA on human health is unknown. Modeling the SOA mass and oligomer fraction in conjunction with an epidemiological study may help researchers to better understand which constituents of SOA are harmful to human health.

The health impacts of aerosols vary based on the composition of the aerosols. Organic aerosols have been shown to have detrimental health effects. However the composition of the organic portion can vary and the presence of oligomers can also vary the physical properties of aerosols. The impact on human health of the chemical and physical properties of organics containing oligomers should be quantified. Also the relationship between acidity, oligomers and health should also be investigated to better understand the observed relationship between increased adverse health effects in the ambient with SO₂, but no measurable health effects in animal studies. Modeling the SOA mass and oligomer fraction in conjunction with an epidemiological study may help researchers to better understand which constituents of SOA are harmful to human health.

Overall this study has provided valuable information and has also highlighted how related areas of research are affected by the information learned through this study.

5.3 References

Chow, J.C., Watson, J. G., Chen, L. W. Antony, A., W. P., Moosmueller, H., and Fung, K.. (2004). Equivalence of elemental carbon by thermal/optical reflectance and transmittance with different temperature protocols. *Environmental Science and Technology*. 38: 4414-4422.

Iinuma, Y., Muller, C., Boge, O., Gnauk, T., Herrmann, H.(2007) The formation of organic sulfate esters in the limonene ozonolysis secondary organic aerosol (SOA) under acidic conditions. *Atmospheric Environment* 41: 5571–5583.

Surratt, J.D., Kroll, J.H., Kleindienst, T.E., Edney, E.O., Claeys, M., Sorooshian, A., Ng, N.L., Offenberg, J.H., Lewandowski, M., Jaoui, M., Flagan, R.C., Seinfeld, J.H., (2007). Evidence for organosulfates in secondary organic aerosol. *Environmental Science and Technology* 41: 517–527.

Appendix

A.1 Experimental Instrumentation Description and Calibration

Smog Chamber Instrumentation

Smog Chamber: 2 m³ Teflon chamber. Dimension: 1.0 m x 1.2 m x 1.8 m. Chamber can be partially collapsed by suctioning the air using a vacuum to have a dimension of 1 m x 0.6 m x 1. m. The collapsed dimension is used to vent the chamber.

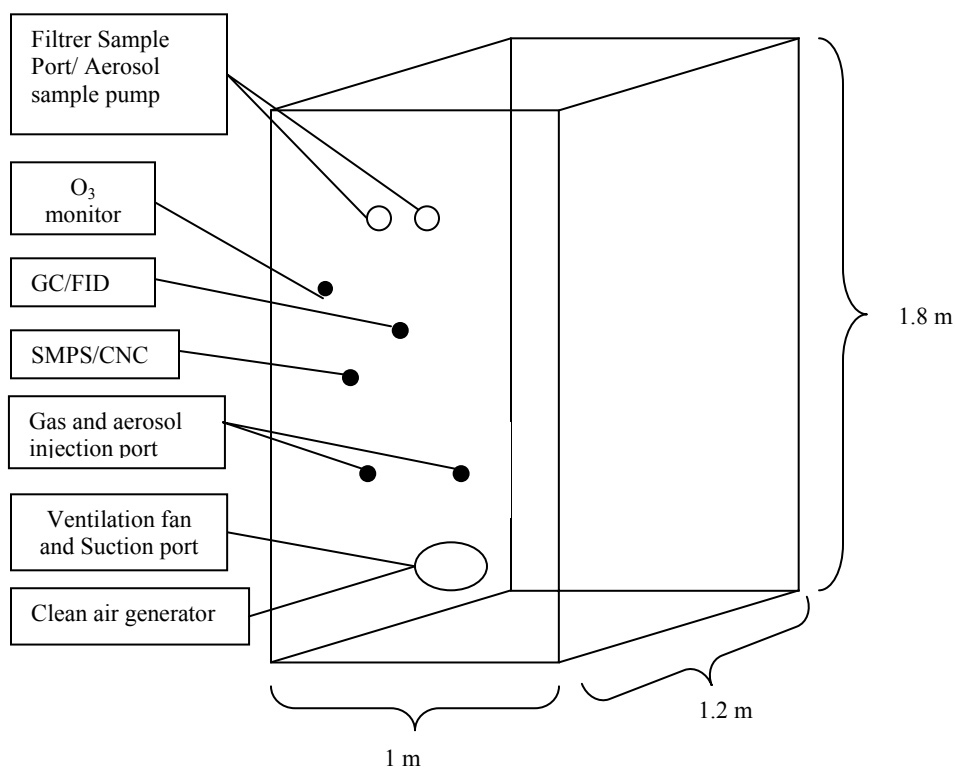


Figure A.1 Smog chamber schematic

Exhaust system: The laboratory exhaust system is used to evacuate the chamber.

Clean Air Generator:

Two clean air generators were used, a Whatman FT-IR purge gas generator (model 75–52) and an Aadco 73. Both were connected to air compression tanks. Room air was pumped into the tanks and compressed to remove excess water and airborne pollutants (tanks should

be emptied of compressed water once a week). Both clean air generators consisted of air filtration systems which further purified the compressed air.

Temperature and Relative Humidity Monitor:

Hanna instruments thermo hygrometer HI 9160C

Gas Chromatograph with Flame Ionization Detector:

HP 5890 GC-FID Capillary column.

N₂ GC carrier gas flow rate 2.5 mL

Column: DB-5 (15m x 0.53mm) fused silica capillary column (J & W Scientific INC, Cat# 1255012)

Gas phase samples are taken through 1/16 in. stainless steel sample line connected to the chamber. A six-port valve was used to sample the chamber air immediately after injecting a sample to the chamber.

Scanning Mobility Particle Sizer in Series with Condensation Nuclei Counter .

TSI (Model 3830) and TSI (Model 3025A) respectively. The SMPS/CNC was configured to sample every 3 minutes for particle sizes 10 nm to 835 nm. Imported data was corrected for multiple charges by the TSI software.

Ozone Photometer

Thermo Electron Instruments UV photometric

O₃ analyzer model 49

Aerosol Sampling Pump

Gast model: DOA-P704-AA

Aerosol Analysis Instruments

Microbalance

Fourier Transform Infrared Spectrometer (FTIR)

Nicolet Magna-IR 560 Spectrometer equipped with a MCD detector

Thermal Gravimetric Analyzer (TGA)

Perkin Elmer Pyris 1

N₂ Purge gas, and actuator gas

A.2 Experiment Protocol

A.2.1 Smog Chamber Experiments

Initialization

1. Evacuate chamber of air using exhaust system. Fill with room air twice and vent. Repeat twice.
2. Fill chamber with clean air from clean air generator, humidify if necessary.
 - a. Humidification:

Pass clean air through bubbler inserted into flask containing deionizer water, and connected to chamber. If humidity needs to be raised more than 20% then use a hot water bath to maintain an elevated flask water temperature. Air bubbled through water is pumped into the chamber.

3. Once chamber is full, monitor the particle number concentration using the SMPS/CNC. If the number of particles at any diameter exceeds 20, then vent chamber and repeat steps 1-3. If all diameters are less than 20 then proceed to next step.

Injection

1. Inorganic seed solution is injected into the chamber using a TSI atomizer to form the inorganic seed aerosol. The inorganic seed aerosol is composed of 0.01M solutions of NH_4HSO_4 , H_2SO_4 and $(\text{NH}_4)_2\text{SO}_4$ all from Sigma Aldrich (99%, 95% and 99%).
2. Terpene is injected by passing clean air through ozone generator and into the chamber at a rate of 5Lpm. Monitor chamber ozone concentration during injection using ozone monitor, stop when desired concentration is achieved.
3. Ensure the seed aerosol mass is not increasing. SMPS/CNC should report a stable or slightly declining aerosol volume. An increasing volume is a sign of a gas phase contaminants partitioning to the seed aerosol. If this occurs, stop experiment and vent chamber.
4. Terpene is injected into chamber using a heated manifold (Figure A.2)

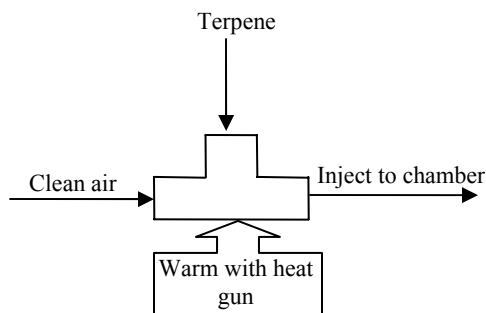


Figure A.2 Terpene injection manifold

5. Using GC/FID take gas phase samples to monitor terpene concentration. Initially take sample as frequently as possible (~every 3 minutes). As terpene decay begins to GC/FID samples can be taken with less frequency
6. Manually record O₃ concentrations when GC/FID samples are taken.
7. Monitor SOA mass using SMPS/CNC. Samples are automatically taken every 3 minutes.
8. Experiment is complete when SOA mass stops growing and begins to decline. At this point if aerosol samples are taken is needed.

Aerosol Filter Sampling

1. Two types of aerosol filter samples were collected. Samples for TGA and samples for FT-IR.
2. FT-IR samples are collected in a specially designed Teflon aerosol sampler. The sampler is designed to impact aerosols onto a ZnSe cell.
3. The cell is placed into the FTIR for analysis.
4. Aerosols were also sampled onto filters. Quartz fiber filters were used to sample aerosol for TGA analysis, and Teflon filters were used to compare filters sampled aerosol concentrations with those measured by the SMPS/CNC. The sampling technique was the same for both types of filters.
5. A filter was pre-weighed using the microbalance, and then placed into the filter holder.
6. The filter holder was connected to the chamber at one end and a pump on the other.
7. A stop watch started as the pump is turned on.

8. The volumetric flow rate is measured from the pump exhaust periodically throughout the sampling time. The chamber is manually compressed as the air is suctioned out to maintain atmospheric pressure.
9. After the chamber is fully compressed, the pump is turned off, time is recorded and the filter is weighted again using the micro balance.

A.2.2 Aerosol Analysis

A.2.2.1 Thermal Analysis

PerkinElmer Pyris 1

Furnace Temperature Range: 20-1000°C

Scanning Rates: 0.1°C/minute to 200°C/minute

Temperature Precision: $\pm 2^\circ\text{C}$

Balance Tare: Reproducible to $\pm 2 \mu\text{g}$

Sensitivity: 0.1 μg

Accuracy: Better than 0.02%

Precision: 0.001%

Capacity: 1300mg

Hang-down Wires High temperature quartz, nichrome, or platinum

Sample Pans Platinum 60 μL

Purge Gases: N_2

Temperature Program

Normal: Heating Rate: 10°C/minute to 30°C to 600°C

Isothermal: Heat 30°C to 250°C

Hold at 250°C for 1 hour

Heat 250°C to 600°C

Micro Balance

Materials

Filter: 25 mm tissuquartz filters (Pallflex 2500 QAT-UP, 25 mm)

Ammonium Sulfate Sigma Aldrich, 98%

Sulfuric Acid Sigma Aldrich, 95-98%

Ammonium Bisulfate Sigma Aldrich, $\geq 99\%$

Deionized water

Gast Pump DOA-P704-AA, 30 Lpm maximum flow rate

Filter Holder: Brass 15mm Swage Loc reducing union reconfigured to hold a 13 mm diameter quartz filter

Methods

Aerosol Sampling and Aerosol TGA Method

1. Bake filters to be used for the day at 400°C for 1 hour to remove any contaminants.
2. Cut filter using circular hole punch to 13mm diameter circle.
3. Weigh filter using microbalance and record mass.
4. Place filter in filter holder and attached holder to chamber and pump.
5. Start pump and timer. Record SPMS sample number and time.
6. Measure pump exhaust flow rate using Gilibrator.
7. After chamber appears to be fully evacuated, measure flow rate again using Gilibrator.
8. While taking filter sample prepare TGA and Microbalance

Turn on TGA

Turn of N₂ tanks, check pressure gauges.

Zero the TGA with an empty sample pan

Input file name information

Input temperature program

Remove sample pan from TGA and zero microbalance using sample pan

9. Turn of pump, stop timer, record time and SMPS sample number and time.
10. Immediately remove filter from filter holder and place in pan. Weigh using microbalance.

Record mass

11. Place sample pan with filter on the wire pan hook in the TGA.
12. Record the sample weight using TGA.
13. Start sample run.

Model Compounds Method

Inorganic Aerosol Solutions

1. Using ISOROPPIA determine the molar concentration of the aerosol, specific to initial seed solution composition and relative humidity.
2. Make aerosol solution using the molar concentrations determined by ISOROPPIA
3. Prepare TGA (*Aerosol Sampling 8.*)
4. Measure a pre-baked filter (*Aerosol Sampling 1.*) using the microbalance.
5. Add inorganic aerosol solution to the filter, trying not to add more than 7mg.
6. Weigh filter with inorganic aerosol sample.
7. Follow Aerosol Sampling 11-13

Organic Model Compounds

1. Follow *Aerosol Sampling 8.*
2. Tare Microbalance using PT sampling pan.
3. Add organics directly to sample pan, trying not to add more than 3mg.
4. Follow *Aerosol Sampling 11-13.*

Data Analysis

Raw TGA data is exported from the software in the form of tables of mass, and temperature. The data is imported into excel for data analysis.

A.2.2.2 FT-IR Analysis

The FT-IR is used to identify relative changes in functional groups between samples, thus a calibration curve was not appropriate. Also due to the large numbers of compounds present in SOA it would be extremely difficult to determine specific concentrations with first separating the components.

Analysis was conducted for impacted SOA and samples of pinonic acid and inorganic seed aerosol solutions. The samples were always placed on a ZnSe cell. The detector temperature was lowered using liquid nitrogen, and clean low %RH air was introduced into the chamber which housed the detector to reduce the noise in the spectra gas phase contaminants.

The clean chamber air was used as a zero reference, to compare the sample spectra against. The resultant spectra were exported as raw data and analyzed using excel.

A.3 Instrument Calibration and Measurement Comparison

A.3.1 Gas Chromatograph Calibration

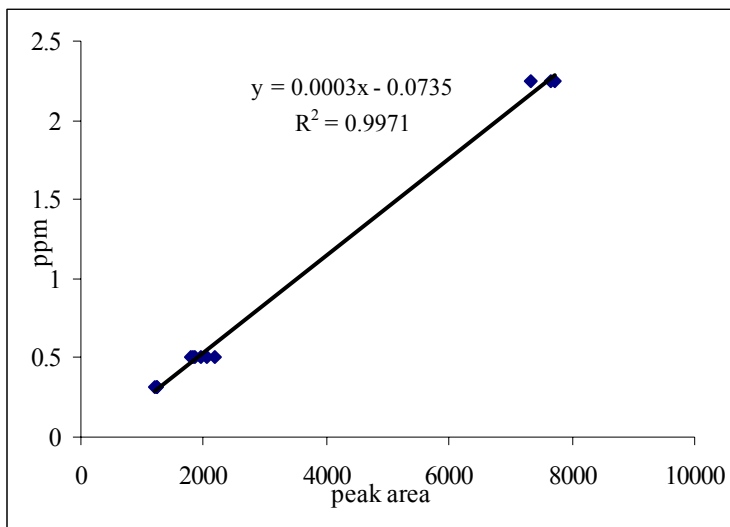


Figure A.3 Example of calibration curve. α -pinene in a Teflon bag with serial dilutions using clean air for concentrations from 2.25 ppm – 0.32 ppm.

GC calibration was conducted using 500L Teflon bag. An initial volume (2- 5 μ L of 10% terpene solution) of terpene was volatilized into the bag by passing clean air through the injection tube and heating the tube with a heat gun. The volumetric flow rate of the clean air was measured using a Gilibrator, the time was

measured resulting in the volume of air in the bag. A sample line was connected the bag and at least three GC measurements were taken at each concentration. The terpene concentration changed by adding air to the bag. The volume of dilution air added was measured using the Gilibrator and air injection time. Flow rates varied between 15-30 Lpm. At least different concentrations were measured for each calibration curve.

The minimum detectable concentration was also measured by incremental serial dilutions until a discernible signal was no longer measured. The minimum detectable concentration was determined as the concentration which was lower than the average standard error of all of the measurements above that level.

Calibration curves were constructed each day, as the calibration factor changed daily.

A.3.2 Mass Concentration Comparison SMPS/CNC vs. Filters

It is not possible to calibrate the SMPS/CNC instrument. In order to determine that the reported measurements were reasonable the aerosol mass measured in the chamber was compared to the

SMPS/CNC estimated aerosol mass concentration. Table A.1 show the results of α -pinene ozonolysis SOA.

The aerosols were filtered on to a Teflon filter which was weighed both before and after sampling.

The sample time was measured with a stop watch and the flow rate was measured every 8 minutes.

The average flow rate was used to determine the mass concentration. Table A.1 shows a comparison between the filter measured aerosol concentration and the SMSP/CNC estimated concentration using an inorganic aerosol density of 1.4 mg/m^3 and an organic aerosol density of 1.4 mg/m^3 .

SMPS/CNC Aerosol Mass $\mu\text{g/m}^3$	Filter Measured Aerosol Mass $\mu\text{g/m}^3$	Percent difference
378	390	3%
249	220	13%
373	352	6%

Table A1 SMPS/CNC estimated mass concentration for SOA from α -pinene ozonolysis in comparison to filter sample derived aerosol concentration.

Using Student's t-test ($t= 0.2$) to compare the filter measured aerosol mass concentration in comparison to the SMPS/CNC estimated concentration shows the values are not statistically different. The SMPS/CNC provides a reasonable estimate for the aerosol mass concentration.

A.3.3 Ozone Monitor Calibration

The ozone monitor was calibrated using a two point calibration. The clean air generator was connected directly a gas phase titration flask. A zero air reading was taken. The offset of the ozone monitor was changed so the reading for the zero air was 0.

Next the flask was connected to an ozone source (Teledyne O_3 Calibration) of 0.5535 ppm of ozone. The source concentration was measured using a different ozone monitor (Teledyne Instruments O_3 Photometer ML9811 series O_3) which had been calibrated using a 5 point calibration curve. The ozone monitor span was reset to give a reading of 0.553 ppm.

A.3.4 TGA Calibration

The TGA was purchased new from Perkin Elmer. The calibration of the instrument was conducted by the installation technician. A periodic calibration of the instrument was not conducted.

The flow rate from the gas tank was periodically checked to ensure that the purge gas flow rate was stable. The volumetric flow rate was measured using a bubble meter (Giliblator). Two N₂ (National Welder, 99.99%) tanks were used. One tank was used to supply the actuator mechanism, and the second tank was for the purge gas flow.

A.4 Chamber Wall Loss

Wall loss calculation is based on the exponential decay of the particle number at each in diameter (equation A.1) (McMurray and Grosjean 1985, see Chapter 3 references). N is the number of particles per cm^3 at diameter D_p . β is the loss coefficient of particles at diameter D_p and t is time.

$$\frac{dN(D_p)}{dt} = -\beta_p(D_p)N(D_p) \quad (\text{A.1})$$

Solving equation A.1 results in an exponential equation (A.2).

$$N_t = N_o e^{(\beta_p t)} \quad (\text{A.2})$$

β_p is found by fitting an exponential decay curve in the form of equation A.2 for each particle diameter size measured by the SMPS/CNC. Table A.1 shows β_p used for a series of experiments. β_p was re-estimated after the chamber was cleaned and when the Teflon in the chamber was replaced.

The wall loss equation is applied after the seed particles are injected into the chamber. Any particles lost to the walls before the injection has finished are not available to participate in partitioning and therefore are not corrected for. Once the particle number distribution is corrected the volume distribution can be determined using the corrected number of particles and the particle volume described as $\text{volume} = \pi D_p^3 / 8$. Figure A.4 shows the resulting cumulative volume distribution from an α -pinene ozonolysis experiment.

Diameter (nm)	β_p
19.81	6.05E-04
21.29	5.10E-04
22.88	4.41E-04
24.58	3.47E-04
26.42	3.79E-04
28.39	2.42E-04
30.51	2.41E-04
32.78	2.59E-04
35.23	2.19E-04
37.86	1.90E-04
40.68	1.84E-04
43.71	1.67E-04
46.98	1.51E-04
50.48	1.33E-04
54.25	1.16E-04
58.29	1.08E-04
62.64	9.70E-05
67.32	8.55E-05
72.34	7.67E-05
77.74	4.14E-05
83.54	2.70E-05
89.77	4.78E-05
96.47	4.02E-05
103.66	3.30E-05
111.40	2.46E-05
119.71	1.86E-05
128.64	8.19E-06
138.24	1.53E-06
148.55	1.68E-06
159.63	2.53E-05
171.54	1.70E-05
184.34	5.12E-06
198.10	1.36E-05
212.88	4.46E-06
228.76	2.50E-05
245.82	2.64E-06
264.16	2.19E-06
283.87	2.53E-06
305.05	6.87E-06
327.81	3.87E-06
352.27	1.82E-05
378.55	5.45E-05
406.79	3.11E-05
437.14	3.17E-05
469.76	1.28E-05
504.81	6.24E-05
542.47	4.78E-05
582.94	3.31E-05
626.43	1.33E-04
673.17	7.91E-05
723.39	5.65E-05
777.37	3.40E-05
835.36	3.40E-05

Table A.2 Particle wall loss coefficients.

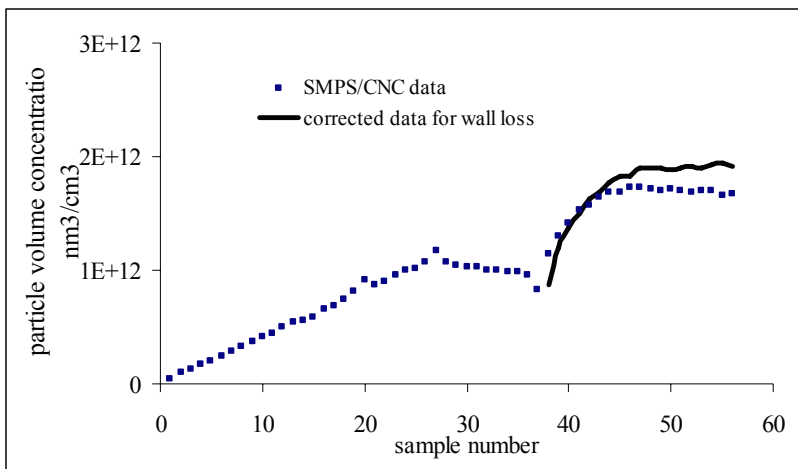


Figure A.4 Particle wall loss for α -pinene ozonolysis and neutral seed. Loss calculation starts at end of seed injection.

A.5 Nebulizer Seed Aerosol Size Distribution

The particle number distribution mode varied by seed aerosol acidity. Figures A.5-A.7 show the particle size distribution for the seed aerosols used in this study.

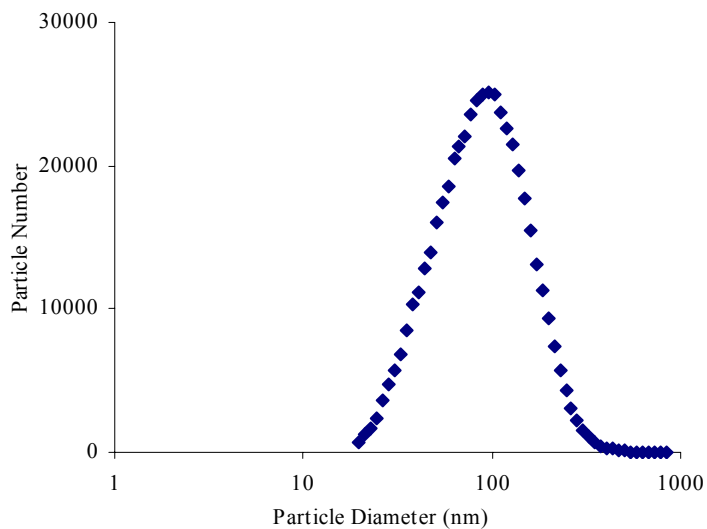


Figure A.5 Acid seed particle number distribution, 25%RH Mode: 103

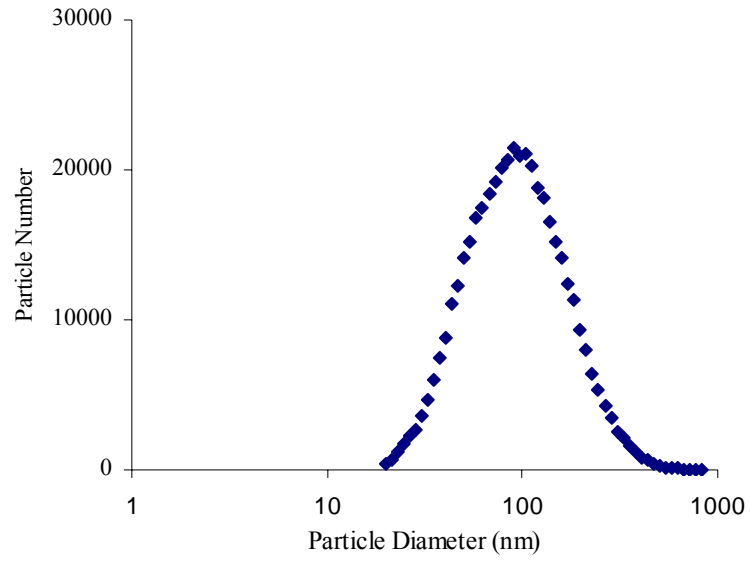


Figure A.6 Mid acid seed particle number distribution, 25%RH Mode: 89

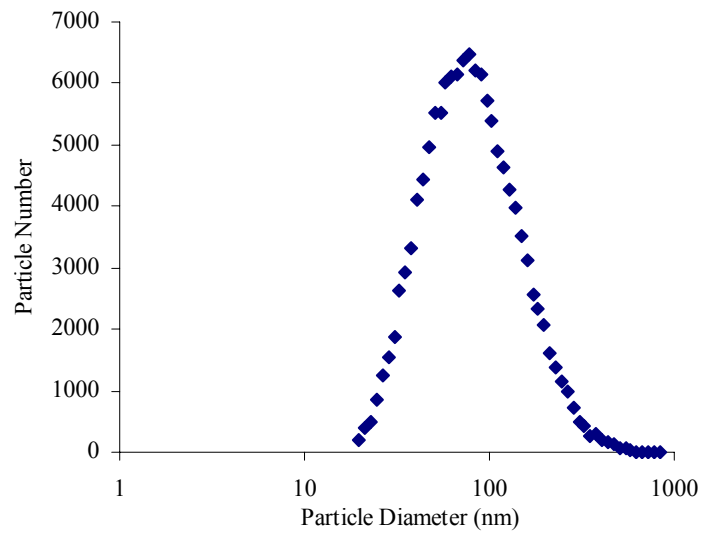


Figure A.7 Neutral seed particle number distribution, 42%RH Mode: 98